OAK RIDGE NATIONAL LABORATORY
operated by
UNION CARBIDE CORPORATION
for the
U. S. ATOMIC ENERGY COMMISSION

ORNL - TM - 2893, Vol. 2
COPY NO. - 64
DATE - October 7, 1970

TOWER SHIELDING REACTOR II
DESIGN AND OPERATION REPORT: VOL. 2 - SAFETY ANALYSIS

L. B. Holland and J. O. Kolb

BLANK PAGE

PREFACE

Information on the Tower Shielding Reactor II is contained in the TSR-II Design and Operation Report and in the Tower Shielding Facility Manual.

The TSR-II Design and Operating Report consists of three volumes:

ORNL-TM-2893, Volume 1, "Description of the Tower Shielding Reactor II and Facility," by L. B. Holland

ORNL-TM-2893, Volume 2, "Safety Analysis of the Tower Shielding Reactor II," by L. B. Holland and J. O. Kolb.

ORNL-TM-2893, Volume 3, "Assembly and Testing of the Tower Shielding Reactor II Control Mechanism Housing," by D. R. Ward and L. B. Holland.

The Tower Shielding Facility Manual contains current operating, maintenance, and emergency procedures; operating safety limits; descriptions of the facility, the reactor, and auxiliary equipment and records for their operation and maintenance; delineation of the administrative organization and programs for training and qualifying personnel.

The TSR-II was conceived, designed, and fabricated by ORNL personnel. It is not feasible to give credit to the many individuals who have contributed to the overall effort but some should be singled out. At the suggestion of A. M. Weinberg that a reactor having a wide utility shielding be designed, E. P. Blizard proposed that the reactor be spherical. In order to minimize flux perturbation by control rods, C. E. Clifford proposed that the control be achieved in a central nonfueled region. P. E. Oliver first suggested the control mechanism design, which utilized only metal and water in the core region. The diligent efforts of the TSF staff in carrying on development studies was a fine compliment to the many individuals who contributed to the design.

CONTENTS

CONTENTS (continued)

1. INTRODUCTION

The Tower Shielding Reactor II is a spherically symmetrical experimental reactor that was installed at the Tower Shielding Facility in 1960. In order to measure reactor parameters and to gain operating experience with this reactor, initial approval was requested,[1] and granted,[2] for operation at 100 kW, both at ground level and at elevated positions. It is now proposed that, as a result of the safety analysis contained in this report, the TSR-II be operated at a power level of 1 MW with the three following limitations: 1) the core life will be limited to 3000 MWhr, 2) continuous operation at 1 MW will be limited to periods of 75 hr or less, and 3) operation at a power level of 1 MW will be initiated only if the afterheat from previous operation has decayed to a sufficiently low value.

The factor considered in the safety analysis for operation at the proposed power level of 1 MW were the lack of a containment barrier around the primary core coolant system, the operation of the reactor while suspended from the TSF towers, and the minimum exclusion distance of 4085 ft from the reactor to the nearest point of public access at the general exclusion fence. The investigation was directed primarily to the adequacy of the fuel plate cladding as a barrier to fission-product release and to the amount of fission-product release that could be tolerated under the Maximum Credible Accident (MCA) conditions.

References

1. C. E. Clifford and L. B. Holland, Description of the Tower Shielding Reactor II and Proposed Preliminary Experiments, ORNL-2747 (June 1959).
2. Letter dated September 29, 1959, from H. M. Roth to J. A. Swartout: "Proposed Preliminary Experiments with the Tower Shielding Reactor II (TSR-II) at the Tower Shielding Facility (TSF)."

2. SITE DESCRIPTION

2.1. Site Location

The Tower Shielding Facility is located on a knoll with an elevation of 1069 ft 2.35 miles south-southeast of ORNL, 6 to 13 miles from the city of Oak Ridge, and 17 to 25 miles from the city of Knoxville (see Fig. 2.1). The Melton Hill Dam of the TVA is located 0.8 mile south of the TSF on the Clinch River, which forms a natural boundary of the restricted area. The nearest ORNL facilities are the Health Physics Research Reactor (HPRR) and the High-Flux Isotope Reactor, both of which are over 6000 ft from the TSF and separated from it by Copper Ridge, which has a maximum elevation of 1356 ft (see Fig. 2.2). The immediate terrain on all sides of the tower structure slopes below ground level at the base of the towers; approximately 400 ft to the north of the towers the grade gradually rises to the top of Copper Ridge.

The Tower Shielding Facility is situated within a general exclusion area which is enclosed by a 6-ft-high chain-link fence topped with three strands of barbed wire (see Fig. 2.2). The closest approach to the reactor at this fence is a distance of 3800 ft located on an arc drawn through points M2, M3, and M4 in Fig. 2.2, but the terrain is so steep and heavily wooded that this area is not considered accessible to the general public. However, where the TVA lands of Melton Hill Lake are adjacent to the exclusion fence, the fence is reasonably accessible for pedestrians from a road that runs along the lake. The nearest point of possible access to the reactor from this area is at M1 (Fig. 2.2), which is 4085 ft from the reactor.

Four gamma-ray sensitive detectors are located at points M1, M2, M3, and M4 along the exclusion fence. Calculations[1] have shown that, even if a highly collimated beam from the reactor is directed north, i.e., away from the monitor stations, (see Fig. 2.2) the radiation level along the fence where the monitor stations are located will be higher than it is at any other point on the exclusion fence. If the beam is pointed directly between the two most widely separated monitor stations, the dose at that point is calculated to be approximately 35% higher than that at

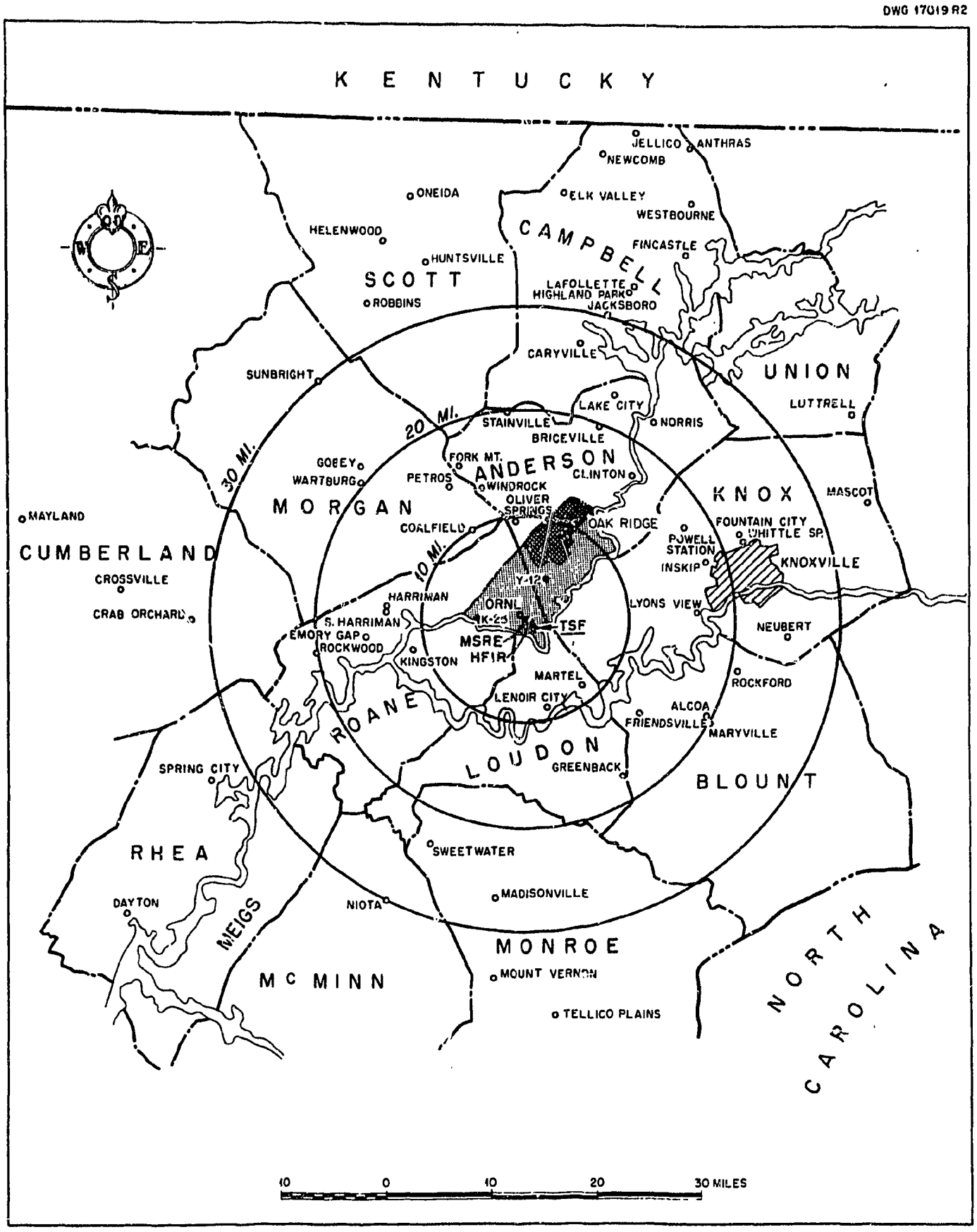

Fig. 2.1. Map of cities and counties surrounding TSF area.

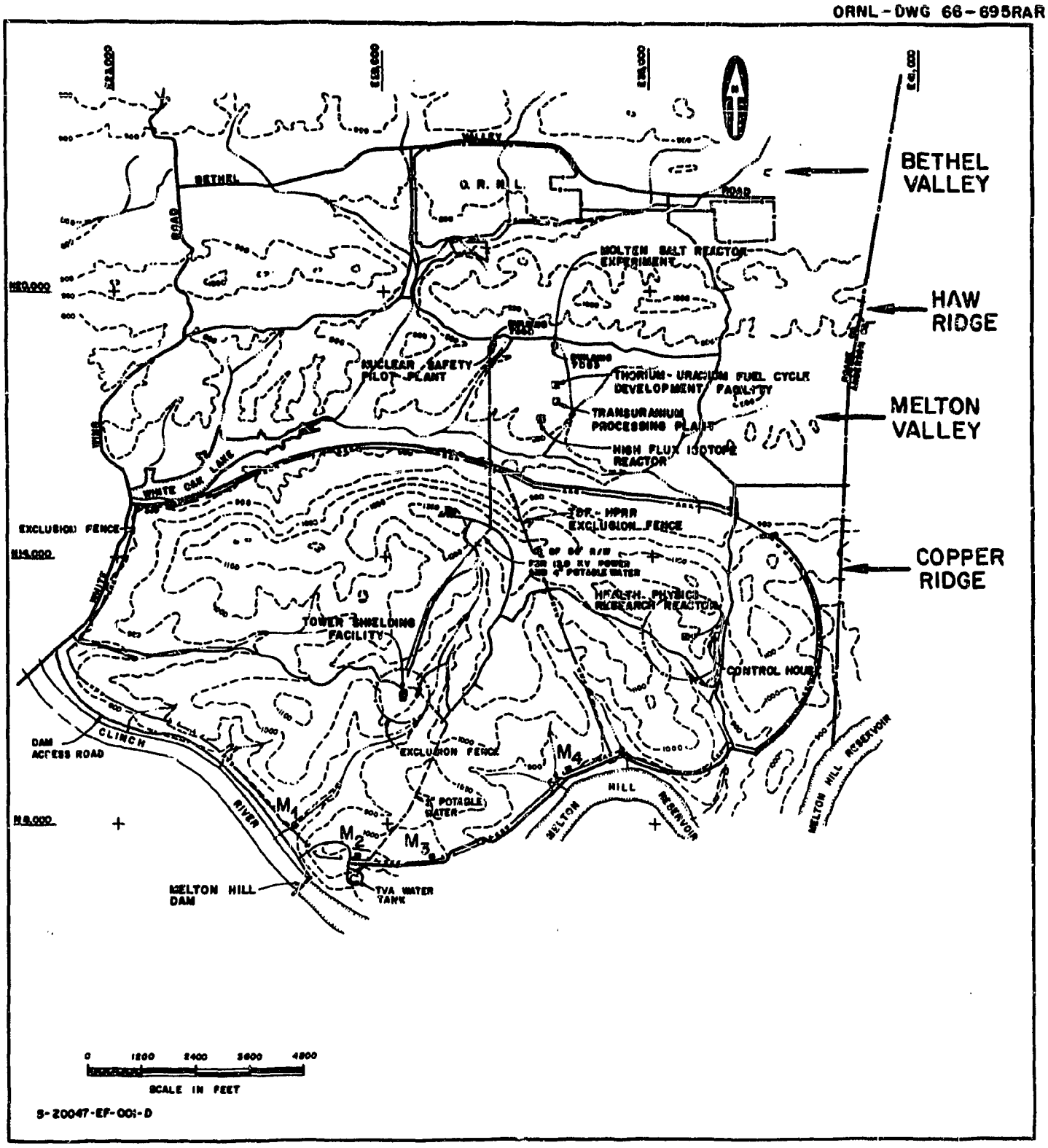

Fig. 2.2. Area topography.

the monitor stations nearest to the beam direction. This area, however, is a heavily wooded peninsula that is not readily accessible to the general public. The gamma-ray dose rates at the four monitor stations are continuously recorded on a strip chart in the control room. With the TSR-II operated at 100 kW in the beam shield, no radiation above background has been detected at the fence. If the radiation level at the perimeter fence for a new reactor shield configuration is above background level, the neutron-to-gamma ratio will be measured. (For the TSR-II in the COOL-I shield it was measured to be 2.23.) This ratio will be used with the monitor readings to calculate the daily dose accumulated at the exclusion fence. The daily dose is recorded in the operations log book, and the total dose at the fence is published in operating reports that are now issued semiannually. The allowable dose to an individual in an uncontrolled area is 500 mrem/year. The TSR-II will be operated such that at the point of closest public access to the reactor, the 4085-ft point, the dose will be limited to 500/mrem/year.

2.2. Climatology and Meteorology of the TSF Site[2]

Weather instruments have been used at the Tower Shielding Facility since March 1954. When supplemented by meteorological observations from Melton Valley and X-10 (ORNL), these instruments provide extensive information on temperature, dew point, wind velocities, wind directions, and vertical temperature gradient in the TSF area. The climatological differences at the TSF site, Melton Valley, and X-10 are quite marked and will be discussed in detail. This material can be considered as supplementary to the climatological discussion of the TSF area contained in ORNL-1550.[3]

2.2.1. Stability in the Lower Layers of the Atmosphere

In order to discuss the stability in the lower layers of the atmosphere, the following terms are first defined:

Lapse: a decrease of temperature at the height increases, the normal daytime state of the atmosphere.

Inversion: a state of the atmosphere wherein the temperature of the air at a lower level is less than or equal to the temperature at some higher level. True inversions cover a large area of space (more than a city block) and are characterized by lack of vertical and horizontal mixing.

Stability: a function of the existing degree of lapse or inversion condition; the greater the degree of the lapse condition, the more unstable the air becomes.

Great stability decreases effluent mixing to practically zero. (Instability, conversely, is accompanied by comparatively rapid dispersal of contaminants, often in an erratic vector pattern.) Stability, measured from the temperature difference between two elevations, varies not only as a function of the season and time of day but also as a function of site location. The average number of hours of inversion per day (up to 1958) as a function of season and location is shown below:

	Average Daily Inversion (hr)		
	TSF	Melton Valley	X-10
Winter	10.1	11.1	8.1
Spring	10.1	11.1	9.2
Summer	12.7	11.1	9.3
Fall	12.7	12.7	9.8

The X-10 site has the fewest hours of inversion compared with TSF and Melton Valley, whose yearly totals are about equal. The reason for the comparatively few hours of inversion in X-10 is that there are very few large trees in this area and in Bethel Valley itself, in contrast to the wooded environment of TSF and Melton Valley. The forested regions inhibit the freedom of air movement near the surface, and the moist, shaded forest floors strongly affect the temperatures in and near wooded areas. Therefore temperature variations are damped, and once an inversion is started in a wooded area, it tends to persist. By contrast, in open areas such as at the X-10 site, temperatures vary rapidly with cloud cover, time of day, and wind variations. All three sites show the greatest number of hours of inversion during the fall, which is to be expected.

Measurement of the temperature gradient at each site is made by means of thermocouples placed at two convenient levels. The lowest temperature probe is 4 to 5 ft from the ground. With this type of instrumentation, we can state only that an inversion exists near the surface and can only surmise the total depth of the inversion layer. At the TSF, where the upper thermocouple is 300 ft above the ground, surface conditions are not sufficient criteria for the estimation of meteorological conditions at the higher elevations. It may be many hours before an inversion which originated at the base of the TSF tower reaches the top of the tower, or it may never reach there.

The expected frequency, by season, of inversions with a length equal to or greater than "n" hours is shown in Fig. 2.3. Inversions of long duration represent an undesirable condition because of a reduction in wind velocity, in turbulence, and in atmospheric mixing below the inversion layer and create two problems: an increase in the pollution near the ground and an increase in the depth of the inversion with time offsetting somewhat the advantage of increased source height.

2.2.2. Wind Flow

For simplicity the wind behavior of the TSF region may be divided into two categories, the surface wind and the "free air," or upper wind, which may be considered separately. The surface winds may be regarded (for simplicity only) as the first 10 to 20 m of air movement above the

ORNL-DWG 67-13507

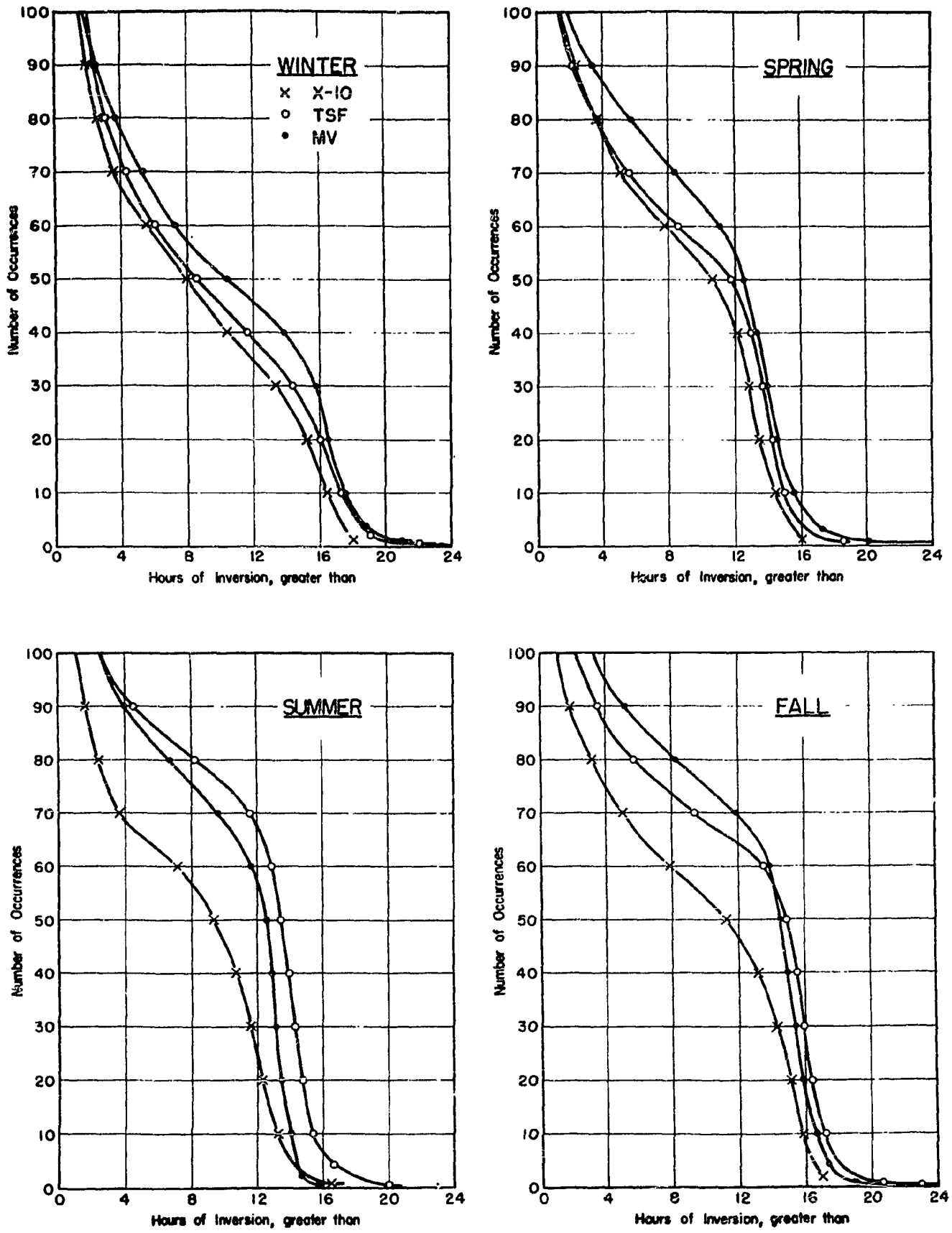

Fig. 2.3. Seasonal frequency of inversions as a function of duration for X-10, TSF, and Melton Valley.

ground. Surface winds are distinct from upper winds only during strong inversion conditions, when the dense cold air follows a down-valley path analogous to the flow of a river. As an inversion lessens or as the lapse condition becomes stronger, the air has less tendency to resist vertical perturbations. It follows therefore that at night, under deep inversions, wind flow in the valley will be northeasterly, following the ridge profiles of the East Tennessee area. In the morning, as the inversion weakens and disappears, the surface wind mixes with the upper winds, destroying the northeasterly circulation and following the upper winds with a fidelity that is a function of low-level turbulence and upper-wind direction and strength.

The wind roses for the TSF (Figs. 2.4 and 2.5) show the effect of stability conditions on wind patterns. The wind roses for Melton Valley are shown in Figs. 2.6 and 2.7. During lapse conditions, the wind direction has a distinct tendency toward a west-southwest component, resulting from turbulent mixing with the "prevailing westerlies" that are at about 5000 ft measured from sea level (MSL). During inversion conditions the wind directions are oriented more along a southwest-northeast axis, reflecting the domination by terrain of winds below 2000 ft MSL in this area.

Although during inversion conditions winds usually decrease at a given level, wind friction with the ground is reduced, thereby allowing the upper winds to reach their maximum theoretical speeds (and directions). Thus during inversion conditions the wind velocities at the top of the TSF tower often increase because of the comparatively great height of the tower. The average wind velocities for TSF and Melton Valley by season, during lapse and inversion conditions, are given below:

ORNL-DWG 67-13500

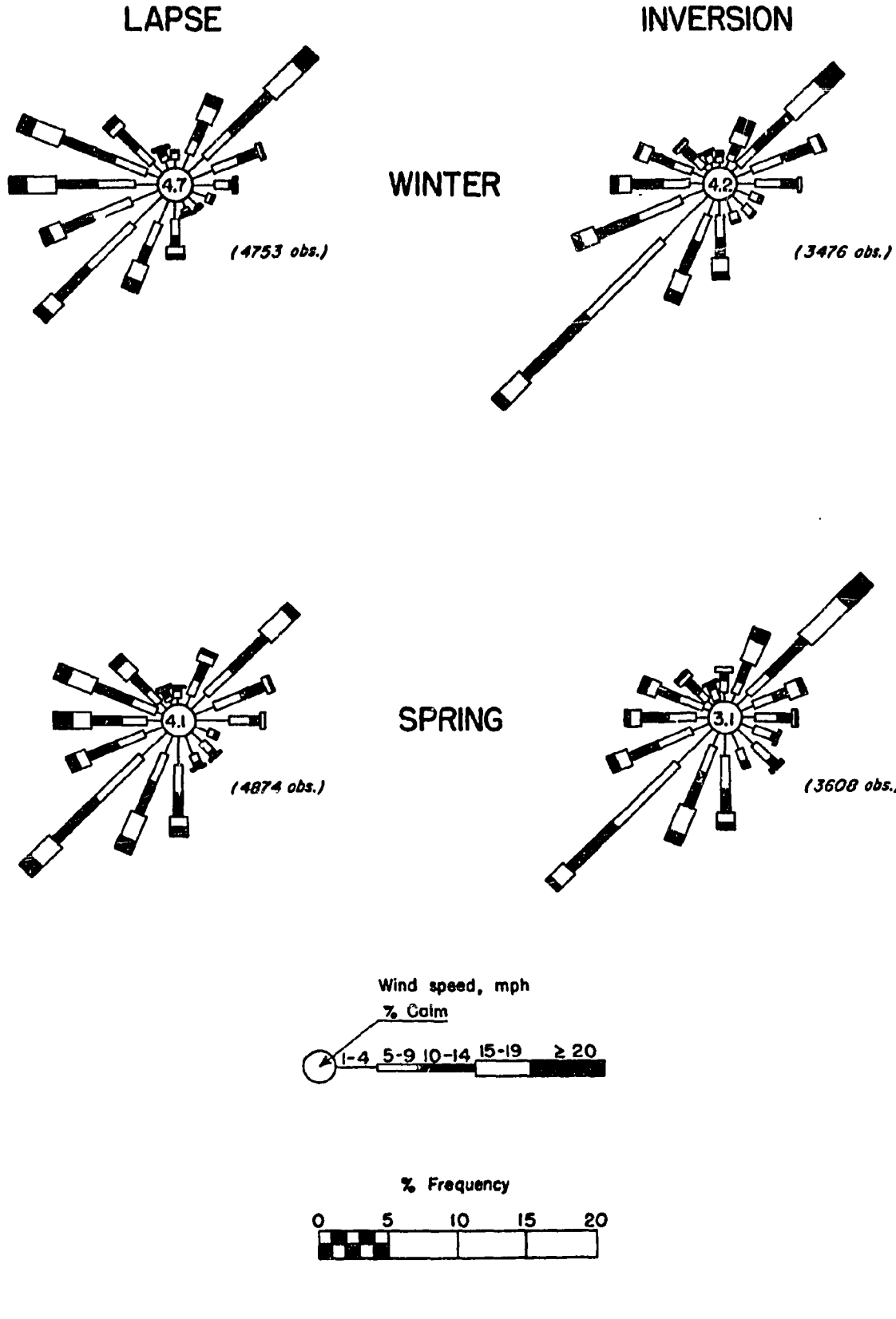

Fig. 2.4. Wind roses for the Tower Shielding Facility - winter and spring.

ORNL-DWG 67-13496

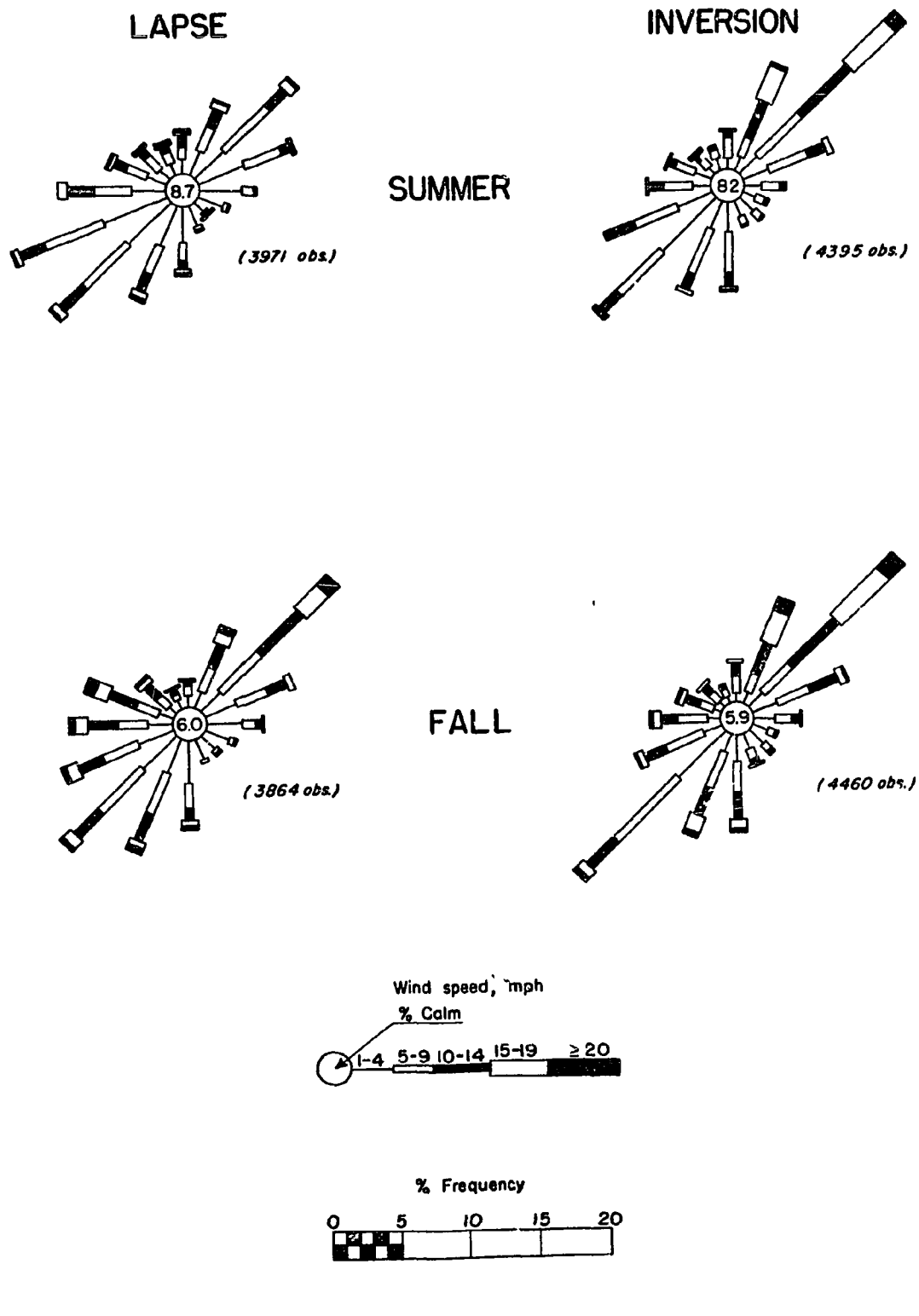

Fig. 2.5. Wind roses for the Tower Shielding Facility - summer and fall.

ORNL-DWG 67-13506

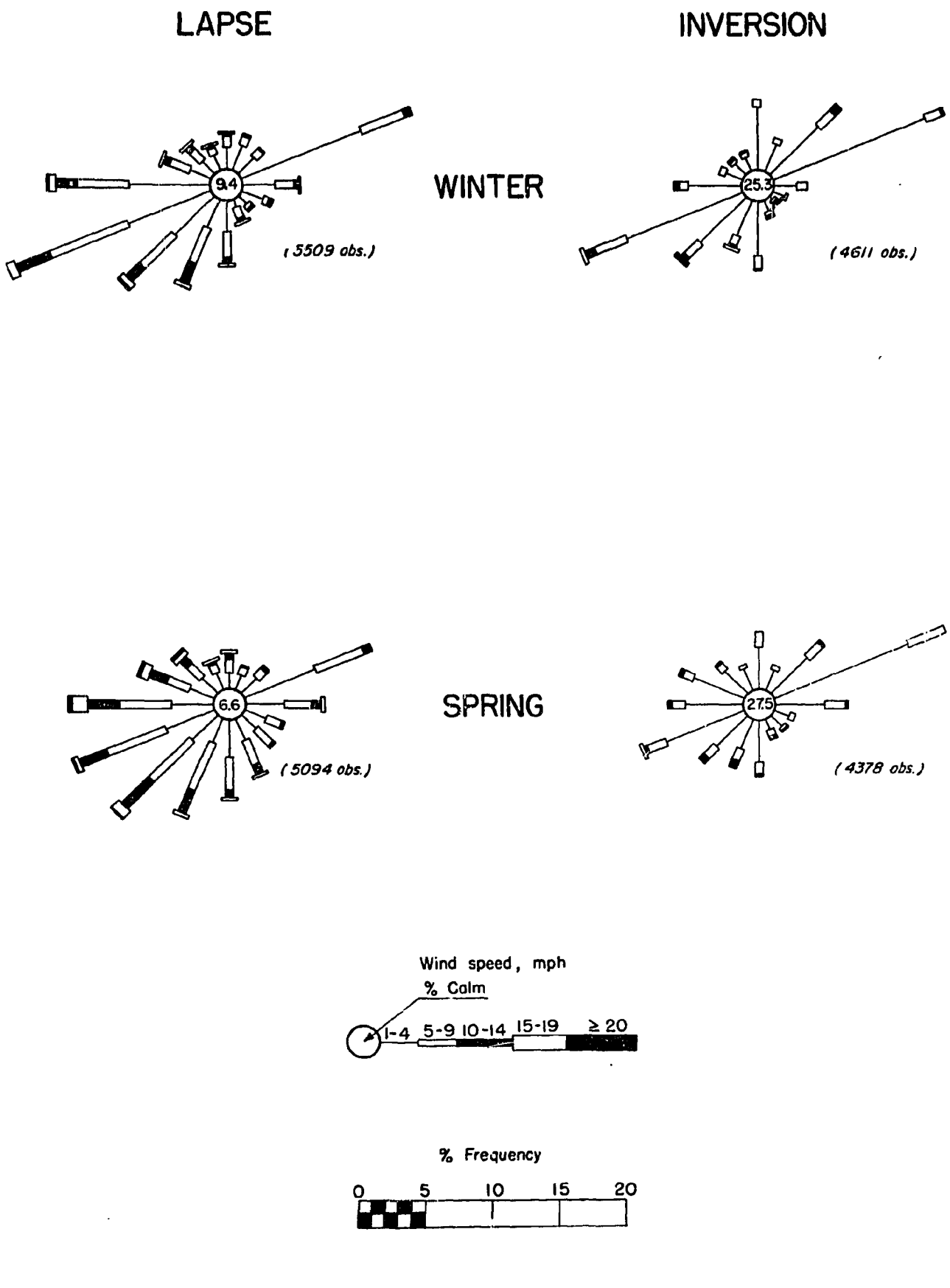

Fig. 2.6. Wind roses for Melton Valley - winter and spring.

ORNL-DWG 67-13503

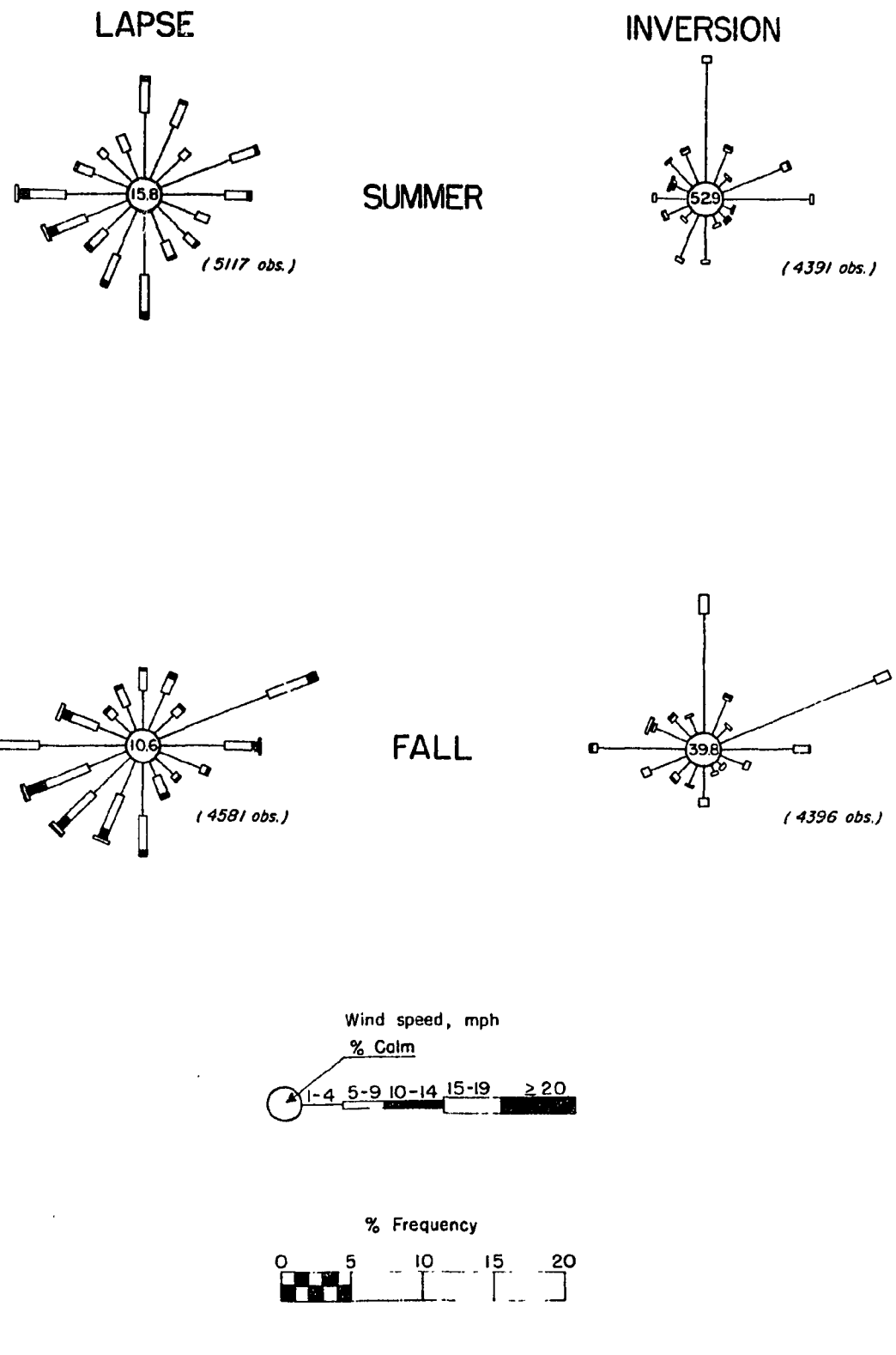

Fig. 2.7. Wind roses for Melton Valley - summer and fall.

	Wind Velocity (mph)	
	During Lapse	During Inversion
Winter		
TSF	9.7	9.5
Melton Valley	5.2	2.9
Spring		
TSF	10.0	9.9
Melton Valley	6.2	2.8
Summer		
TSF	6.1	7.3
Melton Valley	3.7	1.4
Fall		
TSF	7.9	8.7
Melton Valley	4.5	2.0

The consequences of the inversion-wind relationship are quite interesting. Should a contaminant be released from the maximum operating height (185 ft), it would probably be carried away from the site quite rapidly regardless of time of day or inversion condition. A contaminant released at ground level, however, would be dispersed as a function of the stability conditions existing at the time. An elevated release during lapse conditions would be more likely to send effluent over Knoxville than would such a release during inversion conditions when the predominant wind pattern follows Haw Ridge quite faithfully. Effluent released at the ground would follow the terrain with a fidelity proportional to the degree of inversion present. In either case, ground or elevated release, the effluent would be dispersed more rapidly during lapse conditions.

The frequency (or percentage of time) that winds arriving at the TSF travel toward the various plant sites and Oak Ridge is shown below:

	Frequency (% of Time) of Wind Travel from TSF				
Condition	To X-10	To Melton Valley	To Y-12	To K-25	To Oak Ridge
Lapse					
Winter	1.2	4.3	7.3	1.7	11.6
Spring	2.6	7.4	9.4	1.8	16.8
Summer	1.8	5.1	7.6	2.3	12.7
Fall	1.9	6.6	9.1	2.5	15.7
Inversion					
Winter	1.9	5.8	8.3	2.0	14.1
Spring	2.8	7.4	8.8	2.8	16.2
Summer	2.0	6.6	7.3	1.8	13.9
Fall	2.5	7.3	8.2	1.9	15.5

The high percentage for Oak Ridge results from combining all winds that occur from the east to the west side of the town. Actual percentage toward any one section of Oak Ridge is approximately half of the given percentage.

Figure 2.8 is a compilation of Knoxville and Nashville wind roses for various altitudes. Note the dissimilarity of patterns between Knoxville and Nashville at an elevation of 500 m and the tendency toward similarity with increasing altitude. From 500 m up, Oak Ridge would have a wind rose almost exactly equal to that for Knoxville. The effect of local ridge terrain is marked at 500 m, slight at 1500 m, and almost totally absent at 3000 m.

The upper-wind patterns at Nashville show a characteristic southerly wind direction, which is most prevalent during precipitation periods. No such preference is found in studies made of surface wind during periods of precipitation at Oak Ridge.

An extract of Oak Ridge and X-10 climatological data is given in Tables 2.1 and 2.2.

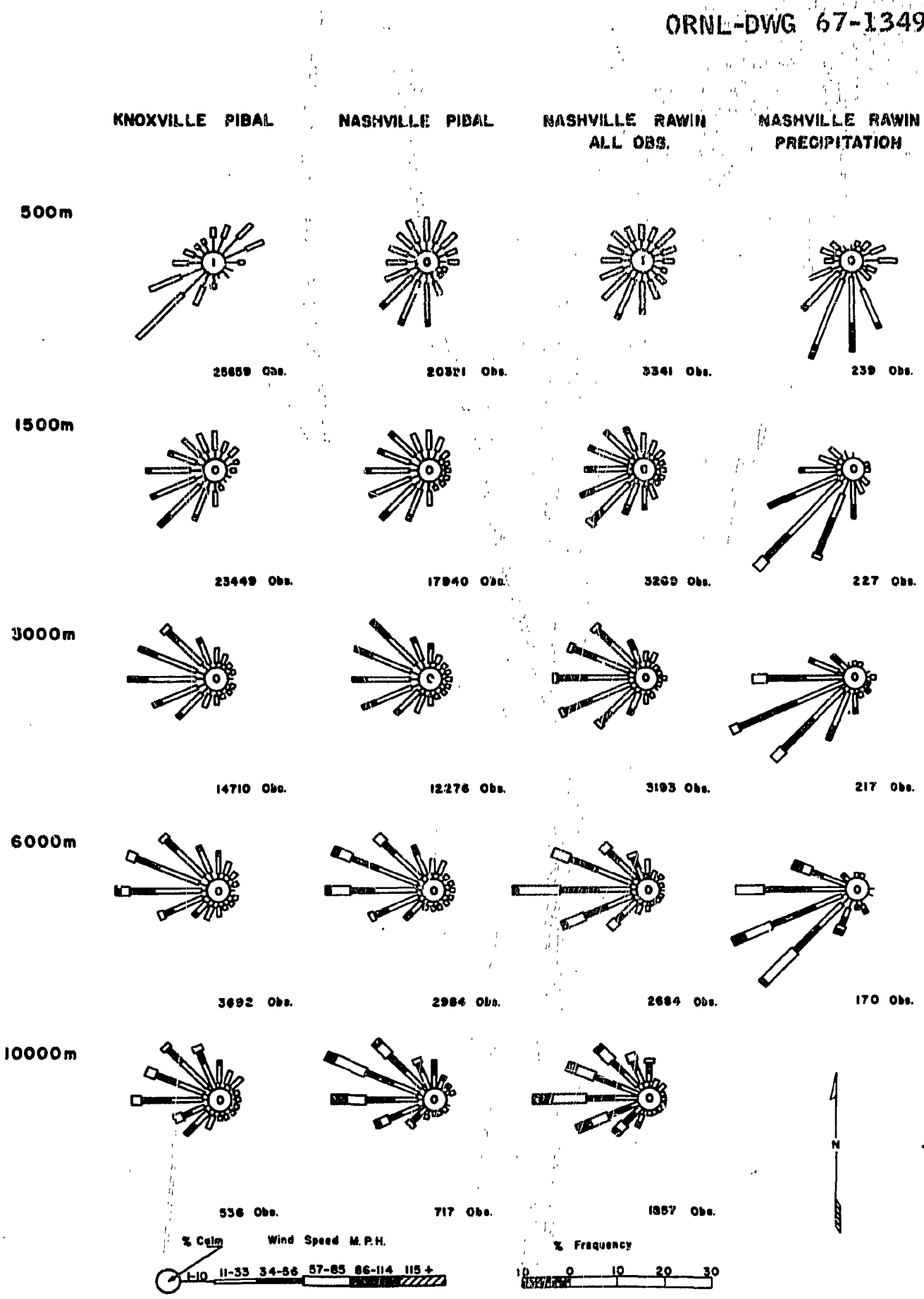

Fig. 2.8. Pibal and rawin roses for Knoxville and Nashville for various altitudes.

Table 2.1. Normals, Means, and Extremes for Oak Ridge

Month	Temperature (°F)							Normal Degree Days[a]	Precipitation (in.)											Wind (mph)		Mean Sky Cover Sunrise to Sunset[d]	Mean Number of Days											
	Normal			Extremes											Snow, Sleet								Sunrise to Sunset							Temperatures			
																														Max		Min	
	Daily Maximum[a]	Daily Minimum[a]	Monthly[a]	Record Highest	Year	Record Lowest	Year		Normal Total[a]	Maximum Monthly	Year	Minimum Monthly	Year	Maximum in 24 hr	Year	Mean Total	Maximum Monthly	Year	Maximum in 24 hr	Year	Mean Hourly Speed	Prevailing Direction		Clear	Partly Cloudy	Cloudy	Precipitation 0.01 in. or More	Snow, Sleet 1.0 in. or More	Thunderstorms	Heavy Fog	90°F and Above	32°F and Below	32°F and Below	0°F and Below
				11[b]		11[b]				11[b]		11[b]		11[b]		11[b]	11[b]		11[b]		10[b]	10[b]	6[b]	11[b]	11[b]	11[b]	11[b]	6[b]	10[b]	8[b]	11[b]	11[b]	11[b]	11[b]
J	48.8	29.2	39.0	75	1952	4	1948	806	6.06	13.27	1954	2.44	1955	4.25	1954	2.1	10.7	1948	5.7	1948	4.9	SW	7.3	6	6	19	14	1	1	2	0	1	18	0
F	51.6	30.4	41.0	74	1951[c]	1	1958	672	5.79	10.47	1956	1.90	1952	3.05	1948	1.3	4.0	1948	4.0	1948	4.9	W	6.5	6	7	15	13	1	2	2	0	1	13	0
M	59.9	36.2	48.1	83	1948	13	1955	532	5.69	8.09	1951	2.13	1957	2.80	1952	0.2	1.0	1951	1.0	1951	5.2	SW	6.7	7	8	16	13	0	3	1	0	<½	11	0
A	70.2	45.0	57.6	89	1955	24	1950	230	4.08	9.71	1956	1.39	1950	3.74	1956	T[e]	T[e]	1956[c]	T[e]	1956[c]	5.7	SW	5.8	10	7	13	10	0	5	1	0	0	2	0
M	78.5	53.4	66.0	93	1953	34	1954	64	4.18	7.05	1950	1.23	1951	2.20	1953	0.0	0.0		0.0		4.4	SW	6.1	11	9	11	11	0	8	2	2	0	0	0
J	86.3	62.1	74.2	101	1954	43	1956	0	3.91	4.83	1951	1.18	1952	2.01	1957	0.0	0.0		0.0		3.9	SW	5.2	10	12	8	10	0	8	2	10	0	0	0
J	88.3	65.1	76.7	105	1952	51	1952[c]	0	5.34	8.51	1949	2.72	1957	3.48	1954	0.0	0.0		0.0		3.7	SW	5.6	10	12	9	12	0	11	3	14	0	0	0
A	86.9	63.6	75.3	100	1954	51	1956	0	4.06	5.94	1950	0.54	1953	2.20	1955	0.0	0.0		0.0		3.4	E	4.4	13	10	8	10	0	9	3	13	0	0	0
S	83.1	58.4	70.8	102	1954	37	1949	38	2.55	9.10	1957	1.14	1948	2.61	1957	0.0	0.0		0.0		3.8	E	4.8	14	8	8	8	0	4	3	6	0	0	0
O	71.7	45.9	58.8	90	1954[c]	21	1952	216	2.42	6.11	1949	0.41	1958	2.13	1949	T[e]	T[e]	1957	T[e]	1957	3.7	E	4.9	14	7	10	7	0	1	8	<½	0	2	0
N	58.2	35.7	47.0	82	1948	0	1950	540	3.98	12.22	1948	1.37	1949	2.97	1957	0.9	6.5	1950	6.5	1950	4.1	E	5.6	10	7	13	9	0	2	7	0	<½	14	<½
D	49.3	29.9	39.6	74	1951	6	1957	787	5.66	10.31	1956	2.43	1958	4.73	1954	0.4	2.1	1954	1.8	1954	4.4	SW	6.4	8	8	15	11	<½	1	2	0	1	19	0
Year	69.4	46.2	57.8	105	July 1952	0	Nov. 1950	3835	53.72	13.27	Jan. 1954	0.41	Oct. 1958	4.73	Dec. 1954	4.9	10.7	Jan. 1948	6.5	Nov. 1950	4.3	SW	5.8	119	101	145	128	2	55	36	45	3	79	<½

[a]Normal values are based on the period 1921–1950, and are means adjusted to represent observations taken at the present standard location.

[b]Length of record, years.

[c]Also on earlier dates, months, or years.

[d]Sky cover is expressed in a range of 0 for no clouds or obscuring phenomena to 10 for complete sky cover. The number of clear days is based on average cloudiness 0–3 tenths, partly cloudy days on 4–7 tenths, and cloudy days on 8–10 tenths. Monthly degree day totals are the sums of the negative departures of average daily temperatures from 65°F. Sleet was included in snowfall totals beginning with July 1948.

[e]Trace.

Table 2.2. Normals, Means, and Extremes for X-10

Month	Temperature (°F)							Normal Degree Days[a]	Precipitation (in.)							Wind (mph)		Mean Number of Days				
	Normal			Extremes															Temperatures				
																			Max		Min	
	Daily Maximum[a]	Daily Minimum[a]	Monthly[a]	Record Highest	Year	Record Lowest	Year		Normal Total[a]	Maximum Monthly	Year	Minimum Monthly	Year	Maximum in 24 hr	Year	Mean Hourly Speed	Prevailing Direction	Precipitation 0.01 in. or More	90°F and Above	32°F and Below	32°F and Below	0°F and Below
				14[b]		14[b]				15[b]		15[b]		15[b]		11[b]	11[b]	12[b]	12[b]	14[b]	14[b]	14[b]
J	48.7	30.4	39.6	77	1952	1	1948	787	5.11	12.37	1954	1.11	1944	3.96	1954	5.6	NE	13	0	1	18	0
F	51.2	31.5	41.4	77	1948	0	1958	661	5.21	10.01	1956	1.89	1947	3.23	1948	5.9	NE	11	0	2	14	$<\frac{1}{2}$
M	59.3	37.3	48.3	87	1945	14	1955	534	5.64	8.91	1951	2.06	1957	2.85	1952	6.7	SW	12	0	$<\frac{1}{2}$	11	0
A	69.5	45.9	57.7	89	1948[c]	24	1950	227	4.29	8.54	1956	1.25	1952	2.96	1956	6.8	SW	11	0	0	2	0
M	77.7	54.2	66.0	94	1956	34	1954	64	3.78	7.01	1950	0.90	1951	2.09	1955	4.9	NE	10	1	0	0	0
J	85.7	62.7	74.2	99	1952	41	1946	0	4.18	5.87	1945	1.18	1956	3.08	1945	4.2	SW	9	10	0	0	0
J	87.8	65.6	76.7	103	1952	49	1947	0	4.83	8.13	1950	2.14	1954	2.40	1948	3.9	NE	11	13	0	0	0
A	86.6	64.2	75.4	99	1957[c]	44	1946	0	4.45	10.31	1950	0.50	1953	2.34	1950	3.2	NE	9	13	0	0	0
S	83.0	59.1	71.1	103	1954[c]	33	1949	41	2.97	12.84	1944	1.07	1945	7.75	1944	4.1	NE	7	6	0	0	0
O	71.8	46.7	59.3	91	1954	21	1952	206	2.77	6.43	1949	0.48	1958	2.32	1949	4.0	NE	6	$<\frac{1}{2}$	0	1	0
N	58.4	36.6	47.5	82	1950	4	1950	531	3.94	12.00	1949	1.01	1949	3.20	1948	4.8	SW	10	0	$<\frac{1}{2}$	12	0
D	49.3	30.9	40.1	76	1951	4	1957	772	5.21	10.28	1954	1.98	1958	4.38	1954	4.8	NE	10	0	1	19	0
Year	69.1	47.1	58.1	103	Sept. 1954[c]	0	Feb. 1958	3823	52.38	12.84	Sept. 1944	0.48	Oct. 1958	7.75	Sept. 1944	4.9	NE	119	43	4	77	$<\frac{1}{2}$

[a]Normal values are based on the period 1921–1950, and are means adjusted to represent observations taken at the present standard location.

[b]Length of record, years.

[c]Also on earlier dates, months, or years.

2.3. Geology, Hydrology, and Seismology

The geology, hydrology, and seismology of the TSF site and surroundings have been described previously.[3,4] In brief, the geological structure is a combination of clayish soil and conasauga shale,[5] which results in a high adsorption capacity for most fission products and low ground-water velocities. Surface water flow from high rainfall is therefore the main mechanism for transport of water-borne activity. A natural drain exists to the south of the TSF site (see Fig. 2.2), with surface run-off flowing into the Clinch River below Melton Hill Dam.

Seismic activity in the Oak Ridge area is very low, an average of only one or two earthquakes occurring a year.[6-8] Oak Ridge has been classified by the U. S. Coast and Geodetic Survey as subject to earthquakes of intensity mm-6 measured on the modified Mercalli Intensity Scale. J. Lynch of Fordham University further concluded that a major shock in the Tennessee area was improbable for several thousand years to come.[9]

2.4. Surrounding Population

Population data for nearby cities and counties are shown in Tables 2.3 and 2.4. The distance to the closest population concentration, Gamble Valley of Oak Ridge or the north section of Lenoir City, is about 7 miles. Land along the Clinch River south of the TSF is controlled by TVA for at least 3/4 mile from the TSF. There are no residences within 1 mile of the TSF.

Table 2.3. Population of the Surrounding Towns+

City or Town	Distance from TSF (miles)	Direction from TSF	Population
Oak Ridge	6-13	NNE	27,124
Lenoir City	8	SSE	4,979
Martel	9	SE	500*
Oliver Springs	10	N by W	1,163
Coalfield	11	NW	650*
Windrock	10	N by W	550*
Kingston	12	WSW	2,010
Harriman	13	W	5,931
South Harriman	13	W	2,884
Petros	14	NW by N	790*
Fork Mountain	15	NNW	700*
Emory Gap	15	W	500*
Friendsville	15	SE	606
Clinton	16	NE	4,943
South Clinton	16	NE	1,356
Powell	17	ENE	500*
Briceville	19	NNE	1,217
Wartburg	20	NW by W	800*
Knoxville	18-25	E	111,827
Greenback	20	S by E	960*
Rockwood	21	W by S	5,343
Rockford	22	SE	5,345
Fountain City	22	ENE	10,365
Lake City	23	NNE	1,914
Norris	23	NNE	1,389
Sweetwater	23	SSW	4,145
Neuberts	27	ENE	600*
John Sevier	27	E	752*
Madisonville	27	S	1,812
Caryville	27	N by E	1,234*
Sunbright	30	NW	600*
Jacksboro	30	N by E	577*
Niota	30	SSW	679

+Based on 1960 census except where indicated by an asterisk, which figures were based on 1950 census.

Table 2.4. Rural Population in Surrounding Counties

County	Total Area[a] (sq mi)	Rural Population[b]	Density (No. people per sq mi)	Estimated Population Within 10-mile Radius	Within 20-mile Radius	Within 30-mile Radius
Anderson	338	26,600	79	395	14,200	22,800
Blount	584	38,325	66	0	6,720	23,200
Knox	517	138,700	238	13,100	46,400	96,000
Loudon	240	18,800	78	6,080	16,900	18,700
Morgan	539	13,500	25	225	3,625	8,630
Roane	379	12,500	33	3,070	9,170	11,110

[a] Does not include area within Oak Ridge reservation.

[b] 1960 census - does not include communities with population of 500 or more.

REFERENCES

1. V. R. Cain, Additional Fencing and Radiation Monitoring Required for 5-MW Operation of the TSR-II, ORNL-CF-60-8-7 (August 1960).
2. This section is based on a revision by W. M. Culkowski, U. S. Weather Bureau Office, Oak Ridge, Tennessee, November 1958 of the TSF Climatology (Appendix F of ORNL-1550).
3. C. E. Clifford, The Tower Shielding Facility Safeguard Report, ORNL-1550 (June 9, 1953).
4. J. H. Buck and W. B. Cottrell, Aircraft Reactor Experiment Hazards Summary Report, ORNL-1407 (November 24, 1952).
5. P. S. Stockdale, Geological Conditions at the Oak Ridge National Laboratory (X-10) Area Relevant to the Disposal of Radioactive Waste, ORO-58 (August 1, 1951).
6. B. C. Moneymaker (TVA), "Earthquakes in Tennessee and Nearby Sections of Neighboring States, 1851-1900," J. Tenn. Acad. Sci. 30(3), 222-233 (1955).
7. B. C. Moneymaker (TVA), "Earthquakes in Tennessee and Nearby Sections of Neighboring States, 1901-1925," J. Tenn. Acad. Sci. 32(2), 91-105 (1957).
8. B. C. Moneymaker (TVA), "Earthquakes in Tennessee and Nearby Sections of Neighboring States, 1926-1950," J. Tenn. Acad. Sci. 33(3), 224-239 (1958).
9. Letter from J. Lynch (Fordham University) to M. Mann (ORNL), November 3, 1948.

3. ACCIDENT ANALYSIS

The accident conditions and analyses presented here relate to the TSR-II as described in Volume I of the Design and Operations Report,[1] which should be consulted for a detailed description of the reactor and its primary suspension system. Since the reactor has been operated from 1960 at power levels of up to 100 kW, the mechanical system and the instrumentation systems for reactor operation and protection have been tested, the reactivity coefficients have been measured (see Appendix D for TSR-II core characteristics), and the probability of accidents from operational causes has been reduced, although not, of course, eliminated through actual operating experience. The accident analysis investigation was therefore primarily concerned with fission-product release due to reactivity accidents and to reduction or loss of core coolant. A major topic is the probability of a dropped core, the one conceivable accident that will cause a loss of coolant. The possible mechanisms for minor release of fission-products are also discussed, but the mechanism for a major release of fission-products is discussed in Chapter 4. In Chapter 6 it is shown that such a release will not occur.

3.1. Reactivity Accident

A reactivity accident is the addition of reactivity to the reactor in an uncontrolled manner at a rate sufficient to cause the reactor power to increase to a level where damage occurs.

In the present analysis a TSR-II startup accident is compared with SPERT experiments in which only intrinsic shutdown mechanisms limited the reactor excursions to safe levels. The capability of the reactor protection system with only neutron level trips to protect the reactor from even larger reactivity insertions without any intrinsic shutdown mechanisms is also examined. For any real reactivity accident the intrinsic shutdown mechanisms and the reactor protection system would act to limit the power excursion and the shim-safety plates would be inserted to eliminate any subsequent power pulses. Reactivity additions from other possible mechanisms are shown to be smaller than that from the startup accident.

BLANK PAGE

3.1.1. Startup Accident with Intrinsic Shutdown Only

The conventional startup accident is considered to be a situation in which all of the control rods or, in the TSR-II, the control plates are withdrawn at their maximum rate, and all the instrumentation for reactor operation and for reactor protection, except for the neutron level trips, fails to operate. In the following analysis of SPERT experiments it is shown by analogy that the intrinsic shutdown mechanisms in the TSR-II are sufficient to protect the reactor from reactivity additions that are greater than any that can be added by the shim-safety plates.

At the position where the clean-cold core is normally critical the shim-safety plates add reactivity at the rate of 0.066×10^{-2} $\Delta k/k$ per second which from a SPERT empirical relation (see TSR-II Self Shutdown Characteristics, Appendix B) is equivalent to a 0.90×10^{-2} $\Delta k/k$ step increase in reactivity and an asymptotic period of approximately 55 msec. The rate of reactivity addition decreases as it becomes necessary to further withdraw the plates to compensate for temperature rise, fission-product buildup, and fuel depletion.

The probability that the above failures will exist at source-power level is extremely low. The consequences of such an accident can, however, be deduced from SPERT tests[2] with U-Al plate-type fuel elements since only self-shutdown mechanisms were operative in those tests. From the brief discussion of the SPERT test results in Appendix B, which relates the TSR-II with the SPERT B-16/40 core, a 50-msec period excursion in the TSR-II can be expected to be terminated almost solely by coolant and fuel expansion, with essentially no coolant vaporization and no metal-water reaction occurring.

The energy release to peak power from a 50-msec excursion is estimated from SPERT data (see B-16/40 in Fig. B.2) to be approximately 4 MWsec; the accompanying pressure pulse is negligible (see Fig. B.4), and the fuel plate surface temperature rise is approximately $80^{\circ}C$ (see Fig. B.3). The effect of system pressurization (see Appendix B) will no more than double the energy release and the maximum fuel plate temperature rise. Since the TSR-II is larger than the SPERT core, the specific power in the TSR-II for an equivalent energy release is smaller. Therefore, the energy release in the TSR-II to attain equivalent temperatures for shutdown will be larger. Correcting

the energy release to peak power for pressurization and for the ratio in masses of the two cores give a maximum energy release to peak power of 14 MWsec which is not a damaging excursion by SPERT standards.

The inherent self-shutdown characteristics of the TSR-II are better at power-operation core temperatures than they are at the ambient (~20°C) temperature at startup. For example, 0.1 x 10^{-2} $\Delta k/k$ per second reactivity ramp experiments in the SPERT-I B-12/64 core (the SPERT I core which was used for this comparison) yielded inverse asymptotic periods of 15 and 3 sec^{-1} for initial power levels of 5 mW and 10 kW respectively, with corresponding peak powers of 80 and 8 MW.[2] For reactivity insertions at 1 MW from realistic mechanisms such as 0.066 x 10^{-2} $\Delta k/k$ per second for control rod withdrawal in the TSR-II, self-shutdown would occur with less excursion energy than it would at source-power level.

3.1.2. Hypothetical Reactivity Accident with Protection System Action Only

The reactivity insertion that can be controlled by the TSR-II protection system was studied (see "Analog Computer Tests," Appendix A) under conditions that ignored intrinsic shutdown mechanisms and assumed that all control and protection systems except the neutron level system were inoperative. Investigation showed that the power increase from a step reactivity change that results in a 14.5-msec positive period ($\Delta k/k \cong 1.175 \times 10^{-2}$) would be limited by the reactor protection system to a factor of 200 over the operating power level, which for 1-MW operation would be a 200-MW peak power (see Fig. A.1 in Appendix A). The total energy release to peak power is approximately 5 MWsec, which is a fairly mild excursion. Thus with no self-shutdown mechanism acting and no period scram, the protection system is able to protect the core from damaging excursions for step reactivities as large 1.175 x 10^{-2} $\Delta k/k$. In the situations postulated in Sections 3.1.4 - 3.1.7. for possible reactivity additions, it is shown that additions of such magnitude are not credible.

3.1.3. Operation of Control Mechanisms and Shim-Safety Plates

There are five neutron-absoring shim-safety plates in the TSR-II, each of which scrams independently due to a spring force. If the positioning spool in any of the five mechanisms were to bind, the drive motor which drives the positioning spool in all five mechanisms will stall. To keep

foreign material out, the water to the control mechanisms is filtered twice, once at the pump house and again at the reactor, with filters which remove particles down to 3.5 mils. Each of five control mechanisms is so designed that the force of the shutdown spring is balanced by a hydraulic pressure differential across a piston and no load can be transmitted to the positioning spool (see Section 3.6 Vol. 1). Even if the drive motor fails to operate, all five neutron-absorbing shim-safety plates will still scram independently due to the action of the spring on each control mechanism and any one of the plates will shutdown the reactor. The performance of each shim-safety plate is checked periodically and no significant change in performance has been noted for any plate since the reactor has been in operation.

3.1.4. Void Formation

Void formations in all regions of the core except the region internal to the fueled cover plates on the control mechanism housing produce negative reactivity effects As described below it is not credible for any sizeable void to be maintained inside the control mechanism housing without void formations also existing in the core proper and the next reactivity effect is negative.

The measured void coefficient of reactivity in the water inside the control mechanism housing is $+1.06 \times 10^{-6}$ $\Delta k/k$ per cubic centimeter, which is a conservative value (see Section 4.1.6 of Vol. 1). The region contains 20,000 cc of water, which includes the volume inside the control mechanisms and tubing. Conceivably, water pumped into the region could contain voids or voids could be created by excessive heating.

The maximum heat generation inside the control mechanism housing is 8.8 kW (see Appendix C). It is necessary to maintain a water flow rate of 5.5 gpm to the control mechanisms in the housing to keep the reactor critical. Thus the temperature rise cannot exceed $11.0^{\circ}F$ unless the main cooling flow is lost, in which case boiling would occur in the regions exterior and interior to the control mechanism housing.

Assuming that the water inside the housing is completely and quickly removed and that an equal void volume were established just outside the fuel loaded cover plates and extending into the fuel elements, the net effect would be a reactivity reduction of 0.37×10^{-2} $\Delta k/k$. The measured

negative void coefficient (-6.3×10^{-7} $\Delta k/k$ per cc) was used for the unfueled volume outside the housing and the calculated negative void coefficient (-1.5×10^{-6} $\Delta k/k$ per cc) was used for the void that extended into the core proper (see Void Coefficients, Vol. 1).

Two pumps supply water to the region under discussion: the shim pump supplies 5.5 gpm to operate the control mechanisms and an additional 14.5 gpm to cool the control mechanism housing, and the main pump supplies less than 2 gpm of water to operate the seat switches. Float-operated bleed valves (see Fig. 6.1 in Vol. 1) in the shim line at the 120-ft level in tower leg I and at the top of the reactor turret remove any air bubbles that might be trapped in the shim supply line. Even if air were to reach the control turret, air directed to the control mechanisms would reduce resistance to the spring-actuated shim plates and cause a shutdown before more than a few hundred cc of air could enter. An average reactivity ramp of $+0.127 \times 10^{-2}$ $\Delta k/k$ per second would result if air were added to replace the water at a rate of 19 gpm. The probability of a critical reactivity addition from this mechanism is very low because of the inherent shutdown action of the control mechanisms with air addition; the protection afforded by the protection system; the low probability of air reaching the control turret; and the tendency of air to escape from the control mechanism housing. The 2-gpm total flow of water to the seat switches is too small to be of any consequence in introducing voids.

3.1.5. Cold-Water Slug

The possibility of a slug of cold water entering the reactor is minimized by reactor control interlocks. The reactivity effect that would accompany any conceivable reduction in the inlet cooling water temperature is shown to be very slow and easily counteracted by the protection system (see Appendix A).

If the reactor could be started with little or no cooling water flow, it is conceivable that the water in, say, the air coolers or the holdup tank would be at a lower temperature than the water in the rest of the system. Initiation of flow would then cause a cold slug of water to enter the core. Since the control system interlocks require that the cooling water be pumped through the reactor at the maximum rate for 3 min before

the reactor can be started, any large changes in water temperature would be displayed for the operator. Nevertheless, analog studies were made to determine what would happen if the water leaving the air coolers was well below the operating temperature. The studies showed that the reactivity effect of the slug of cold water would stretch out in time so that the power level would increase at a slow rate and that the neutron level sensors would trip the protection system at 150% of maximum permissible power seconds before the fuel plate temperature reached the saturation temperature in the core. Thus in the actual case the power swing would be reversed by a fast shutdown, and no excessive heating or damage would occur.

3.1.6. Core Structural Changes

The probability of a reactivity accident due to core structural changes is virtually nil while the reactor is in service. The reactor core is located at the lower end of a closed pressurized tank so that the fuel elements are not accessible for manipulation. Furthermore, the geometry of the fuel in the core is fixed and all the volume in the core is occupied so that inadvertent movement is not likely.

The metal-to-water ratio of the core was optimized so that any change in the ratio would make the reactor less critical. Thus if the reactor is compressed so water is removed or if the core starts to expand, the reactor becomes less critical.

Regularly scheduled measurements are made of the worth of the regulating plate and the operating position of the shim-safety plates is recorded to ensure that no unexpected change has been caused by burnout of the boron, packing and settling of the boron carbide powder, or development of holes in a stainless steel control plate, followed by spilling or leaching of the powder.

A significant possibility of generating a reactivity accident occurs only when the reactor is in a dismantled state. Dismantling and reassembly are performed with the reactor at ground level and are adequately covered in maintenance procedures. The four upper central fuel elements, which must be removed before the control housing can be removed, contain 17% of the fuel,

and their removal leaves the reactor many dollars subcritical, even after the control housing has been removed. The hazard is associated with the possibility of accidental insertion of one of the upper central elements before the control housing is reinstalled. If an element were lowered to the center of the reactor, a region of high importance, a nuclear excursion would result. The amount of excess reactivity that would be introduced in this way is not known, but in the initial critical experiments it was shown that the reactor would be critical in this abnormal configuration with the water level only a little above the core mid-plane.

Such an accident, which appears to be the only way that fuel handling could cause trouble, will be diligently guarded against by reviewing maintenance procedures each time a control mechanism housing is removed and a new one installed.

3.1.7. Shield Configuration Changes

No dangerous reactivity effects can occur due to shield changes with the presently available shields. The reactivity worths measured for various shield configurations are given in Table 3.1.

When a new shield is to be installed around the reactor or when the configuration is changed in any other way that could influence reactivity, a critical experiment will be made according to procedures in the Tower Shielding Facility Manual. The TSR-II will not be operated with the excess reactivity exceeding 1.9×10^{-2} $\Delta k/k$, which is approximately half the worth of the shim-safety plates.

3.2. Changes in Core Cooling

The action of the instrumentation for operation and protection of the reactor will prevent damage from loss of heat sink or loss of coolant flow. The loss of some coolant from the system is a minor problem. Loss of all coolant from the reactor requires a catastrophic failure which is very improbable.

3.2.1. Loss of Heat Sink

The heat sink of the heat removal system consists of a forced-draft water-to-air heat exchanger in which two large variable-pitch fans blow

Table 3.1. Reactivity Change Associated with Shield Changes

Shield Configuration	Abbreviated* Nomenclature	Reactivity Change $(\frac{\Delta k}{k})$ from Bare Reactor in Water
Lead-Boral Reflector Replaced with a 3/4-in.-Thick Aluminum Shell		
Bare reactor in air	Bare A3	-0.31×10^{-2}
Bare reactor in water (nominal case)	Bare B3	0.0
Reactor in beam shield	Beam A3	-0.08×10^{-2}
Reactor in beam shield with water drained from shield	Beam B3	-0.05×10^{-2}
Cool-I shield (1 1/2 in. lead) in air	CI-C3	-0.01×10^{-2}
Cool-I shield in water	CI-D3	$+0.09 \times 10^{-2}$
Cool-II shield in air	CII-A3	$+0.05 \times 10^{-2}$
Cool-II shield in water	CII-A4	$+0.14 \times 10^{-2}$
Lead-Boral Reflector in Place Around the Core		
Bare reactor submerged in water	Bare B1	-0.21×10^{-2}
Bare reactor in air	Bare A1	-0.29×10^{-2}
Reactor in beam shield	Beam A1	-0.04×10^{-2}
Reactor in beam shield with water drained from shield	Beam B1	$+0.16 \times 10^{-2}$
Lithium hydride shield	PW-A1	$+0.07 \times 10^{-2}$
Fuel in water (reference only)	Bare B6	$+0.17 \times 10^{-2}$

*For a description of the abbreviated nomenclautre, see Appendix A, Volume 1 of the Design and Operating Report.

air across aluminum tube-and-fin radiators. Fan blade pitch can be automatically controlled to maintain a constant exit temperature from the heat exchanger. To prevent freezing damage, louvers have been installed in the radiators which close automatically when the water temperature drops to a preset value. Reduction in air flow across the radiators would result in a water temperature rise at the core inlet. When the core outlet temperature reaches 150°F, the reactor would be shut down. Since the maximum core temperature would still be well below the saturation, no damage would occur.

3.2.2. Loss of Coolant Flow

The reactor protection system will automatically scram the reactor if the water flow rate through the core becomes less than 500 gpm or if the pressure drop across the reactor falls below that equivalent to the 500-gpm flow rate. Also an annunciator would alarm when the coolant temperature rise across the core reaches 12°F and a reactor shutdown would occur when it reaches 14°F. Analog studies (see Appendix A) have shown that the time lag is of the order of seconds between cessation of water flow and elevation of the fuel temperature to the water saturation temperature for 10-psig overpressure. Therefore there is more than adequate time for the protection system to shut down the reactor before any core damage could occur if flow were to cease.

3.2.3. Loss of Coolant

Although it is not possible to drain all the water from the reactor pressure vessel, loss of some water from the reactor pressure vessel could result from rupture of the hoses or pipes supplying cooling water. Any break in the system which causes a reduction in water flow through the reactor causes a reactor shutdown as noted in Section 3.2.2. Any break, however, causes a reduction in the base pressure which operates two annunciators to alert the operator so that he may take any action that is necessary. If the rupture started a syphoning action, the syphoning would be stopped when the water level reached the lower end of the central cylinder from which the reactor core is suspended. If the syphoning action resulted from a break in the outlet cooling hose, additional cooling water could be added to the core through the inlet hose. if the break occurred in the

inlet hose, water could be supplied to the core through the shim pump line. Furthermore, the heat capacity of the core, including trapped water, would limit fuel temperatures to below the point at which any fuel element melting would occur.

If the reactor were dropped from an elevated position, the coolant lines to the reactor would undoubtedly be severed and it is possible that all of the coolant water would be drained from the pressure vessel. It is also possible, depending on the manner in which the accident proceeded, that water would remain in some enclosures in the pressure vessel, e.g., in the chamber wells, in the lead-water shield, or in some portion of the pressure vessel itself. The probability of an accident which would result in a dropped core is discussed in the following section.

3.3. Dropped-Core Accident

A failure of the reactor suspension system, comprised mainly of the tower legs, suspension cables, and connectors, could initiate a dropped-core accident. An independent stress analysis indicated that there is a very low probability that the reactor will be dropped because of mechanical failure. Current operating and maintenance practices further reduce this probability. Prescribed Federal Aviation Agency requirements have been met to alert low flying aircraft to avoid the structure.

The design of the suspension system[3] required conventional safety factors of 3 to 6 in all components except the tower structure. Since the intended use of the towers required that there be a minimum amount of neutron and gamma-ray scatter from the steel in the towers, the towers were designed to have a minimal but adequate safety factor for the worst conceivable condition. This worst condition was for a wind loading of a 105 mph, a wind velocity that has not been observed in this area.* Operating

---

*The highest wind mile reported over a 40-year period in the Knoxville area prior to the erection of the TSF was 71 mph.[4] Through December 1966, the highest wind velocity in the area was 73 mph on July 6, 1961. From January 1, 1956 through July 31, 1970 the wind velocity at the TSF site has exceeded 60 mph on the average of once a year with a maximum of 78 mph occurring on February 25, 1956.[5]

procedures[6] have been developed to prevent situations that may impose unusual loads or service conditions, and inspection procedures[7] have been developed to provide means of detecting any deterioration or change in the suspension system with time.

Operating stresses in the tower suspension system and TSR-II components have been reviewed and checked in an independent ORNL stress analysis.[8] The study re-examined stress levels in the tower legs to determine the effect of changing the live load (TSR-II in place of the original TSR-I) and in changes in the wind load resulting from additions to the tower area and a higher assumed wind pressure. From this analysis, which is summarized below, it is concluded that there is a very low probability that the reactor will be dropped because of a mechanical failure.

The minimum yield stress for structural grade steel (ASTM-A7 carbon steel) is 33,000 psi. The allowable unit stress for the TSF calculated with a formula recommended by the American Institute of Steel Construction (A.I.S.C.) in "Specifications for the Design, Fabrication, and Erection of Structural Steel for Buildings," is 14,400 psi for normal conditions. The AISC specifications permit the allowable stress to be increased to 19,200 psi when wind forces are considered.

In the recheck of the original calculations, the maximum stress in a tower leg considering the static load (tower weight plus prestressing on guy wires) and the effect of supporting a 55-ton reactor and shield elevated to 185 ft* midway between tower legs I and II is only 10,487 psi. This is well below the 14,400 psi for normal conditions.

In the original engineering calculations[3] it was found that the maximum stresses were created during wind loading on the entire structure. For a 30-psf wind load (105 mph) they calculated a maximum stress of 19,978 psi, which exceeds slightly the 19,200 psi but is well below the 33,000 psi. In the review of these calculations,[8] minor items that were neglected in the

---

*The cables which support the reactor extend from the top of tower legs I and II to a pear shaped ring and the reactor is suspended from the ring. With a short suspension from the ring a 55-ton load can be lifted to an elevation of 200 ft. The TSR-II suspension system is such that the elevation of the reactor is limited to 185 ft. The stress in the tower legs, however, is the same.

original calculations or items that were added since the original construction increased the maximum stress to 23,572 psi. If the assumed wind velocity were reduced from 105 mph to 80 mph, the maximum calculated tower leg stress would not exceed the allowable AISC stress with the reactor hoisted.

In the review an additional calculation was made using the "American Standard Building Code Requirements for Minimum Design Loads in Buildings and Other Structures" (ASA A58.1-1955). This code requires a greater shape factor, a larger projected area and a higher wind load (40 psf above 100 ft, which is equivalent to a 120-mph wind velocity) all of which resulted in a maximum stress of 27,822 psi. This value, which is based on an unusual high wind velocity, is still below the minimum yield stress. The reactor, however, is not elevated for operation whenever wind speeds exceed 40 mph. When there is thunderstorm activity in the locality which may be accompanied by high wind gusts, the TSF operators use weather radar to observe the course and speed of thunderstorms and then lower the reactor if a storm is expected to cross the TSF area.

The probability of a dropped-core accident obviously cannot be quantitatively determined since adequate "failure rate" type of data does not exist for the suspension system components. The many years of successful operation of the TSR-I and TSR-II from the reactor suspension system verify that the basic design and operation procedures have been adequate to date. The inspection procedures and techniques in use with the TSR-II have been made as exhaustive and extensive as practical, especially for the hoist equipment and cables. Therefore factors that contribute to the overall reduction in the probability of a dropped-core accident are (1) a design which allows a generous margin between working stresses and yield stresses in structural and hoist components for all hoist operation with moderate wind velocity, (2) operating procedures which prohibit hoisting the reactor from a secure position when the wind velocity is above 40 mph and lowering it from the maximum elevated position when the possiblity exists of winds approaching 80 mph (e.g. during thunderstorms), (3) inspection and maintenance of the suspension system which enables significant deterioration of the system's strength capabilities to be detected and corrected, and (4) prudent operation of the hoists. A subjective evaluation of these

factors, which is the only evaluation procedure one has, leads to the conclusion that there is a very low probability that the reactor will be dropped because of a catastrophic failure of the suspension system during the useful life of the TSR-II. It is, however, one of the conditions necessary for the maximum credible accident discussed in Chapter 4.

3.4. Fission-Product Release

Fission-product release can result in minor contamination or in a major accident. The first category, leakage of fission products from one or several fuel plates, is discussed below. A major accident, which would be the meltdown of several percent of the core when it contains a heavy inventory of fission products, is discussed in Chapter 4, even though it is shown in Chapter 6 that such an accident is not deemed credible.

Leakage of fission products from fuel plates could result from several types of core fabrication errors such as inadequate clad bonding, improper fuel plate spacing, or inclusions in the aluminum cladding. During the ten years of operation at powers up to 100 kW, there has been no detectable fission-product leakage from the TSR-II core. The TSR-II system is capable of handling fission-product leakage from a defective fuel element as described below.

A fission-break monitor is located in a small by-pass line between the heat exchanger inlet and the suction of the main pump. The gamma-sensitive monitor* is set to annunciate on a significant rise in count rate above background from induced sodium activity in the cooling water. If fission-product activity were detected by the fission-break monitor, the reactor would be shut down manually by the reactor operator. No automatic shutdown by the control system or safety system is provided in the TSR-II on indication of fission-product activity in the cooling water since a rapid power reduction would not be expected to significantly decrease the amount of fission-product leakage resulting from a cladding failure. Particulate fission products would be contained in the closed cooling water system and most of the gaseous fission products (Kr, Xe, I) would be entrapped in

*Victoreen Model No. 900-69.

the cooling water as long as full flow is maintained. When the cooling water flow is stopped, some of the gaseous fission products may migrate to float-operated vent valves and escape to the atmosphere.

Contaminated cooling water can be dumped into the 5000-gal holding water system, and the contamination can be subsequently handled with adequate safeguards.

The amount of fission products that would be released if fuel elements were damaged in handling or in a dropped-core accident is not significant. In a study conducted by the ORNL Reactor Chemistry Division to measure the release of fission products from U-Al fuel plates at elevated temperatures, samples were sheared from irradiated fuel plates.[9] Measurements indicated that the amount of fission products released during the shearing operation was infinitesimal.[10]

REFERENCES

1. L. B. Holland, Tower Shielding Reactor-II, Design and Operation Report, Vol. I, ORNL-TM-2893.
2. S. G. Forbes et al., Analysis of Self-Shutdown Behavior in the Spert I Reactor, IDO-16528 (July 1959).
3. Knappen-Tibbets-Abbett-McCarthy (KTAM), Design Calculations, (unpublished) (1953).
4. Completion Report on the Tower Shielding Facility by the Engineering and Mechanical Division, CF-55-1-165 (February 11, 1955).
5. Personal communication from Barlow H. Goad, USAEC Weather Bureau, to L. B. Holland, September 28, 1970.
6. L. B. Holland, TSF Procedures Manual (limited distribution).
7. Programmed Maintenance TSF (limited distribution).
8. T. W. Pickel et al., Review of Stress Calculations for the TSR-II, (unpublished report) (May 27, 1963).
9. G. W. Parker, G. E. Creek, W. J. Martin, and R. A. Lorenz, "Release of Fission Products on Out-of-Pile Melting of Reactor Fuels," Nuclear Safety Program Semiannual Progress Rept. Period Ending June 30, 1963, ORNL-3483 (September 3, 1963).
10. Personal communication G. W. Parker to L. B. Holland October 7, 1970.

4. MAXIMUM CREDIBLE ACCIDENT

Three conditions must exist before a Maximum Credible Accident (MCA) could occur in the TSR-II: (1) maximum fission-product inventory in the core, (2) maximum afterheat in the core, and (3) complete loss of coolant from the core. The fission-product inventory will be limited by limiting the total fuel element exposure to 3000 MWhr (see Chapter 5).

The initiating incident of the MCA is assumed to be that the reactor has been dropped and all the water has been lost from the pressure vessel; the latter assumption is conservative because some water will adhere to the fuel plate surfaces and some will be trapped in the lead shot above the core.* Such an improbable accident appears to be the only mechanism whereby water flow could be interrupted and all water drained from the core (see Sections 3.2 and 3.3). One would expect the major extent of damage from a dropped-core accident to be confined to the pressure vessel and shield. The fuel sections and control mechanism housing are rigidly assembled, and so would be expected to move as a unit. Any metal-to-metal contact between the fuel plates and the supporting structure would enhance heat conduction, but no credit is taken for this. The meltdown calculations are also conservative in that the value of the afterheat generation was always greater than the actual value, the values for the heat capacity and the heat conduction were selected on the low side, and finally the surface area to remove heat was less than half the actual pressure vessel surface area.

---

*The effect of water adhering to surfaces was noted in experiments to measure the temperature rise of U-Al fuel elements under loss of cooling water conditions.[1,2] The temperature rise levels off momentarily at the boiling temperature of water indicating that some water adheres to the fuel elements.

Measurements with a single TSR-II element that was lifted from a water bath and allowed to hang vertically to drain in dry moving air for over a minute indicate that over 3/4 lb of water would remain in the fuel elements. Similarly, measurements indicate over 13 lb of water would be retained in the lead shot above the fuel elements after the water is drained. A considerable amount of water would also remain on the several hundred square feet of aluminum surface inside the pressure vessel and in the control mechanism pockets and small diameter tubes leading to the control mechanisms.

BLANK PAGE

If the reactor were operating, shim-safety plate action from loss of water pressure at the control mechanisms would reduce reactivity by 2.0×10^{-2} $\Delta k/k$ in 160 msec and shutdown the reactor (see Section 3.1). Also, scram signals would result from loss of cooling water flow or from a low pressure drop across the reactor core. In any case the loss of water moderator would make the reactor inoperative.

With no water coolant available, core temperatures would rise initially but for the 1 MW operation proposed (see Chapter 6) would not reach melting because of convection heat losses and available heat capacity. For purposes of the MCA analysis, however, an instantaneous release of fission products from a melted portion of the core volume is assumed. Also, fission products released from the fuel are assumed to have been released directly to the atmosphere with no deposition on fuel plate or pressure vessel surfaces.

Calculation of maximum off-site doses following the MCA have been based on the conservative assumptions that are summarized below:

Type of release	Instantaneous cloud
Release fraction from melted fuel	Halogens, 50%; noble gases, 100%; bone-seeking nonvolatiles, 1%
Release height above exposure elevation	Zero
Atmospheric dispersion conditions	Moderate inversion or weak lapse from instantaneous ground-level source
Ground deposition	Maximum washout from neutral atmospheric conditions (see Table 5.7)

These assumptions constitute a model for the fission-product release, dispersion, and exposure conditions following the MCA of the TSR-II. It should be noted that the atmospheric dispersion and ground deposition conditions were selected to give the highest dose rates.

As described in Chapter 6 there would be no melting of the fuel in the preceding accident and therefore personnel at the exclusion boundary and at the TSF would not be exposed to radiation from fission product release.

References Chapter 4

1. J. A. Cox and C. C. Webster, Water Loss Test at the Low-Intensity Testing Reactor, USAEC Report ORNL-TM-632, Oak Ridge National Laboratory (August 14, 1964).

2. R. M. Summerhays, "Afterheat Experiments with the ASTRA," paper No. FZM-1012, presented at the Second Winter Meeting of the American Nuclear Society, New York, October 28-30, 1957.

5. FISSION-PRODUCT RELEASE FOR MAXIMUM EXPOSURE AT THE SITE BOUNDARY

The maximum doses following an MCA are established[1] as 300 rem to the thyroid and 25 rem to the whole body in 2 hr at the exclusion boundary or at the "low-population" zone boundary. A study was made to determine how much of the core could melt before these maximum dose limits would be reached. The study involved investigation of two operation schemes at 1 MW thermal power for a core life of up to 3000 MWhr.

5.1. Fission-Product Release Fractions

It was assumed that the fractional release values for melted fuel plates would be 100% of the noble gases, 50% of the halogens, and 1% of the controlling bone-seeking nonvolatiles (Sr, Y, Zr, Nb, Ba, La, Ce, Pr, and Nd). These release fractions were taken from TID-14844[2] and, for low fuel burnup, are conservative in comparison with the data of Parker *et al.*[3] Burnup of the ^{235}U in the TSR-II elements in this study is assumed to 1.5% which is equivalent to 3000 MW hr of operation.

5.2. Fission-Product Inventories

Fission-product inventories were conservatively estimated for the following two operating modes: 1 MW for 8 hr each day and continuous operation at 1 MW for 1000 hr. Two methods were used to estimate fission-product inventories for cyclic operation: for long-lived fission products (half-lives greater than 11 days), the inventories were estimated from the data of Blomeke and Todd[4] for continuous operation at 3000 hr at 1 Mw; for shorter lived fission products, inventories were estimated by the method of Burnett,[5] which assumes an infinite number of cycles. Both methods tend to over estimate the fission-product inventories: in the method of continuous buildup the fission-product decay during reactor shutdown periods is neglected, and in Burnett's method the fission product buildup is assumed to have reached equilibrium. Inventories were estimated for the fission products listed in Table 5.1. The formulas

BLANK PAGE

Table 5.1. Fission Products Listed According to Type and to Half Life

Fission products with long half lives	
Noble gases*	10.3-y ^{85}Kr, 12-d ^{131m}Xe
Nonvolatiles	51-d ^{89}Sr, 28-y ^{90}Sr, 58-d ^{91}Y, 63-d ^{95}Zr, 12.8-d ^{140}Ba, 33-d ^{141}Ce, 282-d ^{144}Ce, 11-d ^{147}Nd
Short-lived fission products with half lives long compared with those of their precursors	
Halogens	8.1-d ^{131}I, 20-h ^{133}I, 6.7-h ^{135}I
Noble gases	4.4-h ^{85m}Kr, 15.6-m ^{135m}Xe, 9.2-hr ^{135}Xe, 2.3-d ^{133m}Xe, 5.3-d ^{133}Xe, 2.8-h ^{88}Kr
Nonvolatiles	17-h ^{97}Zr, 32-h ^{143}Ce
Short-lived fission products with half lives comparable with those of their precursors	
Halogens	2.4-h ^{132}I, 53-m ^{134}I, 114-m ^{83m}Kr
Nonvolatiles	35-d ^{95}Nb

*78-m ^{87}Kr and 3.2-m ^{89}Kr are assumed to saturate within 4 hr.

Burnett developed for estimating the short-lived fission product inventories are given below:

$$A_d = \frac{A_{s,d}(1 - e^{-\lambda_d t})}{1 - e^{-\lambda_d(\tau+t)}}, \tag{1}$$

$$A_d = A_{s,p}\left\{\frac{\lambda_d}{\lambda_d-\lambda_p}\left(1 - e^{-\lambda_p t}\right)\left(\frac{1}{1 - e^{-\lambda_p \tau}} - \frac{1}{1 - e^{-\lambda_d \tau}}\right)\right.$$

$$\left. + \left[\frac{\lambda_d}{\lambda_d-\lambda_p}(1 - e^{-\lambda_p t}) - \frac{\lambda_p}{\lambda_d-\lambda_p}(1 - e^{-\lambda_d t})\right]\frac{1}{1 - e^{-\lambda_d \tau}}\right\} \tag{2}$$

where

A = activity, curies,

t = operating time per cycle,

τ = time for cycle (24 hr),

s = saturation,

p = parent,

d = daughter,

λ = decay constant.

Halogens - Activities of ^{131}I through ^{135}I are required to calculate thyroid and submersion doses. Specific dose factors, D(rem/inhaled μcurie), were obtained for thyroid exposure by revising Burnett's[5] D values using inhalation dose data of the 1959 report of the International Commission on Radiological Protection (ICRP).[6] The revised D value for ^{131}I was 1.484 rem/inhaled μcurie; ratios of D values of other iodine isotopes to that of ^{131}I are listed in Table 5.2. These ratios were used as weighting factors on the iodine activities to obtain an equivalent ^{131}I activity for calculation of thyroid dose. Activities of the individual and totaled equivalent ^{131}I inventories are shown in Table 5.2 for the two operating cycles specified above. For subsequent submersion dose calculation, Table 5.3 contains effective energy data, E_s, from Blomeke and Todd and also individual iodine inventories.

Table 5.2. TSR-II Iodine Data for Thyroid Dose

Isotope	$D_i/D_{^{131}I}$ Dose Relative to ^{131}I	Equivalent Curies of ^{131}I At 1 MW, 8 hr/day[a]	Equivalent Curies of ^{131}I At 1 MW for 1000 hr[b]
		X 10^4[c]	X 10^4[c]
^{131}I	1.0	0.86	2.5
^{132}I	0.036	0.047	0.14
^{133}I	0.269	0.62	1.5
^{134}I	0.017	0.11	0.11
^{135}I	0.083	0.26	0.42
		1.9	4.7

[a]Data are for an infinite number of cycles.

[b]All iodine isotopes reach saturation.

[c]Multiplying factor for equivalent curies.

Table 5.3. TSR-II Iodine Data for Submersion Dose

Isotope	E_s[a] (MeV/dis)	Core Inventory, Q(curies)		$E_s Q$ (MeV curies/dis)	
		At 1 MW, 8 hr/day	At 1 MW for 1000 hr[b]	At 1 MW, 8 hr/day	At 1 MW for 1000 hr
		X 10^4[c]	X 10^4[c]	X 10^4[c]	X 10^4[c]
^{131}I	0.58	0.86	2.5	0.50	1.5
^{132}I	2.4	1.3	3.8	3.2	9.3
^{133}I	1.0	2.3	5.5	2.3	5.5
^{134}I	1.9	6.5	6.6	12.0	12.0
^{135}I	1.9	3.1	5.0	5.7	9.3
				24	38

(a) $E_s = E_\gamma + 1/3\ E_\beta$.

(b) All iodine isotopes reach saturation.

(c) Multiplying factor for equivalent curies.

Noble Gases. - Calculated inventories of krypton and xenon are listed in Table 5.4. For ^{133}Xe and ^{135}Xe, fractions from the precursors ^{133}I and ^{135}I were conservatively assumed. Values of the effective energy E_s for these noble gases are also listed for subsequent submersion dose calculation. The isotopes ^{87}Kr, ^{88}Kr, and ^{89}Kr contribute 80% or more of the dose from all the noble gases considered.

Nonvolatile Fission Products. - Inventories of nonvolatile fission products are shown in Table 5.5. The data in the last column represent the specific bone dose factors, D, corrected again for 1959 ICRP data,[6] combined with the fission-product inventories and a 1% release fraction. The isotopes making the major contributions to the bone dose are ^{89}Sr, ^{90}Sr-Y, ^{91}Y, ^{140}Ba-La, and ^{144}Ce-Pr.

5.3. Atmospheric Dispersion Conditions and Calculations

The climatology and meteorology of the TSF site are discussed in Section 2.2, where data are also included on inversion duration, wind roses, and climatology. Predominant wind flow is shown to follow a NE-SW pattern during nocturnal inversion conditions, with increased wind flow to the W-SW direction during daytime lapse conditions. Therefore the major population centers of Oak Ridge and Knoxville do not lie in the path of the predominant wind flow from the TSF site.

In the event of an MCA, fission products released from melted fuel are assumed to be dispersed in the atmosphere as an instantaneous point source. Even though much of the terrain along the AEC security fence south of the TSF is 300 to 400 ft lower in elevation than the TSF, the atmospheric dispersion conditions discussed below were chosen to estimate χ/Q' (defined below) from a ground-level, instantaneous point source at a distance of 1000 m.

Radioactive cloud concentrations downwind from an instantaneous point source were estimated with the dispersion models of Sutton[7] and of Pasquill[8] and Meade.[9] The Pasquill-Meade model was used in addition to the traditional Sutton model because it has greater fidelity with experimental results at distances greater than 1 km, and also so that

Table 5.4. Krypton and Xenon Inventories for TSR-II

Isotope	E_s (MeV/dis)	Q(curies) At 1 MW, 6 hr/day	Q(curies) At 1 MW for 1000 hr	$E_s\dot{Q}$ (MeV curies/dis) At 1 MW, 6 hr/day	$E_s\dot{Q}$ (MeV curies/dis) At 1 MW for 1000 hr
		X 10^4[a]	X 10^4[a]	X 10^4[a]	X 10^4[a]
^{83m}Kr	0.042	0.31	0.42	0.013	0.017
^{85m}Kr	0.041	0.95	1.3	0.39	0.54
^{85}Kr	0.23	0.006	0.0018	0.0014	0.00042
^{87}Kr	1.6	2.4	2.4	3.8	3.8
^{88}Kr	2.4	2.8	3.1	6.7	7.4
^{89}Kr	1.3	4.0	4.0	5.2	5.2
^{131m}Xe	1.6	0.026	0.019	0.0042	0.0031
^{133m}Xe	0.23	0.049	0.13	0.011	0.030
^{133}Xe	0.20	2.7	5.7	0.53	1.1
^{135m}Xe	0.52	1.5	1.6	0.78	0.83
^{135}Xe	0.57	2.8	4.4	1.6	2.5
				19	21

[a]Multiplying factor for equivalent curies.

Table 5.5. TSR-II Bone Dose Data

Isotope	Specific Dose Factor (rem/inhaled μcurie)	Q(curies) At 1 MW, 8 hr/day	Q(curies) At 1 MW for 1000 hr	fDQ(rem)[a] At 1 MW, 8 hr/day	fDQ(rem)[a] At 1 MW for 1000 hr
		X 10[4][b]	X 10[4][b]		
^{89}Sr	0.418	3.3	1.7	140	71
^{90}Sr	44.55	0.043	0.014	190	62
^{91}Y	0.336	4.0	1.9	130	64
^{140}Ba	0.0896	5.4	4.6	48	41
^{141}Ce	0.0199	4.8	2.9	9.6	5.8
^{143}Ce	0.0228	2.1	5.3	4.8	12
^{144}Ce	1.446	1.4	0.49	200	71
^{95}Zr	0.0617	4.1	2.0	25	12
^{95}Nb	0.0132	2.1	0.66	2.8	0.87
^{97}Zr	0.0055	2.4	5.2	1.3	2.9
^{147}Nd	0.0149	2.3	2.1	3.4	3.1
				760	350

[a] f = 1% release fraction.

[b] Multiplying factor for equivalent curies.

the results obtained with the two models could be compared by using meterological parameters applicable to the TSF site.

The downwind fission-product concentration for an instantaneous ground-level point source based on the Sutton model[10] was calculated as follows:

$$\frac{\chi}{Q'} = \frac{2}{\pi\bar{\mu}C_y C_z X^{2-n}} \quad ,$$

where

χ = curie sec/m^3,

Q' = curies of fission product released,

C_y, C_z = vertical and cross wind virtual diffusion coefficients, $m^{n/2}$,

$\bar{\mu}$ = average wind speed, m/sec,

X = downwind distance, m, from release point,

n = stability parameter, dimensionless.

Values for the Sutton dispersion parameters in Table 5.6 were chosen from previous recommendations of the Oak Ridge Weather Bureau[11,12] for the ARE and EGCR reactors in Melton Valley.

The Pasquill-Meade model is employed by choosing a meteorological condition for which dispersion parameters have been observed as a function of downwind distance.[13] These meterological conditions are given in Table 5.7, along with the percentage of the time that such a condition will exist.[14] The predominant meteorological condition is a slightly unstable one, C, while the worst dispersion condition, F, is estimated to occur 10% of the time. Categories C and F were therefore chosen to represent the most likely and the worst atmospheric dispersion conditions, corresponding to the weak lapse and moderate inversion Sutten dispersion conditions. The decreasing magnitude of the group, $(\bar{\mu}\chi/Q')$, with increasing downwind distance is shown in Fig. 5.1 for all the Pasquill-Meade meteorological categories.

Table 5.6. Sutton Dispersion Parameters for TSF Site

Meteorological Condition	Parameters		
	$\bar{\mu}$ (m/sec)	n	$C_y C_z$ ($m^{n/2}$)
Moderate inversion	1.5	0.35	1×10^{-2}
Weak lapse	2.3	0.23	9×10^{-2}

Table 5.7. Meteorological Conditions in the Oak Ridge Area

Meteorological Condition[a]	Occurrence (%)[b]
Extremely unstable, A	0
Moderately unstable, B	8
Slightly unstable, C	40
Neutral, D	20
Slightly stable, E	22
Moderately stable, F	10

[a]Applicable to heavy overcast day or night, see Reference 9.

[b]See Reference 12.

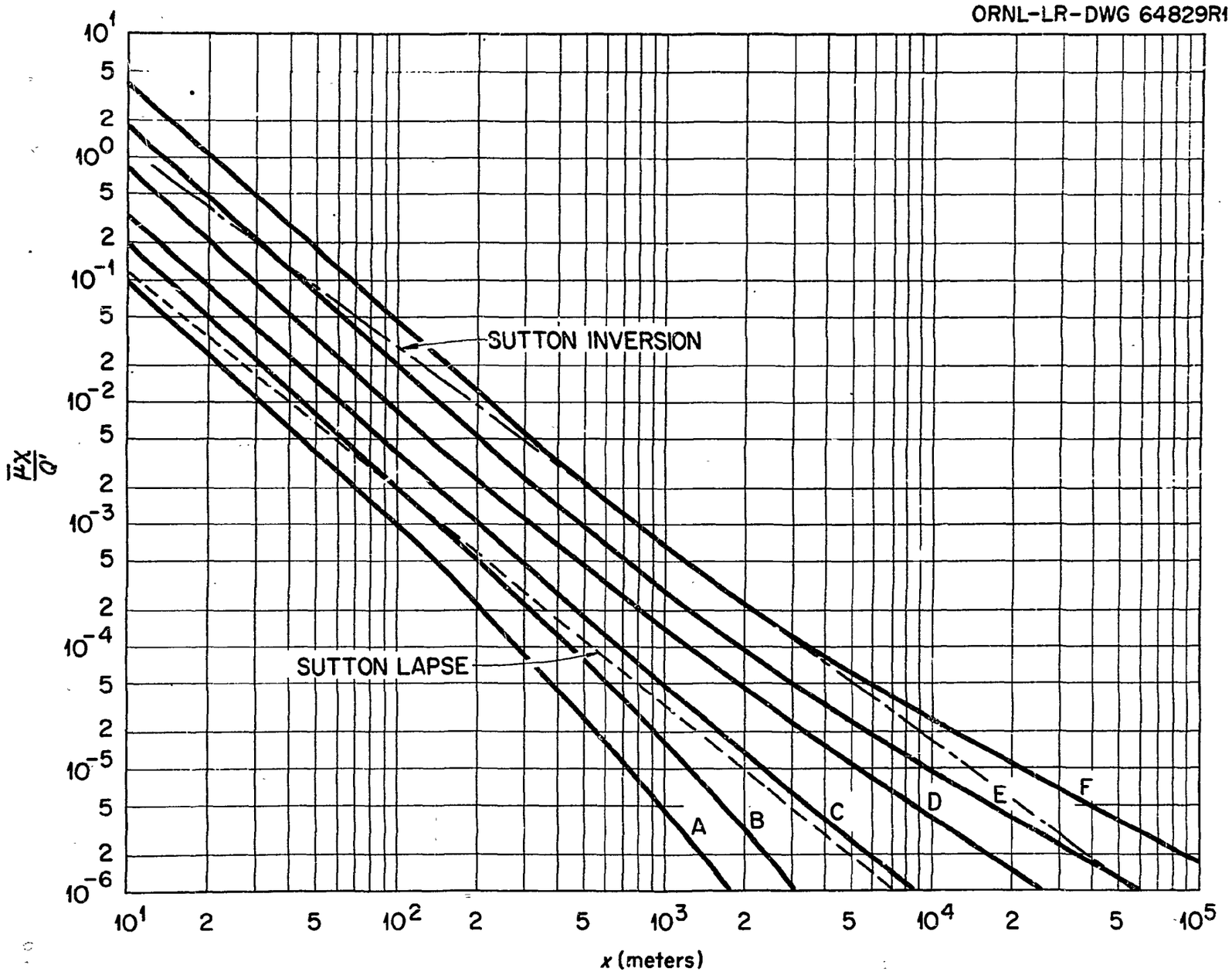

Fig. 5.1. Values of $\frac{\bar{\mu}\chi}{Q'}$, as a function of downwind distance, χ, for various weather types; source at surface (see Table 5.7 for weather types).

From Fig. 5.1 it is seen that at 10^3 m downwind distance the value of (χ/Q') from Sutton's model and from the Pasquill-Meade model is essentially the same for inversion conditions (F), whereas the Pasquill-Meade model for category C gives slightly higher results than the Sutton model. Numerical results for (χ/Q') at 10^3 m are summarized in Table 5.8, with average wind speeds $(\bar{u})$ of 1.5 and 2.3 m/sec used for inversion and lapse conditions, respectively.

The (χ/Q') results from Pasquill-Meade's model were used to calculate the following exposure doses.

5.3.1. Inhalation Doses

Thyroid. - Calculation of the thyroid dose at the 10^3 m distance follows from the relation

$$\text{dose (rem)} = fDQI \frac{\chi}{Q'} \times 10^6 \quad ,$$

where

D = specific dose factor for ^{131}I
  = 1.484 rem/inhaled μcurie,

I = inhalation rate
  = 5×10^{-4} m^3/sec (30 liters/min),

Q = equivalent curies of ^{131}I present, or core inventory,

f = fraction released of available fission product.

Using a release fraction of 50% and the equivalent ^{131}I inventories in Table 5.2, the thyroid doses calculated for the specified operation are shown in Table 5.9. The allowable core melting fraction for a maximum allowable thyroid dose of 300 rem was obtained from the ratio of 300 rem to the calculated dose. Thus allowable melting fractions (see Table 5.10) are 0.036 and 0.80 for 1-MW operation for 1000 hr with inversion and lapse dispersion conditions, respectively.

Table 5.8. Values of χ/Q' for Inversion and Weak Lapse Conditions at 10^3 m from TSF

Dispersion Model	χ/Q' $\left[(\text{curie sec/m}^3)/(\text{curies released})\right]$	
	Inversion[a]	Weak Lapse[b]
Sutton	4.80×10^{-4}	1.50×10^{-5}
Pasquill-Meade	4.80×10^{-4}	2.17×10^{-5}

[a]Average wind speed: 1.5 m/sec.

[b]Average wind speed: 2.3 m/sec.

Table 5.9. Doses at 10^3 m for Melting of Entire TSR-II Core

Operation Mode	Dose (rem)					
	Thyroid		Bone		Submersion	
	Lapse	Inversion	Lapse	Inversion	Lapse	Inversion
1 MW, 8 hr/day	150	3400	8.1	180	1.8	39
1 MW for 1000 hr	370	8300	3.8	83	2.3	50

Table 5.10. Core Melting Fractions for Thyroid Dose of 300 rem from Iodine

Operation Mode	Core Melting Fractions	
	Lapse	Inversion
1 MW, 8 hr/day	2	0.089
1 MW for 1000 hr	0.80	0.036

Bone. - Bone dose by inhalation of bone-seeking fission products is calculated by the same relation used for calculating the thyroid dose. Using the Pasquill-Meade (χ/Q') values from Table 5.8, bone doses calculated (Table 5.9) for 1000 MWhr of steady operation at 1 MW are 83.45 rem (inversion) and 3.89 rem (lapse). Using 25 rem as the maximum dose to the bone, the allowable core melting fraction is (25/83.45) = 0.300 for inversion conditions and > 1 for lapse conditions following operation at 1 MW for 1000 hr. Allowable core melting fractions for bone-dose limits are greater than the corresponding melting fractions for thyroid dose limits.

5.3.2. External Submersion Doses

The whole-body dose from external submersion in a cloud of beta and gamma emitters was evaluated by the relation, after Burnett[5]

$$\text{dose (rem)} = 0.26\, f E_s Q \frac{\chi}{Q'} \quad ,$$

where $E_s = E_\gamma + 1/3\, E_\beta$, MeV.*

The product $E_s Q$ was included in Tables 5.3 and 5.4 for iodines and noble gases. The contribution of nonvolatile fission products to the external submersion dose is negligible[2] for the same release fraction used in this study. Therefore values of submersion doses in Table 5.9 were calculated with the above relation using release fractions of 1.0 and 0.5 for the entire core inventory of noble gases and iodines, respectively. As for the bone-dose results, submersion doses are less than the 25-rem limit for lapse dispersion conditions and with the entire core assumed to have reached melting conditions. For inversion conditions the allowable core melting fraction could be as high as 0.5 for operation at 1 MW for 1000 hr. Submersion exposure is therefore less restrictive than either bone or thyroid exposure, as is the usual result for contained reactor systems.

---

*The term $1/3\, E_\beta$ from Burnett's expression for E_s is the same as Av. E_β from Blomeke and Todd, Table 5.2.

5.4. Activity Deposition by Rainfall

5.4.1. Maximum Rainout Dose

The highest deposition rate of activity from a cloud release results from rainfall through the cloud. The highest surface deposition, curies/m^2, can be obtained from the maximum rainout or washout calculations of Culkowski,[15] which depend only on the choice of a Pasquill-Meade meteorological category. Meteorological condition D was used to obtain values for the washout parameter W_{max}/Q' [(curies deposited/m^2)/(curies released)] at 10^3 m downwind distance.

An estimation of dose rates from deposited gamma activity was based on a calculated dose rate of 10 r/hr at 1 m above an infinite plane covered with 1 curie/m^2 of 0.7-MeV gamma activity.[10] The dose rate from gamma radiation was therefore estimated from the relation

$$\text{dose rate (rem/hr)} = \frac{10 \text{ r/hr}}{(0.7 \text{ MeV})(\text{curie}/m^2)} \frac{W_{max}}{Q'} E_\gamma Q \ ,$$

where $(W_{max}/Q') = 3.5 \times 10^{-6}$ (curies deposited/m^2)/(curies released) at 10^3 m, and E_γ = gamma energy, MeV. Using 50% of the iodine activity and 1% of the gamma-emitting, nonvolatile activity for the 1-MW operation for 1000 hr and E_γ data from Blomeke and Todd,[4] the following values were calculated for a 10^3 m downwind distance:

equivalent ^{131}I deposition = 8.14×10^{-2} curies/m^2,

initial nonvolatile deposition = 8.8×10^{-3} curie/m^2,

dose during first 2 hr = 10.4 rem,

dose during first 24 hr = 45.9 rem,

dose rate at 24 hr = 0.84 r/hr.

The doses at 10^3 m estimated above were based on the assumption of entire core meltdown after 1-MW operation for 1000 hr. The 45.9-rem dose for the first day would be reduced by about 96% if the core-melting fraction is assumed to be that which yields the maximum allowable thyroid exposure (see Section 5.3.1). Therefore long-term (>24 hr) doses from

maximum ground deposition at 10^3 m would be well below the 25-rem limit for MCA exposure for the same core melting conditions that would limit the thyroid inhalation dose to 300 rem. Iodine inhalation exposure is still the controlling exposure mechanism, even with the direct dose from maximum washout deposition at the exclusion boundary considered.

5.4.2. Land and Water Contamination

Land and water contamination following a fission-product release from ~4% of the TSR-II core could result in curtailment of their normal use. Although direct doses from deposited activity would be much less than 25 rem for nearby inhabitants or persons at the exclusion boundary (see Section 5.4.1), appropriate actions would be taken to minimize exposure to and ingestion of deposited fission products by the public. The wide range in possible fission-product deposition precludes establishing any definite course of action in advance. In fact the worst degree of deposition is between two extreme possibilities: high deposition occurring over a small area within the exclusion boundary and therefore not affecting the public and very low deposition from widely dispersed material over a large area and large population but causing a negligible exposure. Therefore field radiation monitoring and deposition sampling by ORNL Health Physics personnel would determine the magnitude and location of contamination and would serve as the basis for any precautionary actions taken.

The ultimate hazard from contamination of the Clinch River stems from its use by municipal water systems such as at Kingston. The main source of water for the Kingston municipal water system, however, is spring water. Some water is pumped from the Clinch River when there is a prolonged dry spell but this could be stopped during the passage of contaminated water. Clinch River water can also flow upstream under Emergy River flow to the Harriman water system intake, but such backflow is very slow and can easily be prevented by reduction of flow in the Clinch River.[16] Clinch River flow is, however, very amenable to control by the Melton Hill and Norris Dams. Therefore the combination of flow control by TVA and activity monitoring by ORNL could be used to

discharge the contaminated volume of water past the Kingston water plant intake and into the Tennessee River.

5.5. Summary of Maximum Fission-Product Releases for the TSR-II Site

The results of the principal exposure doses for release from the entire core show that iodine inhalation is the controlling exposure mechanism. The amount of ^{131}I released under inversion atmospheric dispersion conditions which results in a 300-rem thyroid dose at a distance of 1000 m is 1.7×10^3 curies. This ^{131}I activity would be released if 3.6% of the core melted after 1 MW operation for 1000 hr. The amount of mixed nonvolatile fission products (see Table 5.5) from operation at 1 MW for 1000 hr which results in a 25-rem bone dose from inhalation at 1000 m, as above, is 5.06×10^2 curies; approximately 30% of the core would have to melt before this amount of activity would be released. Therefore inhalation of iodine resulting in 300 rem to the thyroid would be accompanied by a bone dose of about 3 rem for an MCA.

REFERENCES

1. Rules and Regulations, Title 10 - Chapter 1 Part 100, "Reactor Site Criteria," United States Atomic Energy Commission (April 1967), U. S. Government Printing Office, Washington, D. C.

2. J. J. DiNuno et al., Calculations of Distance Factors for Power and Test Reactor Sites, TID-14844 (Mar. 23, 1962).

3. G. W. Parker et al., Nuclear Safety Program Semiannual Prog. Rept. June 30, 1963, ORNL-3483, pp. 9-11 (Sept. 3, 1963).

4. J. O. Blomeke and M. F. Todd, Uranium-235 Fission Product Production as a Function of Thermal Neutron Flux, Irradiation Time and Decay Time, Part 1, Vol. 1, ORNL-2127 (Nov. 12, 1958).

5. T. J. Burnett, "Reactors, Hazard vs Power Level," Nucl. Sci. Eng. 2, 382-393 (1957).

6. "Report of ICRP Committee II on Permissible Dose for Internal Radiation (1959)," Health Phys. 3 (1959).

7. O. G. Sutton, "A Theory of Eddy Diffusion in the Atmosphere," Proc. Roy. Soc. (London) 135A, 143 (1932).

8. T. Pasquill, "The Estimation of the Dispersion of Windborne Material," Meteorlogical Magazine, 90, 33-49 (1961).

9. P. J. Meade, The Effects of Meteorological Factors on the Dispersion of Airborne Material, Rassegna Internazionale Elettronica e Nucleare 6, Atti del Congresso Scientifico, Sezione Nucleare, Vol. II, pp 107-130, Comitato Nazionale per le Ricerche Nucleari, Rome, 1959.

10. Meteorology and Atomic Energy, AECU-3066 (July 1955).

11. Aircraft Reactor Experiment Hazards Summary Report, Appendix C, ORNL-1407 (Nov. 24, 1952).

12. Personal communication, F. A. Gifford, Jr., U. S. Weather Bureau, Oak Ridge, Tennessee, to L. A. Mann, ORNL, January 27, 1961.

13. W. T. Hilsmeier and F. A. Gifford, Jr., Graphs for Estimating Atmospheric Dispersion, ORO-545 (July 1962).

14. Personal communication, W. T. Hilsmeier, AEC-ORO, to T. H. Row, ORNL, June 27, 1963.

15. W. M. Culkowski, Deposition and Washout Computations Based on the Generalized Gaussian Plume Model, ORO-599 (September 1963).

16. Effect of Accidental Spillage of Radioactive Waste into Clinch River: Report No. 1, Time of Travel, Probable Flows, and Dispersion, Tennessee Valley Authority, Division of Water Control Planning, Hydraulic Data Branch, November 1952.

6. AFTERHEAT ANALYSIS FOR LIMITING POSSIBLE CORE MELTDOWN

The objective of this study was to select an operating power level that would preclude any melting of the core if complete loss of coolant occurred following such operation. The methods of calculations and the results of the final study are given below.

The afterheat analysis[1] consisted in calculating the temperature history of all portions of the core to determine the fraction of the core that might reach melting temperature. The main problems connected with this analysis were the choice of the heat removal mechanisms and the establishment of the condition of the core following a dropped-core accident. The heat loss mechanisms in this study were conduction along the central cylinder which supports the fuel elements and heat loss by convection to air from the surface of the pressure vessel. The major assumption of the analysis was that there was no water or steam present in the core. The effect of this assumption was to limit the available heat capacity to the core and pressure vessel structure, to limit heat transfer to conduction, and to reduce the effective conductivity.

The GHTRC computer code, a version of the Generalized Heat Transfer Code[2] revised for the I3M-7090 computer, was used for the temperature transient calculations. The spherical geometry was divided azimuthally into a flat support plate with no fuel, called Segment I, and a 15^{o} wedge containing fuel, called Segment II (see Fig. 6.1). The spherical geometry of the control region, fuel-bearing region, pressure vessel and shielding, and outer boundary was represented by rectangular cross-sectioned cells as shown in Fig. 6.2. The values for heat conduction between the cells and for the heat capacity of the cells were determined in a conservative manner with respect to the actual core geometry. Time-dependent afterheat generation rates were calculated for each fuel-bearing cell because of the size of the cells and the power-density variations between cells.

Afterheat generation was calculated with the PHOEBE code.[3] Calculations were performed for cyclic and continuous operation for 1, 2, and 3 MW. On the basis of the integrated afterheat results from these calculations and of the operating times required for TSR-II experiments, the GHTRC

BLANK PAGE

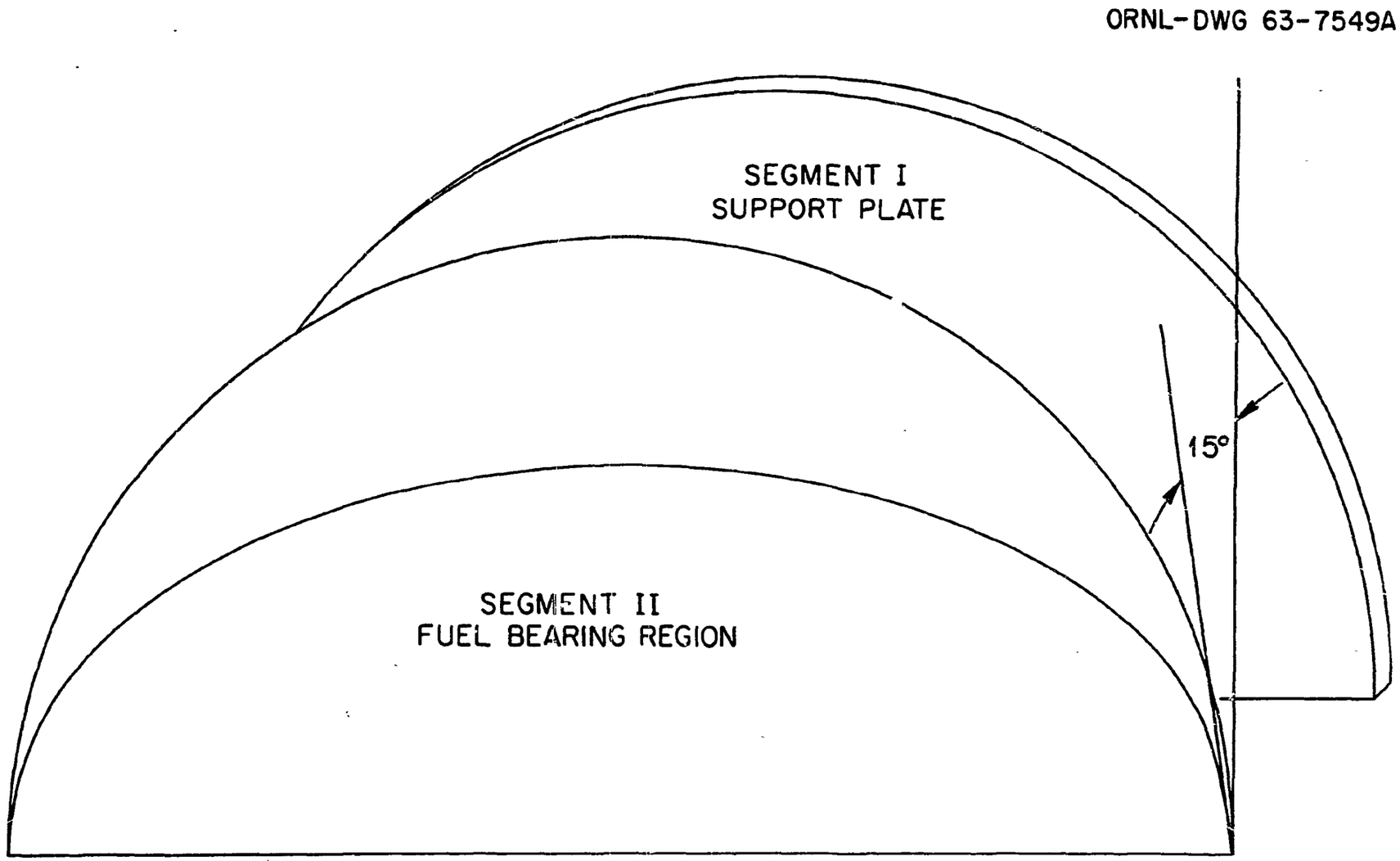

Fig. 6.1. Sector of core used with GHTRC code.

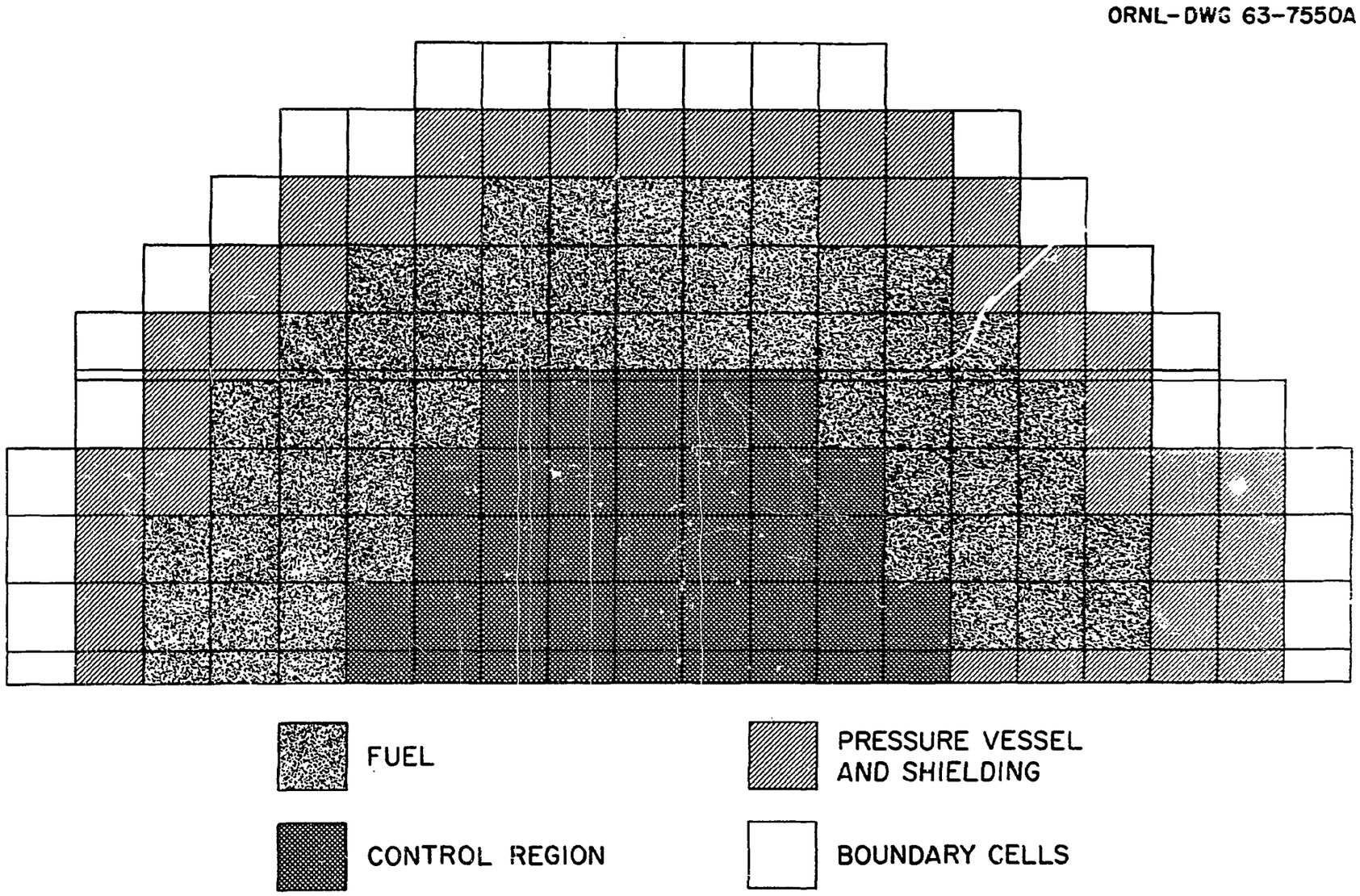

Fig. 6.2. Layout of cells in the TSR-II core for temperature transient analysis.

temperature transient calculations were performed for continuous operation at 1 MW for 75 hr.

The GHTRC calculation for 1-MW operation was extended to a longer time after shutdown[4] and the results are shown in Figs. 6.3 and 6.4. The hottest region in the core, shown in Fig. 6.3, is located on the vertical axis of the core directly below the control mechanism housing and was indicated by the conductance values used in the calculation to be the most thermally insulated region. This region reached a maximum temperature of about 950°F approximately 7 hr after shutdown. This temperature is well below the 1184°F melting temperature of the uranium-aluminum fuel alloy. Since the fuel in this region is only 0.39% of the core loading, an extremely small portion of the core is exposed to the highest temperature. The next hottest portion of the core, which contains approximately 20% of the core loading, reaches a temperature of only about 830°F approximately 4 hr after shutdown.

The last part of the analysis of core-melting conditions was the effect on the maximum core temperature of adding the afterheat due to previous operation (background afterheat) to that from the operation under investigation. In the GHTRC calculations, it was assumed that the reactor was "cold" at the start of each operation; that is to say, the only afterheat was that produced by fissioning during the particular operation under investigation. The following discussion delineates a method of determining the background afterheat generation in the core. It also establishes a limiting value for the background afterheat in the core prior to operation at 1 MW so that when it is added to that from the latest operation, the maximum fuel temperature will still not reach the melting temperature.

The decay of afterheat for several operating times at 1 MW and one cyclic operation as calculated with the PHOEBE code is shown in Fig. 6.5. After operation at 1 MW, the temperature rise across the reactor at a reduced cooling water flow rate will be monitored as a function of time and the values of the flow rate and temperature rise will be used to determine afterheat as a function of time after shutdown. These actual afterheat values will be compared with the values calculated with the PHOEBE code to determine the time at which the afterheat

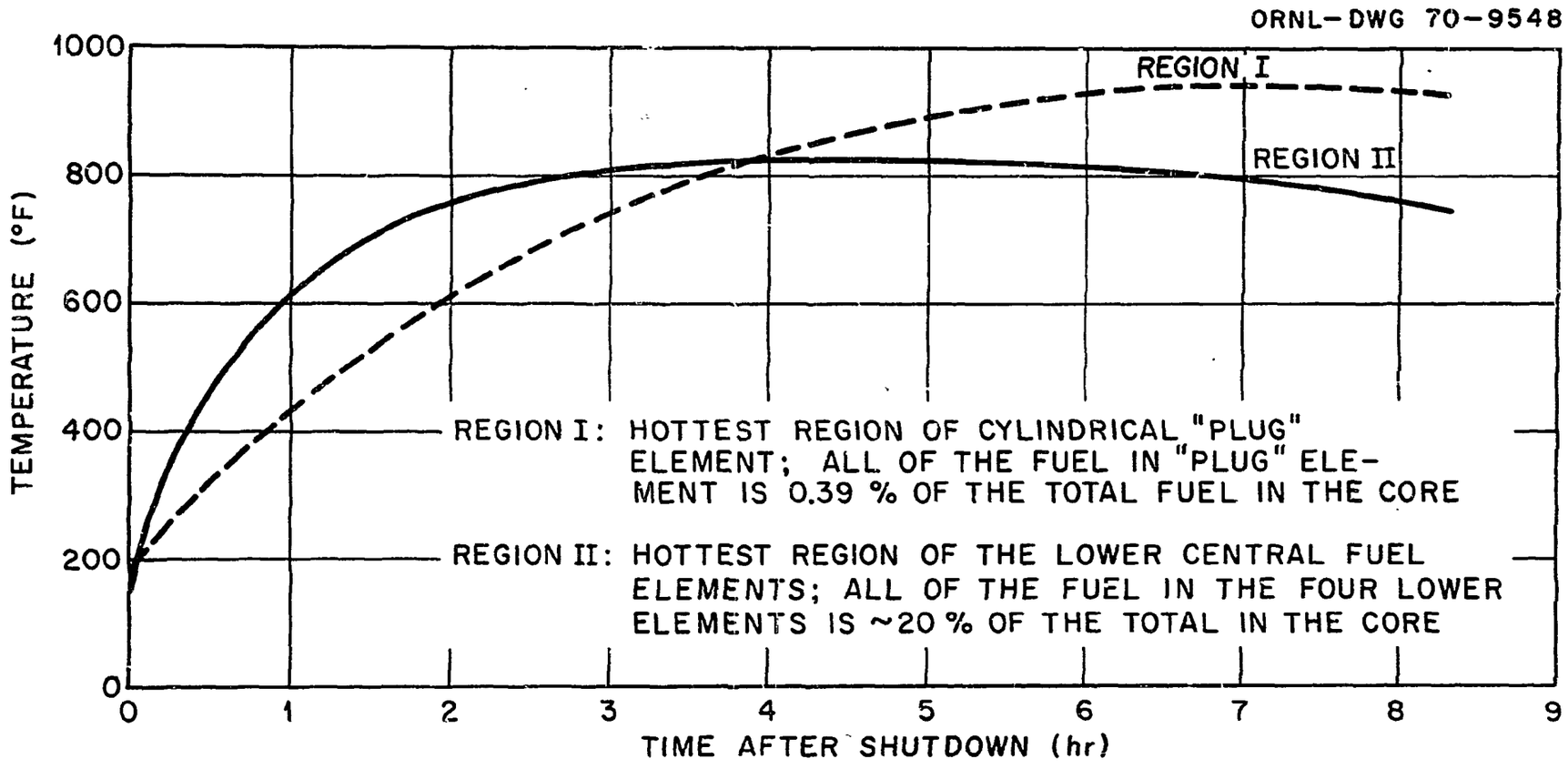

Fig. 6.3. Temperature at the hottest regions in the reactor as a function of time after shutdown for loss of coolant conditions after reactor had been operating at 1 MW for 75-hr period prior to shutdown.

ORNL-DWG 70-10579

					100.0	100.0	100.0	100.0	100.0	100.0	100.0						
			100.0	100.0	342.7	346.7	351.1	365.6	353.9	352.3	351.2	100.0	100.0				
		100.0	333.4	336.4	339.8	630.5	627.2	621.8	625.7	628.0	351.4	351.3	351.7	100.0			
	100.0	329.1	331.5	671.9	669.8	662.9	659.0	655.9	654.3	653.4	655.1	654.2	353.6	355.3	100.0		
100.0	325.9	327.8	668.0	685.1	682.3	676.4	671.1	661.1	661.5	657.0	652.2	646.2	635.6	358.5	362.1	100.0	
100.0	326.1	718.9	711.3	707.9	712.4	682.3	670.2	661.2	653.3	645.4	637.3	621.9	607.2	504.7	386.9	100.0	
100.0	325.1	779.5	778.8	776.6	770.4	444.8	445.0	445.3	445.7	446.0	655.2	654.3	652.4	349.1	384.7	100.0	100.0
100.0	323.0	324.3	790.2	790.4	790.2	443.5	444.0	444.2	444.7	445.3	446.0	446.7	655.9	655.1	654.0	380.6	364.9	349.4	100.0
100.0	322.4	797.0	796.8	796.7	796.2	442.9	443.2	443.6	444.3	445.2	446.4	447.8	654.3	652.4	650.9	649.3	379.8	340.3	100.0
100.0	322.1	798.5	798.8	798.9	441.6	442.2	442.7	443.3	444.1	445.4	447.7	452.2	462.3	644.1	644.2	643.1	384.8	341.6	100.0
100.0	322.1	941.4	941.8	942.0	441.4	441.9	442.5	443.1	444.0	445.3	447.8	453.6	473.0	581.1	608.2	587.1	395.8	343.6	100.0

Fig. 6.4. Map of fuel temperatures (°F) in the TSR-II 1 hr after shutdown following operation of the reactor at 1 MW for 75 hr prior to shutdown.

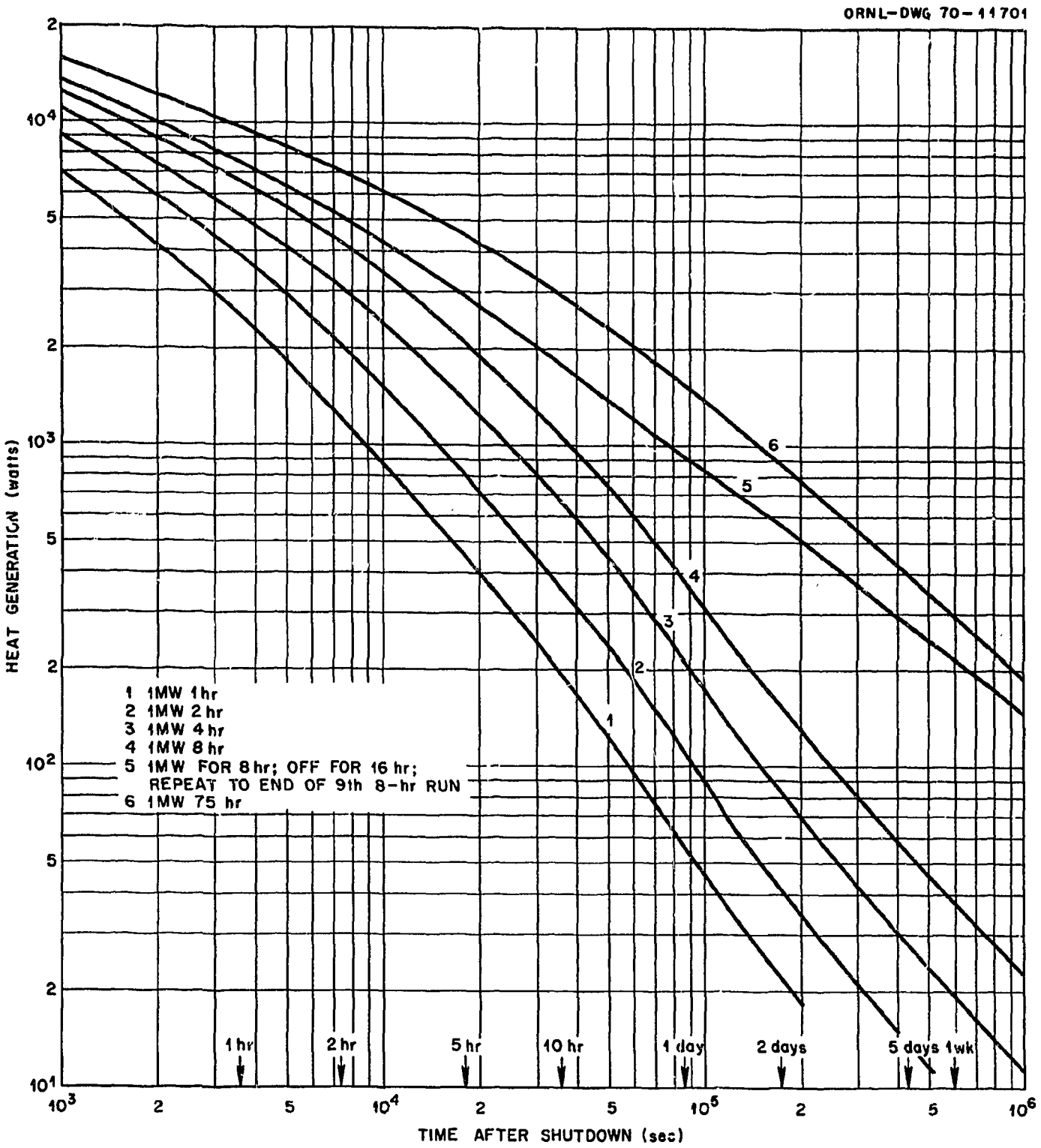

Fig. 6.5. Afterheat generation rate as a function of time after shutdown following operation at 1 MW for several time intervals and following cyclic operation.

The GHTRC results indicated that the maximum core temperature under MCA conditions after continuous operation at 1 MW for about 75 hr is approximately 230°F below the melting temperature. It occurs about 7 hr after shutdown in a portion of the lower fuel region which contains only 0.39% of the fuel in the core (31 g of ^{235}U) and approximately 1.4 lb of aluminum. If the background afterheat at the initiation of operation for 75 hr at 1 MW is 1 kW (see curve 5, Fig. 6.5 at 80,000 sec) at the end of the operation, which is approximately 270,000 sec later, it drops to about 350 watts. Assuming that the background afterheat in the reactor remains at 350 watts during the whole 7-hr period and assuming that none of it escapes from the reactor, the heat deposited in the hottest region is 33 Btu. Using a specific heat of 0.24 Btu per lb for the aluminum, this heat raises the temperature of the fuel plates 97°F which is 133°F below the melting temperature. To raise the temperature of the hottest region to the melting temperature, the background afterheat in the core would have to be 829 watts. To actually melt the 0.39% of the core, the background afterheat would have to be a constant 3.5 kW for the full 7-hr period.

6. REFERENCES

1. G. J. Kidd, Jr., A Procedure for Predicting the Effect of Loss of Coolant Accidents in the Oak Ridge National Laboratory's Tower Shielding Reactor II, ORNL-TM-2853 (May 1970).

2. T. B. Fowler and E. R. Volk, Generalized Heat Conduction Code for the IBM-704 Computer, ORNL-2734 (October 1959).

3. E. D. Arnold, Phoebe - A Code for Calculating Beta and Gamma Activity and Spectra for ^{235}U Fission Products, ORNL-3931 (July 1966).

4. Memo dated July 23, 1970, from G. J. Kidd, Jr., to L. B. Holland, "Additional After-Heat Calculations for the Tower Shielding Reactor II."

7. SUMMARY

Investigation concerning the possibility of fission-product release from the fuel plates under abnormal operating or accident conditions included an analysis of the protection system and the inherent safety characteristics of the TSR-II design and a determination of the consequences of reduced core cooling for loss-of-coolant flow and loss-of-coolant heat sink conditions. It was concluded that fuel damage would not result from any realistic reactivity accident or from reduction in the flow of the core coolant and that release of fission products to the atmosphere from a defective fuel plate would be restricted to noble gases and halogens and would not represent a significant hazard.

Calculations based on 100% release of iodine from melted fuel and on an instantaneous, ground-level release, with atmospheric dispersion from moderate inversion, showed that at least 3.6% of the core would have to melt before the dose to the thyroid of 300 rem would be reached 1000 m from the reactor. Under these conditions the calculated bone dose was 3 rem, and the external submersion dose 1.8 rem. Since these dose levels were calculated for a 1000-m distance, the low population zone boundary could be not only inside the 4085-ft point of closest approach but also inside the 3800 ft minimum distance to the TSF exclusion fence.

Investigation of a dropped-core accident in which the water coolant is drained from the core after operation at 1 MW for 75 hr led to two important conclusions:

1. Maximum core temperatures after 1-MW operation would occur at lease 6.9 hr after shutdown.

2. No fuel melting would occur.

Since the afterheat calculations indicate that there would be no core melting, we believe that the TSR-II can be operated in the proposed manner at a maximum power level of 1 MW with assurance for the safety of the general public and the operating personnel.

APPENDIX A

Analog Computer Tests*

Rod-Drop Test

The TSR-II rod-drop test was performed to determine the minimum period for which the safety system could reverse an excursion in less than a three-decade power rise from the instant that the instruments first detected the excursion. In the analog technique used, the reactor simulator (computer) at time t = 0 is clamped in transient at a low level represented by a voltage of 0.1 to 0.5 V. This voltage is proportional to reactor power or flux and, by proper adjustment of the computer parameters, can be made to represent a nuclear power. At t = 0 the clamp is removed and the safety system is given the information that an excursion is in progress. The simulation allows for the safety system delay, provides the corrective action, and shows the reactor behavior, heat transfer characteristics, and component temperature rises during the complete transient. (Authorization is requested for a maximum power level of 1 MW, whereas the present analysis is for 5-MW maximum operating power.)

In the TSR-II test the initial power of 0.5 (Fig. A.1) corresponds to a power of 5 MW. A three-decade rise then would yield a peak power of 5000 MW. Since the level safety of the TSR-II is intended to actuate a scram at 150% of the maximum power, the level safety was assumed to be 7.5 MW. At 7.5 MW information was supplied to the safety actuator to request a scram. The simulated excursion continued unaltered until reactivity reduction was effected by simulated movement of the shim rods. The corrective action was then initiated, after which the excursion was reversed and the simulated reactor was shut down. Since the test was for the safety system, the effect of the water coolant negative temperature coefficient, which would only have improved the performance of the safety system, was not considered.

The power excursion curves obtained in this test are shown in Fig. A.1, along with the reactivity reduction as a function of time due to the scram

---

*Work performed by R. K. Adams, ORNL.

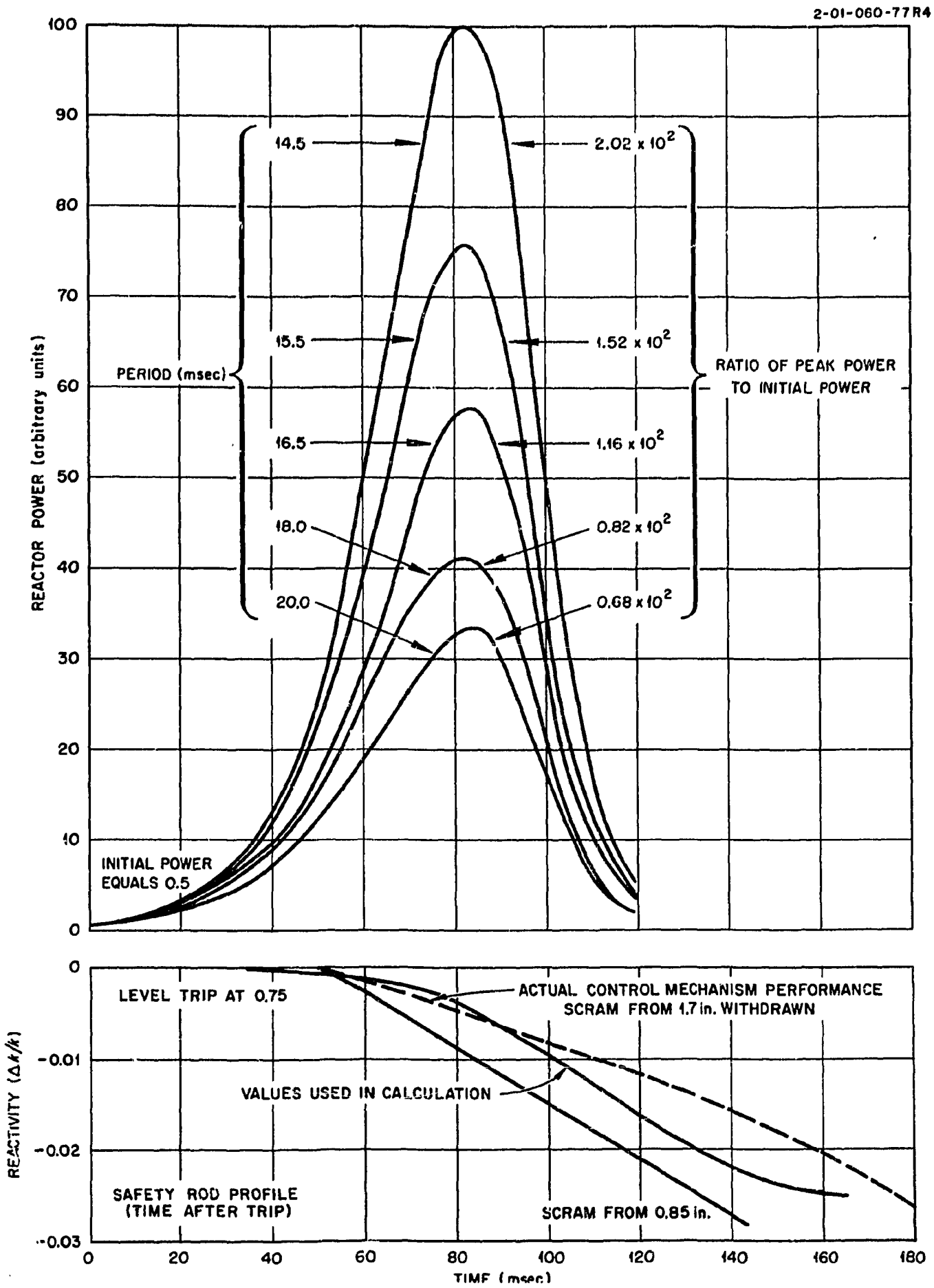

Fig. A.1. Effectiveness of TSR-II safety system in limiting power excursions for various reactor periods.

action of the shim rods used in the calculations. Also shown is the reactivity reduction that can be achieved with the actual TSR-II shim rods at the beginning and the end of core life. The initial reactivity reduction at the end of the core life is close to the value used in the calculations, but for most of the core life it is even better. The total reactivity reduction at the end of the core life is 3.8×10^{-2} $\Delta k/k$, but only the initial 2.6×10^{-2} $\Delta k/k$ reduction is indicated. The associated reactor period is noted alongside each power excursion curve. From these data it can be seen that the TSR-II safety system is capable of reversing a power excursion caused by a 14.5-msec period with a maximum power rise of 2.02×10^{2} above the initial power.

The mean temperature increase of the fuel in the annular elements and the temperature rise of the water in the annular fuel region are shown in Fig. A.2 for each of the power excursions plotted in Fig. A.1.

Cold-Water-Slug Test

Because of the negative coefficient of reactivity of the TSR-II an analog simulator test was performed to investigate the effects of a sudden drop in the reactor inlet cooling water temperature. Figures A.3 and A.4 show the effects on the reactor power and temperature of suddenly changing within 0.5 sec, the inlet cooling water temperature from 145.8°F to 32°F while the reactor is operating at 5 MW. the assumed coefficients in Figs. A.3 and A.4 are -4.28×10^{-5} and -6.5×10^{-5} $\Delta k/k$ per °F, respectively. The measured temperature coefficients at 50 and 145°F are respectively -6.7×10^{-5} and -1.24×10^{-4} $\Delta k/k$ per °F. Prompt gamma-ray heating was included in the simulation. No safety rod action or control rod action was permitted.

The simulation has no validity in the cross-hatched areas of Figs. A.3 and A.4 since no attempt was made to simulate boiling conditions within the reactor. An assumed pressure of 10 psig was used to calculate the boiling temperature of 239°F (the actual core inlet pressure is greater than 30 psig).

The cold-water-slug analysis was carried out without actuating the safety system. It should be noted that there is far more than adequate time for the safety system to shut down the reactor before the fuel

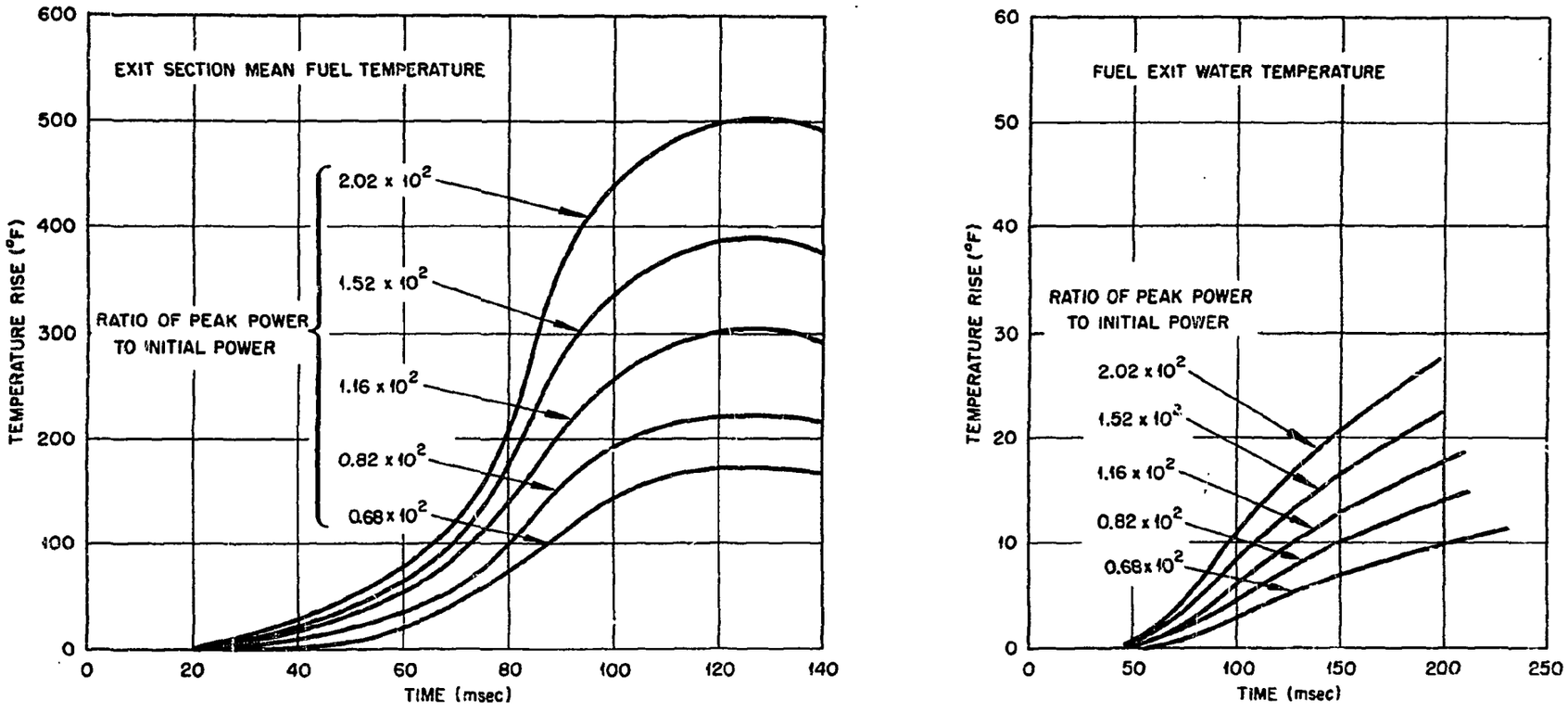

Fig. A.2. Temperature increase in TSR-II annular fuel elements region for various power excursions.

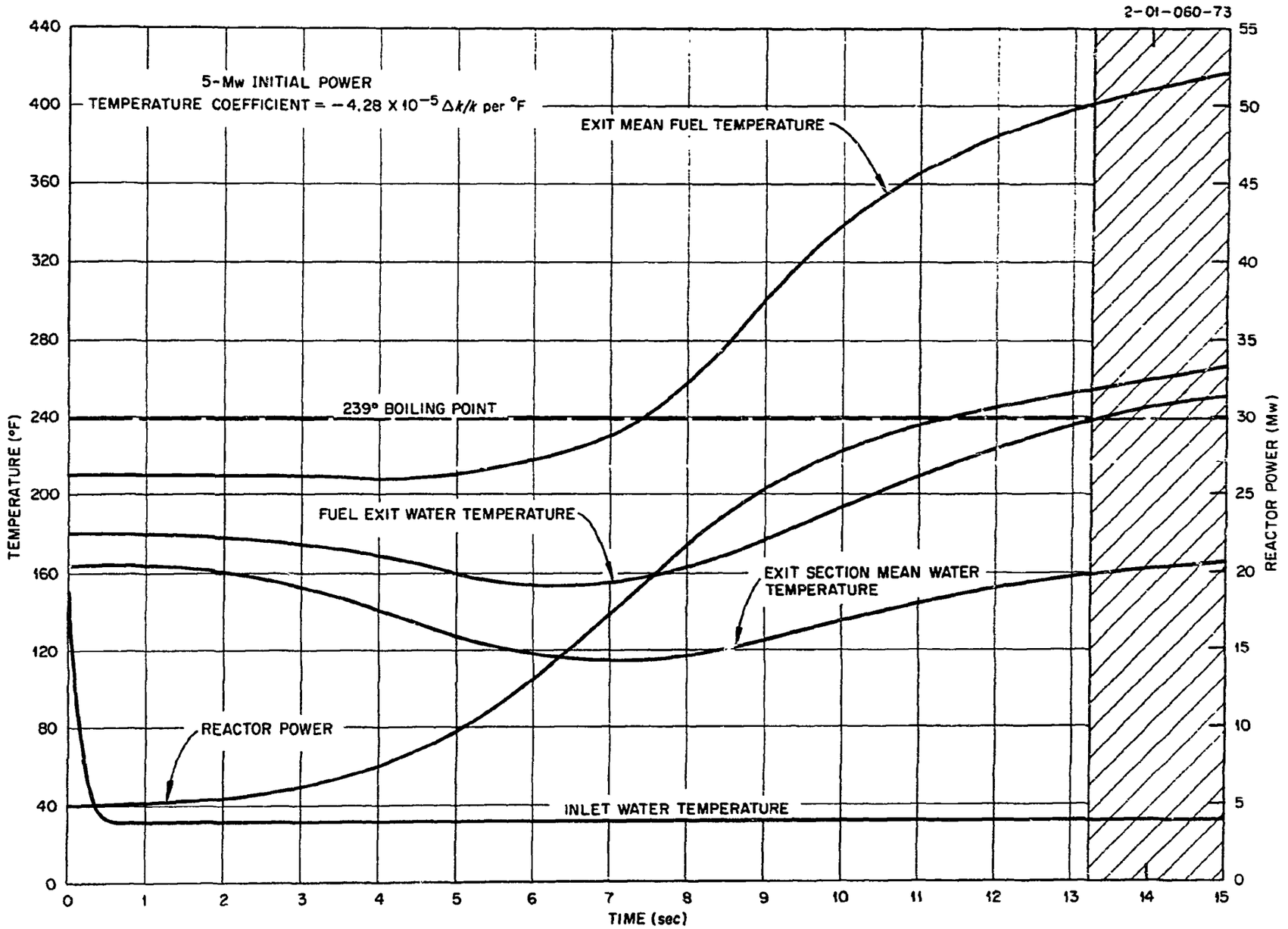

Fig. A.3. Effect on reactor power and temperatures of reducing the inlet water temperature from 145.8°F to 32°F (temperature coefficient = -4.28×10^{-5} $\Delta k/k$ per °F).

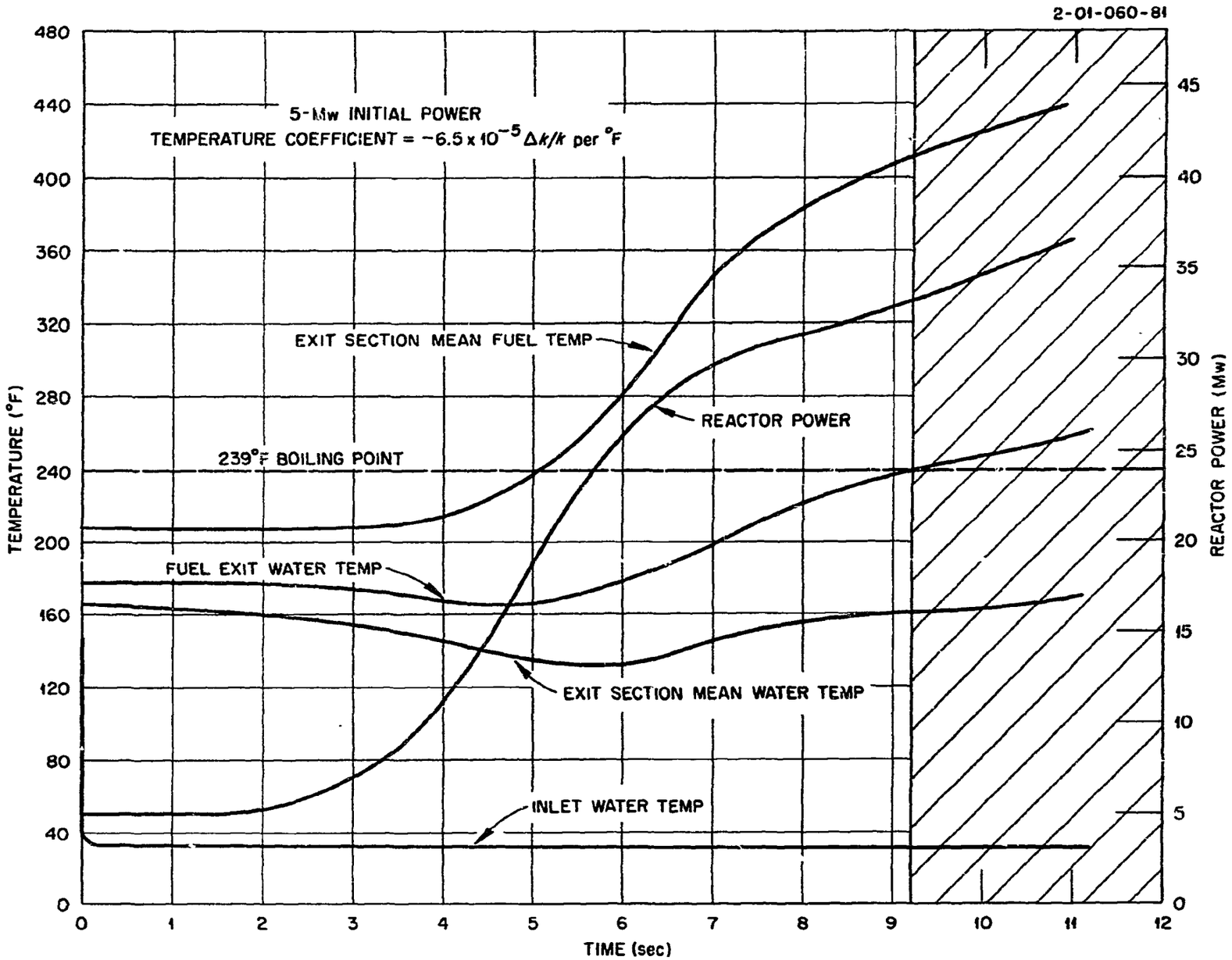

Fig. A.4. Effect on TSR-II power and temperatures of reducing the inlet water temperatures from 145.8°F to 32°F (temperature coefficient = -6.5 x 10^{-5} Δk/k per °F.

temperature rises appreciably since the safety system can complete its action in less than 160 msec (Fig. A.1).

Water-Flow Stoppage Test

Mechanical conditions inherent in the design of the TSR-II cooling water system prompted a test to determine the effects of a sudden stoppage of the coolant water flow. Figure A.5 shows the results for an assumed temperature coefficient of -4.28×10^{-5} $\Delta k/k$ per ^{o}F. Prompt gamma-ray heating was again included in the simulation, and no safety or control rod action was permitted. The simulation included only the annular fuel region of the reactor. Again the simulation has no validity for the cross-hatched area in Fig. A.5. As before, the test showed that the safety system could easily shut down the reactor before any appreciable change occurs in the temperature profile. Conditions would be even more favorable with the actual reactivity reduction due to temperature increase.

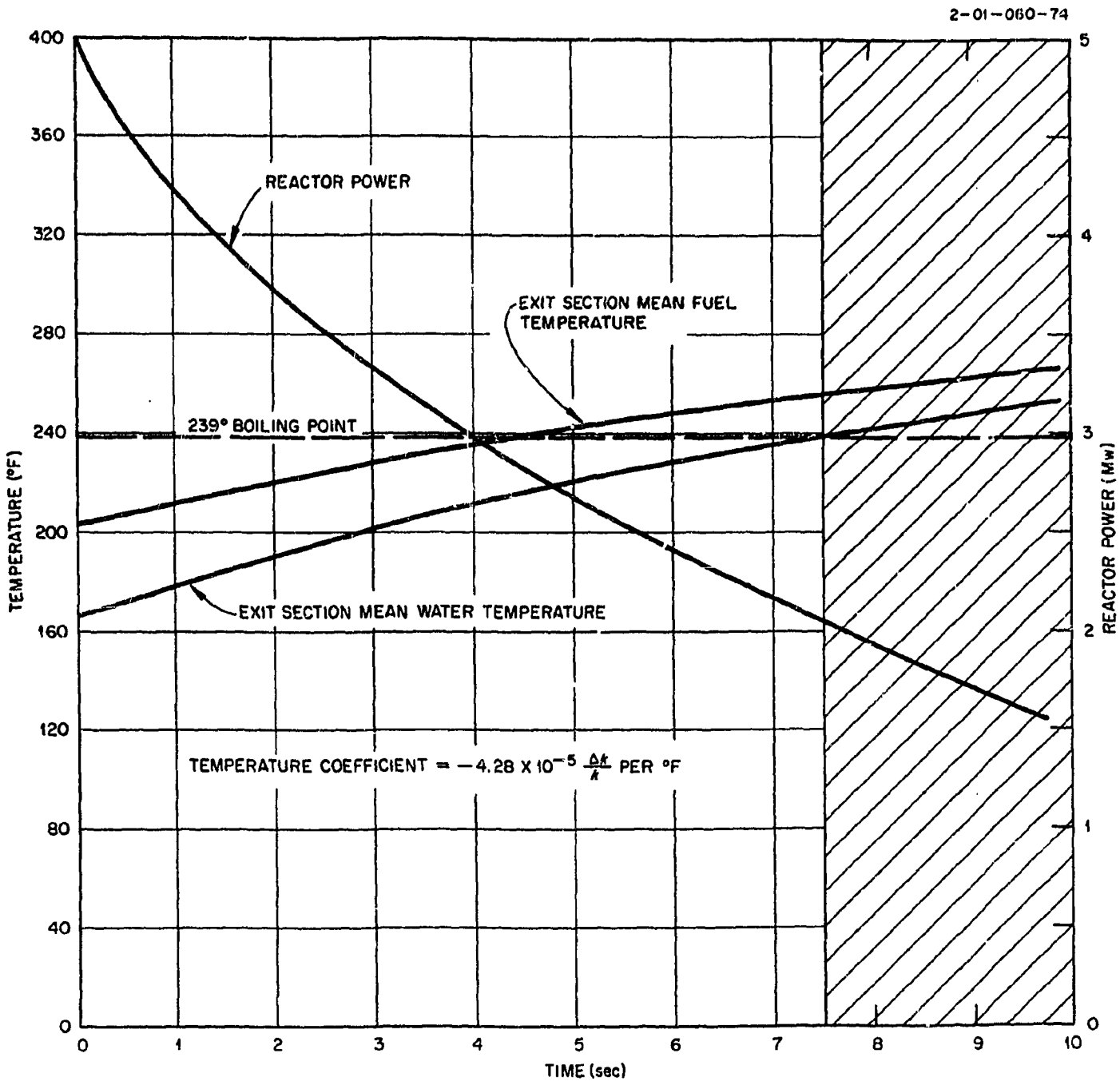

Fig. A.5. Effect of sudden water flow stoppage on TSR-II power and temperatures.

APPENDIX B

Self-Shutdown Characteristics

A reliable reactivity shutdown mechanism has been provided for the TSR-II in the fast-scram protection system described in Volume I of the Design and Operations Report, ORNL-TM-2893. The self-shutdown feature of the TSR-II increases the capability of the reactor to survive reactivity addition accidents with a minimum of core damage and/or fission product release. It is proposed that the self-shutdown characteristics of the TSR-II core can be deduced from the results of the SPERT excursion tests for a wide range of reactivity addition accidents, including the startup accident. The basis for this hypothesis and its application to the TSR-II are presented below. This discussion has been restricted to the highlights of the SPERT program and results as they apply to the TSR-II since more detailed summaries on the SPERT program are readily available.[1-4]

Description of SPERT I Cores

The SPERT I facility was an unpressurized light-water filled, open-tank design with cores composed of 3- x 3- x 24-in.-long box-shaped fuel elements. The aluminum cores consisted of 20-mil-thick highly enriched uranium-aluminum alloy plates clad with 20-mil-thick aluminum. The number of fuel plates per element ranged from 12 to 24 to vary the metal-to-water and hydrogen-to-uranium ratios. Core size varied between 12 and 64 fuel elements per core. Pertinent static nuclear characteristics of the SPERT I cores, including the P-18/19 stainless-steel-clad core, are shown in Table B.1. The first number of the core identification designates the fuel plates per element, the second number the elements in the core; for example, the B-12/64 core contains 64 elements of 12 plates per element.

Response of Spert Cores to Reactivity Additions

The self-shutdown characteristics of the SPERT-I aluminum cores were determined for inverse asymptotic periods (α) as high as 100 to 200 sec^{-1} for step reactivity insertions. Quantitative effects of step reactivity excursions from source power (10^{-4} W) and 20°C ambient temperature are shown by the maximum power, excursion energy to peak power, and fuel plate surface temperature and maximum transient pressure as a function of α in

Table B.1. Static Characteristics of Spert I Cores

Core	Core Identification				
	B-12/64	B-16/40	A-17/28	B-24/32	P-18/19
Cladding material	Al	Al	Al	Al	Stainless Steel
Critical mass, kg of ^{235}U	4.3	3.6	3.9	4.3	7.6
Total ^{235}U loaded, kg	5.4	4.5	4.7	5.4	9.3
H:U atomic ratio	760	540	320	270	120
Metal-water volume ratio	0.46	0.63	0.79	1.14	0.3
Available excess reactivity, $	4.3	5.6	5.2	6.6	4.9
Temperature defect, 20 to 95°C, $	1.44	1.67	1.47	1.73	1.48
Temperature coefficient, 20°C, $/°C	-1.8×10^{-2}	-1.7×10^{-2}	-0.67×10^{-2}	-1.1×10^{-2}	-0.25×10^{-2}
Temperature coefficient, 95°C, $/°C	-2.0×10^{-2}	-3.4×10^{-2}	-2.7×10^{-2}	-3.4×10^{-2}	-3.4×10^{-2}
Central void coefficient, $/cm^3	$+0.8 \times 10^{-4}$	-4.7×10^{-4}	-9.3×10^{-4}	-17×10^{-4}	-18×10^{-4}
Average void coefficient, c_v, $/cm^3	-0.93×10^{-4}	-2.9×10^{-4}	-4.6×10^{-4}	-7.3×10^{-4}	-9.9×10^{-4}
$\ell^*/\bar{\beta}$ (sec)	11×10^{-3}	10×10^{-3}	7×10^{-3}	7×10^{-3}	2×10^{-3}
$\frac{c_v \sqrt{\bar{\beta}}}{\ell^*/\bar{\beta}}$ $\left[(\Delta k/k)/cm^3\right]$/sec	0.9×10^{-2}	3×10^{-2}	7×10^{-2}	10×10^{-2}	50×10^{-2}

Figs. B.1 - B.4. The maximum reactor power showed a break and the excursion energy a minimum at an α value of 5 to 10 sec^{-1}, corresponding to \$1 reactivity addition, indicating the increased energy requirements to generate compensating reactivity once the prompt critical condition is reached. Fuel-plate surface temperature rise at maximum power, Fig. B.3, also exhibited a minimum before saturation temperature was reached at α values of 10 to 30 sec^{-1}. Hence self-shutdown was achieved by moderator and metal expansion effects without moderator boiling for $\alpha < 10$ sec^{-1} in all the SPERT cores listed in Table B.1. Steam generation became an important reactivity compensation mechanism for these unpressurized SPERT I cores at α values of 10 to 30 sec^{-1}, where the temperature rise to time-of-peak power was large enough that the fuel plate surface temperature reached the saturation temperature (see Fig. B.3). The compensated reactivity attributed to steam is illustrated in Fig. B.5 for the A-17/28 core. The transient pressure was of sufficient magnitude to be be measurable only for periods shorter than 35 msec (α = 28.5 sec^{-1})[1] as shown in Fig. B.4.

The effect of system pressurization on the SPERT self-shutdown characteristics is of interest since the TSR-II core coolant is pressurized to ~60 psig. This effect was studied in the SPERT III facility, which allowed pressurization to 2500 psig. For short-period tests at atmospheric pressure, boiling of the moderator is the largest contributor to shutdown. The SPERT III tests have shown that, as the system pressure is raised, the delay and eventual suppression of boiling merely cause an increase in the temperature rise of the fuel plates, with a resultant increase in the reactivity compensation arising from water and fuel-plate expansion and with no gross change in the power burst.[5] Peak power excursion results at atmospheric pressure for the stainless-steel-clad, plate-type SPERT III core are shown in Fig. B.6. The shutdown reactivity coefficient of the SPERT III core was about the same as that for the SPERT I, A-17/28 core (see below); the peak power as a function of α was also the same for the two cores.[6] The effect of system pressurization on SPERT III fuel plate surface temperature and energy release is shown in Fig. B.7 and B.8 for 18- and 11-msec transients (α values of 55 and 91 sec^{-1}). In general, the largest change in the energy release to time-of-peak power occurs in the first 100 psi pressure increase. Above 200 psig the energy release to

ORNL-DWG 67-13497

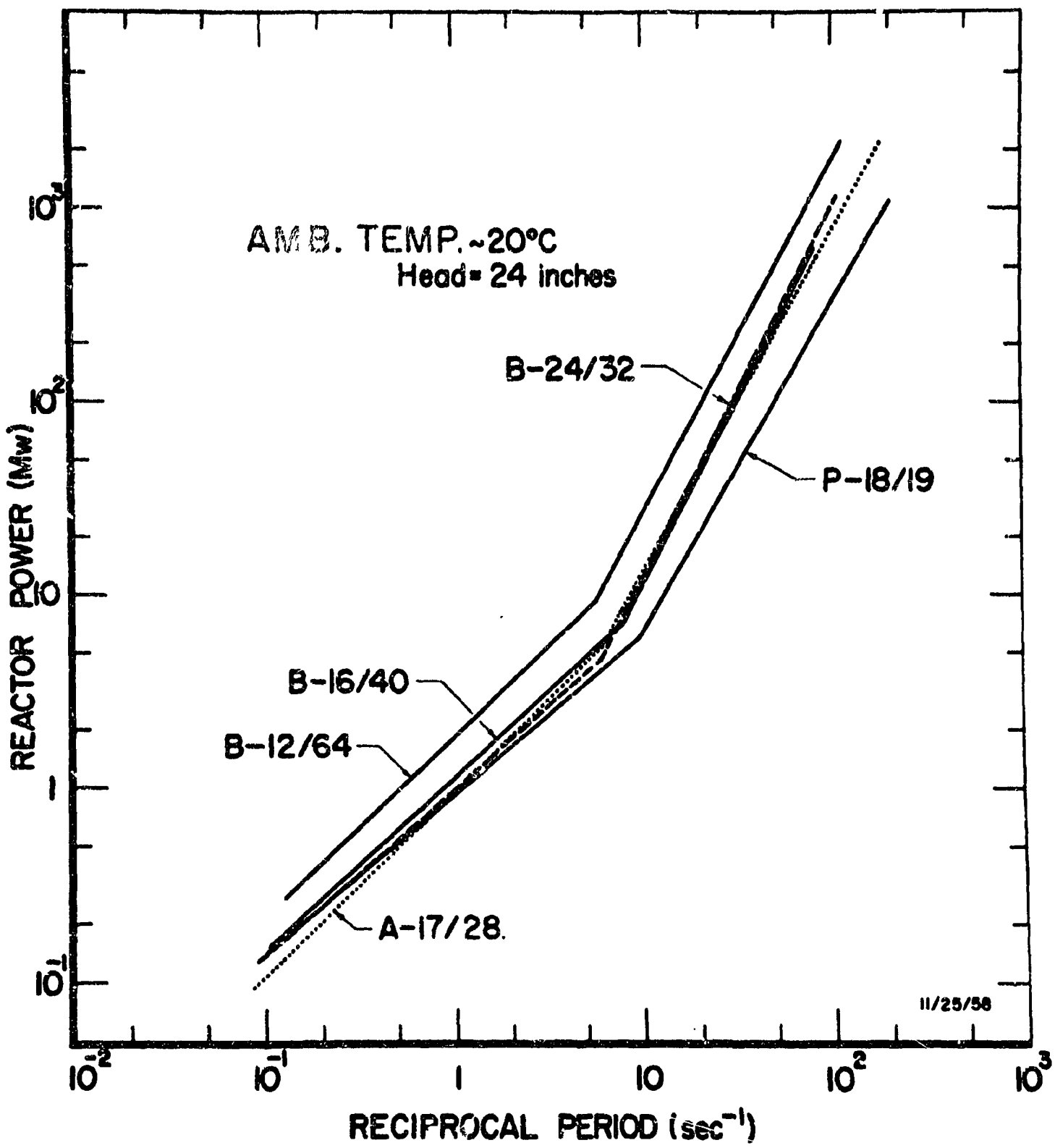

Fig. B.1. Maximum reactor power vs reciprocal period for SPERT I step reactivity excursions from source power (from Ref. 1).

ORNL-DWG 67-13501

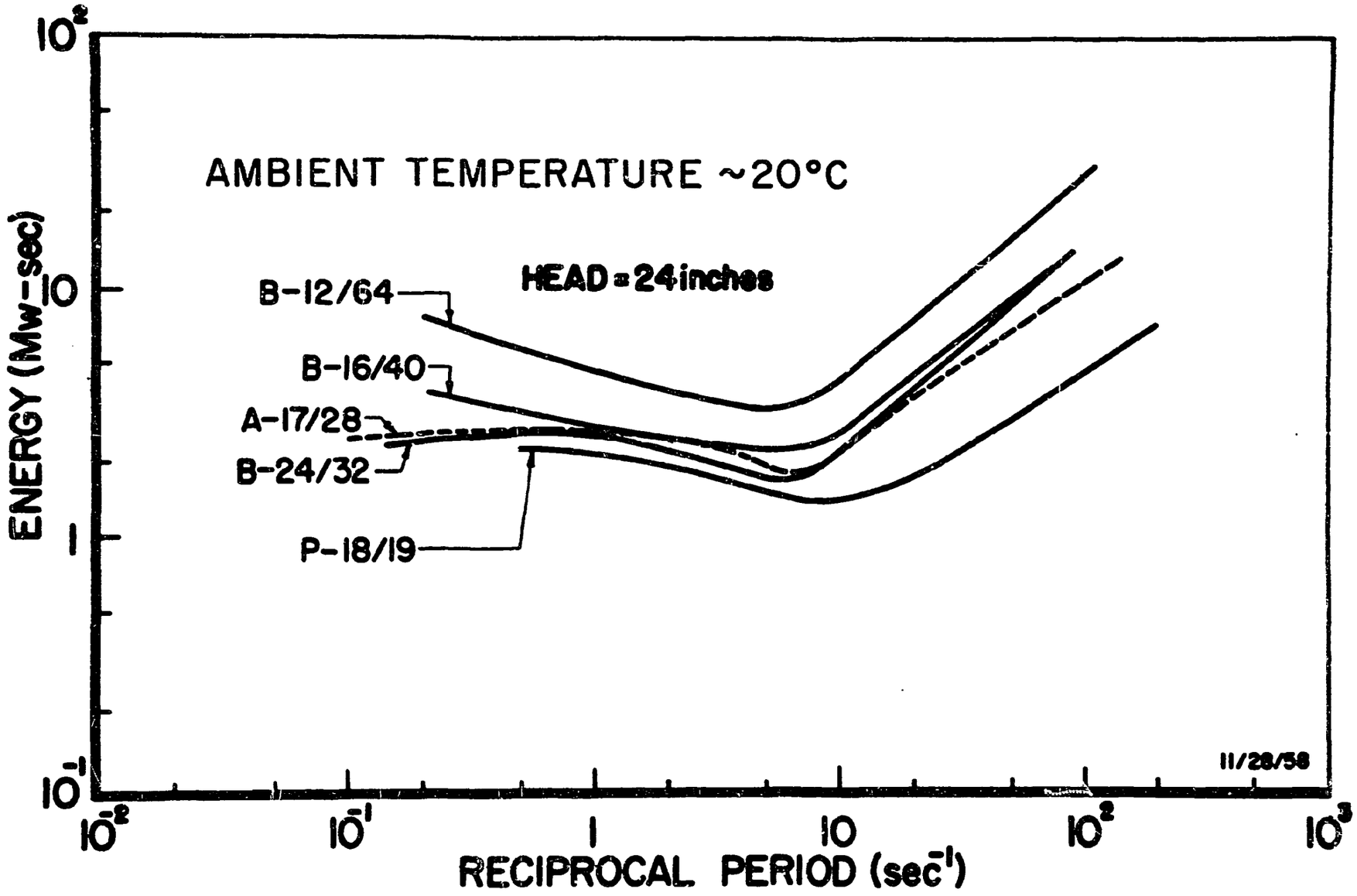

Fig. B.2. Energy to time of peak power vs reciprocal period for SPERT I step reactivity excursions from source power (from Ref. 1).

ORNL-DWG 67-13504

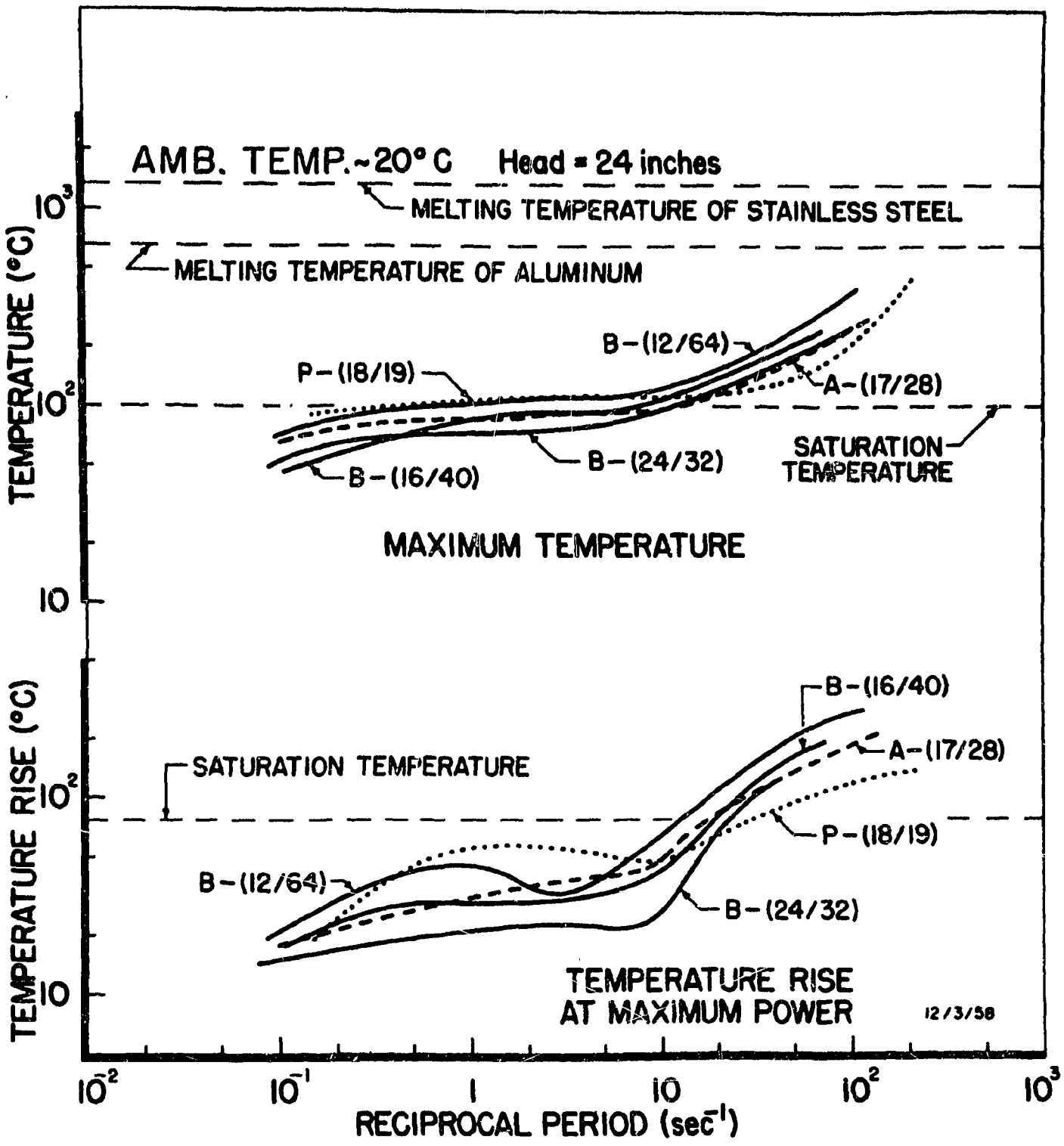

Fig. B.3. Fuel plate surface temperature vs reciprocal period for SPERT I step reactivity excursions from source power (from Ref. 1).

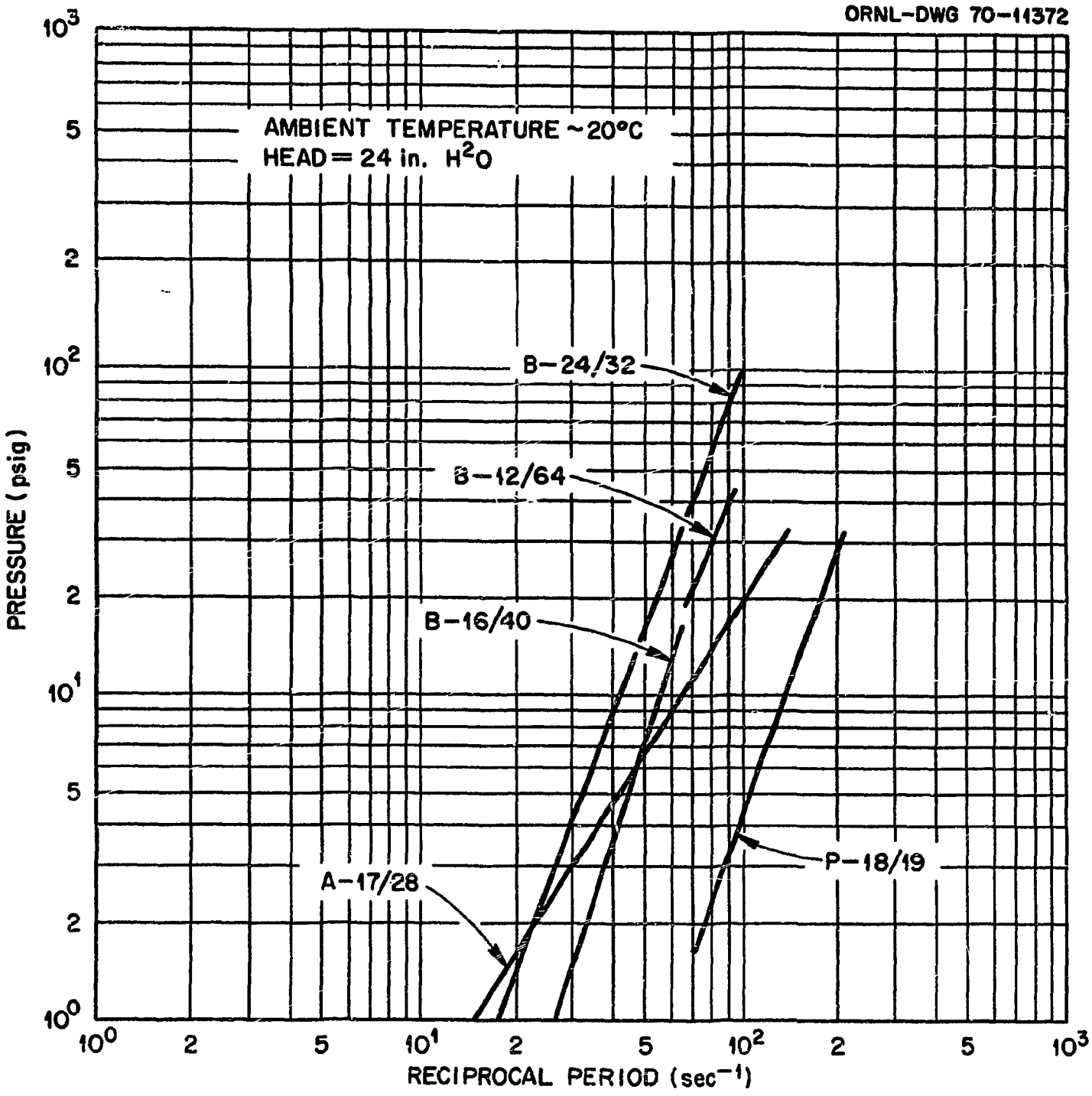

Fig. B.4. Maximum transient pressure vs reciprocal period for SPERT I step reactivity excursions from source power (from Ref. 1).

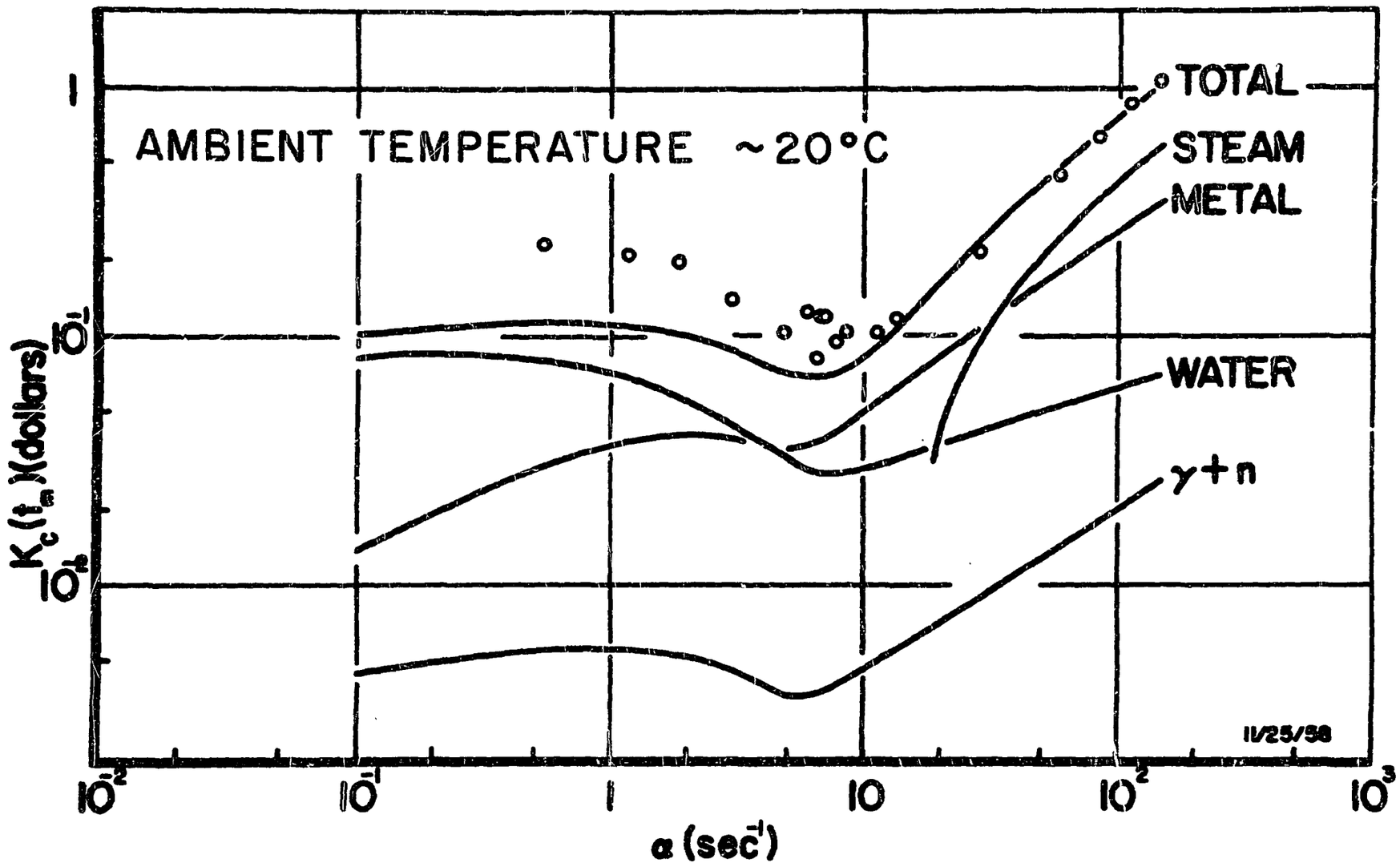

Fig. B.5. Compensated reactivity at peak power, $K(t_m)$, vs reciprocal period for SPERT I core A-17/28 step reactivity excursions from source power (from Ref. 1).

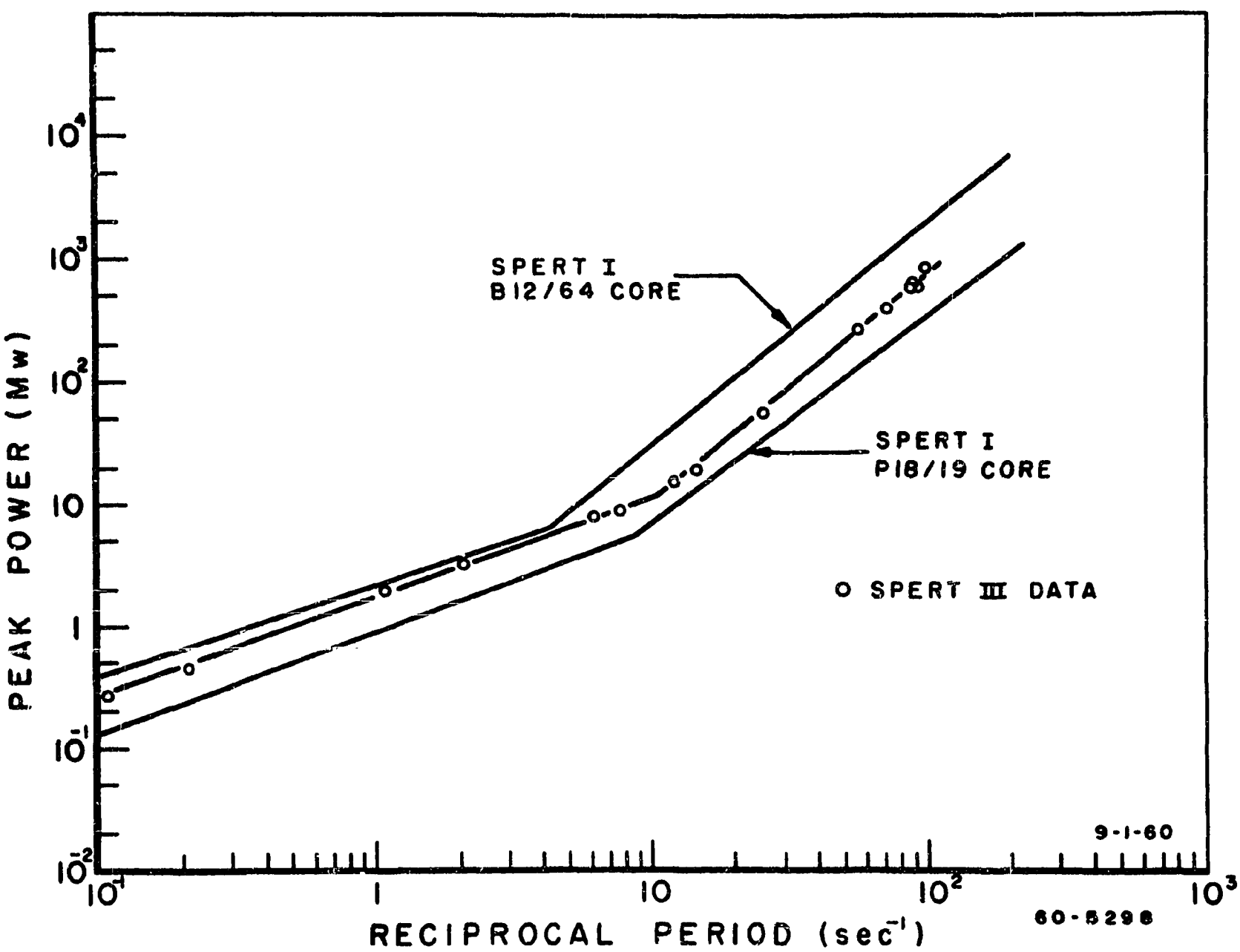

Fig. B.6. Peak power vs reciprocal period for step-transients at room temperature, atmospheric pressure, and no flow (from Ref. 1).

ORNL-DWG 67-13505

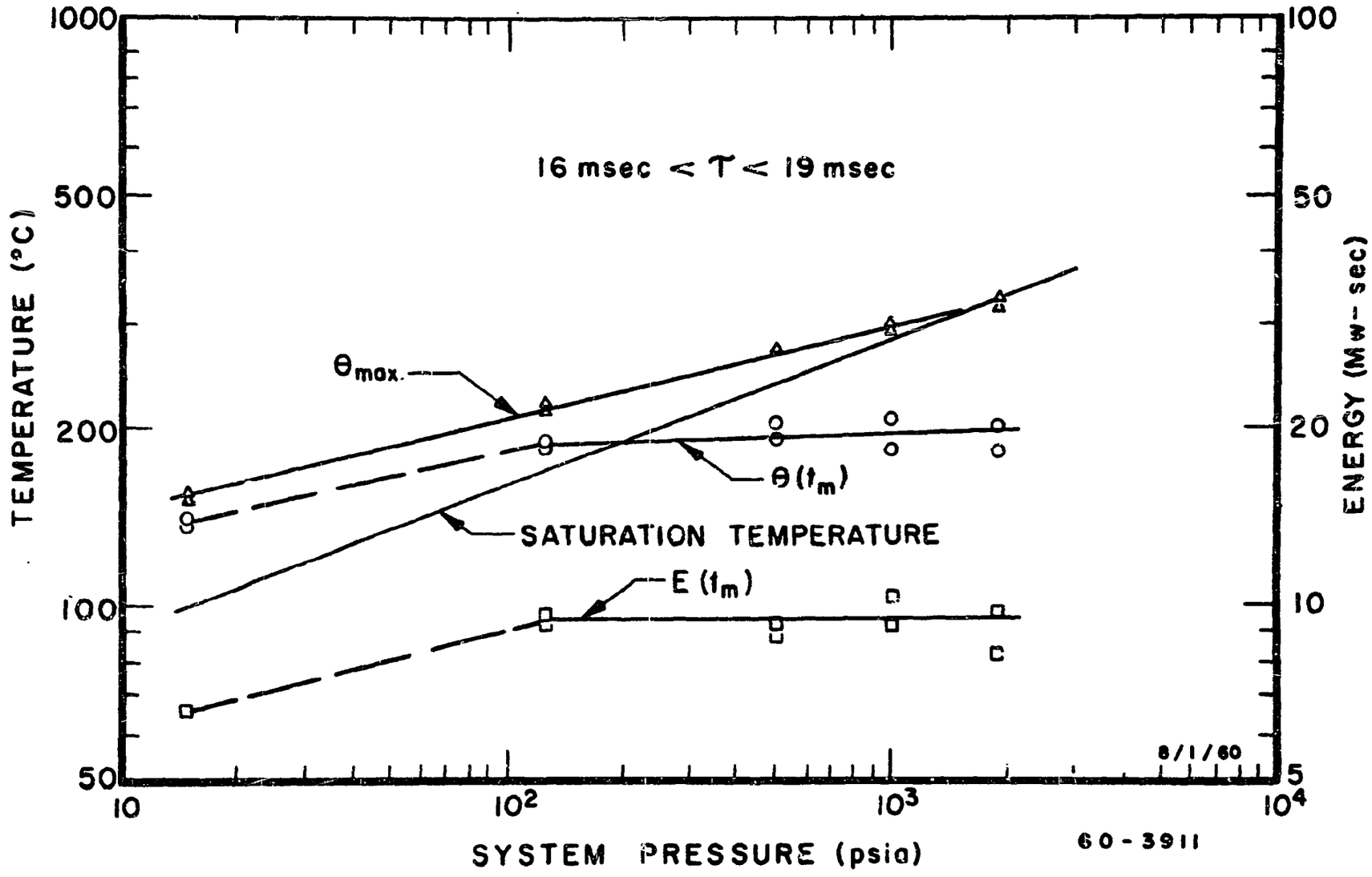

Fig. B.7. Energy release and fuel plate surface temperature at time of maximum power $E(t_m)$ and $\theta(t_m)$, and maximum fuel plate surface temperature, θ_{max}, for 18-msec tests (from Ref. 5)

ORNL-DWG 67-13498

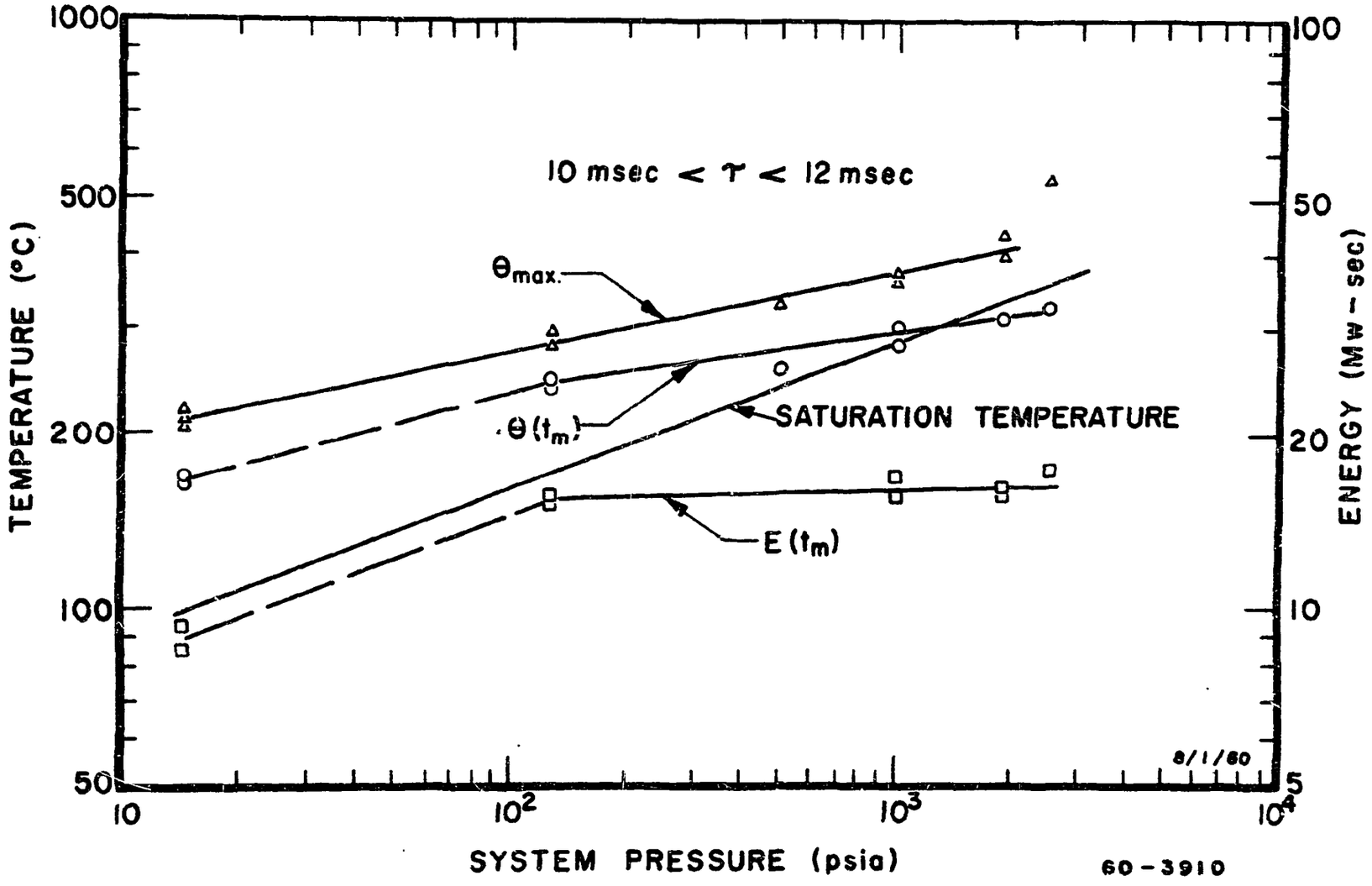

Fig. B.8. Energy release and fuel plate surface temperature at time of maximum power, $E(t_m)$ and $\theta(t_m)$, and maximum fuel plate surface temperature, θ_{max}, for 11-msec tests (from Ref. 5).

to the time-of-peak power is approximately 18 MWsec. For power excursions at 2500 psig with the system initially at room temperature and with the initial asymptotic (steady) period about 11 msec, the total energy release is increased by only a factor of about 2 as compared with tests initiated at atmospheric pressure.[7] Also, for core pressures as high as 2000 psig and for reactor transients as short as 11 msec the maximum fuel-plate surface temperature (see Figs. B.7 and B.8) is less than a factor of 2 above that at atmospheric pressure.

Comparison of the TSR-II and SPERT I Cores

One of the primary objectives of the SPERT I experimental program with highly enriched, plate-type cores was to test an empirical model for the prompt critical power-burst behavior of cores with a range of static nuclear characteristics (see Table B.1) but with the same shutdown reactivity mechanism. The empirical burst model assumed that shutdown was proportional to $b[E(t - \tau)]^n$, where b is a shutdown coefficient, $E(t - \tau)$ is the excursion energy to time $(t - \tau)$ after initiation of the burst, τ is a delay time, and n is a constant. For this model the peak power is proportional to $b^{-1/n}$, where b is proportional to the average void coefficient c_v over the neutron lifetime ℓ. A value of $n = 2$ was found to fit power burst shapes of SPERT I step reactivity addition tests. This empirical burst model predicted therefore that Spert I peak powers at a given value of the inverse asymptotic period α should be proportional to $(c_v/\ell)^{-1/2}$.

The SPERT I cores described in Table B.1 have (c_v/ℓ) values that vary by a factor of 50. On the basis of the relative values of (c_v/ℓ), peak power at a given α should vary by a factor of about 7, with the B-12/64 and P-18/19 cores yielding the highest and lowest peak powers, respectively. Experimentally, the peak power varies by a factor of about 5.5 between the P-18/19 and B-12/64 peak powers (see Fig. B.1). On the basis of the general agreement between the predictions of the elementary power burst theory and the SPERT I step reactivity power burst results, the dominant shutdown reactivity coefficient was concluded to be proportional to $(c_v/\ell)^{-1/2}$.

The TSR-II core was similar to the Spert-I cores in that it consisted of 20-mil-thick highly enriched uranium-aluminum alloy clad with 20-mil-thick aluminum. Basic dissimilarities between the two reactors are the presence of the control mechanism housing in the TSR-II, the spherical annular TSR-II fuel region geometry vs rectilinear fuel region of the Spert cores, and the H_2O reflector of the Spert cores vs the composite reflectors of the TSR-II. However, none of the dissimilarities would be expected to alter the reactivity shutdown mechanism of the moderator expulsion by moderator density decrease, fuel plate expansion, and steam void formation. Therefore, the TSR-II self-shutdown characteristics should be related to Spert-I characteristics by the parameter (c_v/ℓ) for values of α where system pressure does not suppress steam void formation. The TSR-II values of the average void coefficient and neutron lifetime are $c_v = 2.15 \times 10^{-6}$ $(\Delta k/k)/cm^3$ and $\ell = 5 \times 10^{-5}$ sec so that $(c_v/\ell) = 4.1 \times 10^{-2}$ $(\Delta k/k)/cm^3$ per sec. Comparing this (c_v/ℓ) value with those of Table B.1, the TSR-II self-shutdown characteristics should lie between those of the B-16/40 and A-17/28 cores. The more conservative B-16/40 characteristics will therefore be used in the following section to estimate the TSR-II self-shutdown excursion characteristics.

TSR-II Self-Shutdown Characteristics

The most energetic power excursion resulting from a reactivity accident is a function of the maximum rate of reactivity addition, not the maximum excess reactivity available in the system.[3] For the TSR-II the maximum rate of reactivity addition, or reactivity ramp, considered possible is from uncontrolled shim rod withdrawal. The reactivity addition rate of the shim rods is 0.147×10^{-2} $(\Delta k/k)$/sec at the fully insert position, which reduces to 0.101×10^{-2} $(\Delta k/k)$/sec at 0.3 in. withdrawn position and to 0.066×10^{-2} $(\Delta k/k)$/sec at the cold-clean critical position of 0.85 in. Since the reactivity addition rate is even lower if the plates are withdrawn more than 0.85 in., a 0.066×10^{-2} $(\Delta k/k)$/sec ramp is considered the maximum reactivity addition rate that could be attained in the TSR-II during a power excursion.

The SPERT I step and ramp reactivity addition tests provided the following empirical relation for prompt critical excursions:[3]

$$\frac{dk}{dt} = \frac{(k_{ex} - 1)^2}{30(\ell/\beta_{eff})},$$

where k_{ex} = excess reactivity, $; $\frac{dk}{dt}$ = ramp rate, $/sec; and ℓ/β_{eff} = ratio of neutron lifetime to delayed neutron fraction, sec. A 0.066×10^{-2} $(\Delta k/k)$/sec ramp is therefore equivalent to k_{ex} = $1.128 or 0.90×10^{-2} $\Delta k/k$; the corresponding value of α is 18 sec^{-1} calculated from the inhour equation for $\frac{\Delta k}{k} > \beta$ (ref. 8) and using the following values for the TSR-II:

$$\beta = 0.0064 \text{ (ref. 9)},$$

$$\beta_{eff} = \gamma\beta = 0.0080 \pm 0.00002 \text{ (ref. 10)},$$

$$\frac{\ell}{\beta_{eff}} = 6.61 \pm 0.016 \text{ msec (ref. 11)}.$$

Spert I excursion results are therefore of interest for α values up to ~18 sec^{-1} to give TSR-II self-shutdown characteristics.

The rationale by which the quantitative features of the SPERT I B-16/40 core self-shutdown characteristics can be ascribed to the TSR-II has been developed in the foregoing sections. The only limitation that exists in applying the B-16/40 core excursion results directly as a function of α is the effect of system pressure in the TSR-II. Since the basic self-shutdown mechanisms have been demonstrated to be the same for all the SPERT cores under the same operating conditions, with the differences in excursion results attributable to variations in the value of (c_v/ℓ), the effect of system pressure on excursion energy release and maximum fuel-plate surface temperature in SPERT III can be assumed to apply to the SPERT I B-16/40 and TSR-II cores also. Therefore except for differences in initial temperature the TSR-II fuel-plate surface temperature could not exceed twice the maximum temperature of SPERT I B-16/40 shown in Fig. B.3 for $\alpha > 18$ sec^{-1}. For example, using the

B-16/40 data at $\alpha \cong 35$ sec^{-1} (~30 msec asymptotic period),* the TSR-II temperature would not exceed 2 x 170°C or 612°F. Assuming a maximum initial fuel-plate temperature of 175°F for operation at power (105°F higher than the SPERT initial temperature), the maximum fuel-plate temperature would not exceed 717°F. Therefore maximum fuel-plate temperatures for a 30-msec period excursion in the TSR-II would not approach the melting temperature of the fuel (~1184°).

Summary and Conclusions

The SPERT program review and application to the TSR-II presented above have been limited to a maximum α value of 35 sec^{-1}, which is larger than the maximum α value for a startup accident in the TSR-II. On the basis of the SPERT results, it is concluded that for such an α value self-shutdown would cause no damage to the reactor core from high fuel temperatures and there would be no significant pressure pulse.

The shutdown behavior of the TSR-II with reactivity ramps of > 0.2 x 10^{-2} $(\Delta k/k)$/sec giving α values > 35 sec^{-1} would undoubtedly be similar to that of the SPERT III. However, as pressure pulses become more severe with shorter transients, the mechanical damage mechanisms in the TSR-II may differ from those in the relatively straight-through SPERT III coolant passages. Therefore no attempt has been made to predict from the pressurized SPERT III experiments the excursion conditions that would cause incipient fuel damage in the TSR-II. Such fuel damage would require α values between 50 and 100 sec^{-1}, which would require unrealistic reactivity insertion rates.

---

*Equivalent to a 0.98 x 10^{-2} step reactivity addition or 0.20 x 10^{-2} $(\Delta k/k)$/sec ramp addition from source power, higher step and ramp additions from full-power operation.

Appendix B References

1. S. G. Forbes et al., Analysis of Self-Shutdown Behavior in the Spert I Reactor, IDO-16528 (July 23, 1959).

2. W. E. Nyer et al., "Reactor Excursion Behavior," Proc. Intern. Conf. Peaceful Uses At. Energy, Geneva, 1964, 13, 13-22 (1965).

3. W. E. Nyer, pp. 417-445 in The Technology of Nuclear Reactor Safety, Vol. 1, edited by T. J. Thompson and J. G. Beckerley, MIT Press, Cambridge, 1964.

4. J. C. Haire, Jr., "Summary Description of the Spert Experimental Program," Nucl. Safety, 2(3), 15-23 (1961).

5. C. R. Toole, The Effects of Pressure and Flow on Room Temperature Power Excursions in Spert III, IDO-16918 (June 1964).

6. T. Schroeder, editor, SPERT Project, Quarterly Technical Report for April-June, 1960, IDO-16640 (April 7, 1961).

7. T. Schroeder, editor, SPERT Project, Quarterly Technical Report for October-December, 1960, IDO-16687 (June 1, 1961).

8. S. Glasstone and M. C. Edlund, Elements of Nuclear Reactor Theory, p. 309, Van Nostrand, Princeton, N. J. 1957.

9. G. R. Keepin et al., "Absolute Yield of Delayed Neutrons per Fission and Deduced Values of β," Sec. 8-1, p. 8-5 in Nuclear Engineering Handbook, ed. H. Etherington, McGraw-Hill, New York, 1958.

10. J. D. Kington, R. Perez-Belles, and G. de Saussure, Neutron Phys. Div. Ann. Progr. Rept. Sept. 1, 1960, ORNL-3016, pp. 5-12. The BSR-I has the same metal-to-water ratio in the core as the TSR-II; therefore these data were used.

11. G. de Saussure, E. G. Silver, and J. D. Kington, op. cit., pp. 54-55.

APPENDIX C

INTRA-LABORATORY CORRESPONDENCE
Oak Ridge National Laboratory
September 14, 1962

To: L. B. Holland

From: V. R. Cain

Subject: Heat Deposition in the TSR-II Control Mechanism Housing

An upper limit calculation of heat deposition in the control mechanism housing has been done. Sources considered are gamma rays produced by neutron absorption in the fuel, neutron captures in the poison plates, and neutron captures in the housing other than the poison plate captures. The significant assumptions include:

1. 13.5 MeV of gamma-ray energy is emitted per fission (this includes prompt and delayed emission plus emission by virtue of nonfission neutron captures in the fuel).
2. Neutron flux distribution assumed to be that plotted as curve B, p. 49, ORNL-3016. This represents the best present estimate of 5 MW flux distribution.
3. No gamma-ray attenuation in regions external to the control housing.
4. All gamma rays crossing the control housing surface or which originated in it are fully absorbed in the housing.
5. All neutron absorptions in the housing are either in B, producing 2.79 MeV, or in H, producing 2.2 MeV.
6. Heat transfer from the outside of the fuel cover plates is adequate to insure that no fission heat is introduced into the housing (see J. Lewin, "Heat Transfer TSR-II").*

*(Added in press: This report has been published as ORNL-TM-1779.)

Gamma Rays from Fissions in Fuel Annulus

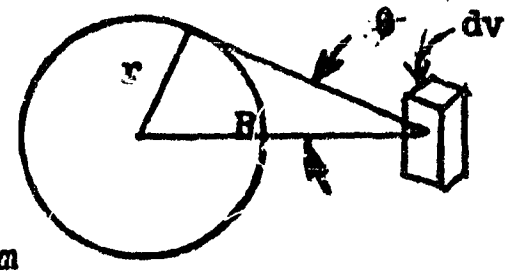

Control Housing

r = 21.6 cm

23 cm ≅ R ≅37 cm

The fraction of gamma rays emitted from dV which strike the housing is

$$\frac{1 - \cos \theta}{2} .$$

Dividing the fuel annulus into 14 1-cm thick regions of total heat deposition rate is:

$$D_{FA} = \sum_{i=1}^{14} F(R_i) \times 13.5 \times \frac{1-\cos \theta_i}{2} \times V(R_i) \frac{MeV}{sec}$$

where

R_i = average radius of spherical annulus, in cm,

$F(R_i)$ = fission rate at radius R_i in fissions . $cm^{-3}.sec^{-1}$,

13.5 = total gamma-ray energy in $MeV \cdot fission^{-1}$,

$V(R_i)$ = volume of spherical annulus around R_i, in cm^3.

This calculation is tabulated in Table 1, giving a net result of 1.96×10^{17} $MeV \cdot sec^{-1}$.

Gamma Rays from Fissions in Housing Cover Plates

The fission rate in the cover plate is:

$$F = \phi AP \text{ fissions} \cdot sec^{-1}$$

where

ϕ = thermal neutron flux in neutrons. $cm^{-2}.sec^{-1}$

A = area of cover plate in cm^2

P = probability of a fission occurring when a neutron crosses the sphere.

P may be broken down into:

$$P = \frac{M\ A_o\ \sigma}{A\ W}$$

where

M = total mass of ^{235}U in the plate, in gm

A_o = Avogadro's number, in atoms.gAW^{-1}

W = atomic weight, in gm.gAW^{-1}

σ = fission cross section, in $cm^2.atom^{-1}$.

Cancelling A, the net result is:

$$F = (9.07 \times 10^{12}) \left(\frac{233}{235}\right) (0.6)\ (583)$$

$$= 3.146 \times 10^{15}\ \text{fiss/sec.}$$

Making the assumptions of 13.5 MeV of gamma rays per fission and that one-half of all gamma-rays emitted enter the housing and are thereby absorbed, the energy deposition rate from this source is:

$$D = \frac{13.5}{2} (3.146 \times 10^{15})\ \text{MeV-sec}^{-1}$$

$$= 2.12 \times 10^{16}\ \text{MeV.sec}^{-1}.$$

Neutron Absorptions in Control Mechanism Housing

Per fission neutron, the probability of an absorption in the region containing the B_4C poison plates is about 0.08 and the probability of an

absorption elsewhere in the housing is about 0.02 (from GNU-II calculations). It is assumed that all the absorptions in the poison plate region are in the boron which emits 2.79 MeV per absorption and all other absorptions are in hydrogen, emitting 2.2 MeV per absorption. This results in a heat generation rate in the B_4C of:

$$D_B = (0.08 \frac{\text{abs}}{\text{fiss·neut}}) (\frac{2.47 \text{ fiss·neut}}{\text{fission}}) (\frac{2.79 \text{ MeV}}{\text{abs}})$$

$$\times (3.1 \times 10^{10} \frac{\text{fiss}}{\text{W-sec}}) (3 \times 10^{6} \text{ W}) =$$

$$= 5.13 \times 10^{16} \text{ MeV·sec}^{-1}.$$

Correspondingly, the absorptions in H give:

$$D_H = (.02) (2.47) (2.2) (3.1 \times 10^{10}) (3 \times 10^{6})$$

$$= 1.01 \times 10^{16} \text{ MeV·sec}^{-1}.$$

Total Heat Deposition

Totaling, we have,

$$\begin{array}{r} 1.96 \times 10^{17} \\ .21 \\ .51 \\ .10 \\ \hline 2.78 \times 10^{17} \text{ MeV/sec, or 44 kW} \end{array}$$

If no credit is taken for the cooling water supplied directly to the housing from the shim line, assuming the only available water is that necessary to maintain the clutch on the five mechanisms, 11 gpm is inserted into the housing.

The temperature rise of the water is:

$$T = (2.78 \times 10^{17} \frac{\text{MeV}}{\text{sec}}) (\frac{1 \text{ BTU}}{6.59 \times 10^{15} \text{ MeV}}) (\frac{\text{min}}{11 \text{ gal}}) (\frac{\text{gal}}{8.33 \text{ lb}})$$

$$\times (\frac{60 \text{ sec}}{\text{min}}) (1 \frac{\text{lb}^\circ\text{F}}{\text{BTU}})$$

$$= 27.6^\circ\text{F}$$

Note by L. B. Holland:

The values used to calculate the temperature rise in Cain's analysis were a power level of 5 MW and a minimum cooling-water flow rate of 11 gpm. Since the maximum power level proposed is 1 MW and since the flow rate required to operate all mechanisms is only 5.5 gpm, the temperature rise is

$$T = 27.6^\circ\text{F} \frac{11}{5.5} \times \frac{1}{5} = 11.0^\circ\text{F}.$$

Table. 1 Calculation of Gamma-Ray Heating from Fissions in Fuel Annulus

Radial Limits of Region	Average Radius R_i	$\frac{1 - \cos\theta}{2}$	$13.5\left[\frac{1 - \cos\theta}{2}\right]$	$F(R_i)$	$F(R_i) \times 13.5 \times \left[\frac{1 - \cos\theta}{2}\right]$	Volume of Spherical Annulus $V(R_i)$	$F(R_i) \times 13.5 \times \left[\frac{1 - \cos\theta}{2}\right] \times V(R_i)$
(cm)	(cm)		(Mev/fission)	Fissions/cm^3.sec	$\frac{Mev}{cm^3.sec}$	(cm^3)	Mev/sec
23 - 24	23.5	.303	4.09	7.02×10^{11}	2.87×10^{12}	6.94×10^3	1.99×10^{15}
24 - 25	24.5	.264	3.56	6.75	2.40	7.54	1.81
25 - 26	25.5	.2342	3.16	6.52	2.06	8.17	1.68
26 - 27	26.5	.2103	2.84	6.39	1.82	8.82	1.61
27 - 28	27.5	.1906	2.57	6.26	1.61	9.50	1.52
28 - 29	28.5	.1738	2.35	6.14	1.44	10.2	1.46
29 - 30	29.5	.1594	2.15	6.01	1.30	10.9	1.42
30 - 31	30.5	.1469	1.98	5.82	1.15	11.7	1.34
31 - 32	31.5	.136	1.84	5.60	1.03	12.5	1.28
32 - 33	32.5	.1264	1.71	5.36	.916	13.3	1.21
33 - 34	33.5	.1178	1.59	5.16	.821	14.1	1.16
34 - 35	34.5	.1102	1.49	4.95	.738	14.9	1.10
35 - 36	35.5	.1032	1.39	4.78	.665	15.8	1.05
36 - 37	36.5	.0969	1.31	4.74	.620	16.7	1.04
							$\sum = 19.6 \times 10^{16}$

APPENDIX D

TSR-II Core Characteristics

I.	Reactor Power Levels, kW	
	A. Maximum steady state (limited by afterheat to periods of 75 hr)	1,000
	B. Reverse point	1,200
	C. Shutdown point	1,500
II.	Neutron Flux at 1 MW, neutrons $cm^{-2}sec^{-1}$	
	A. Maximum thermal for clean cold core	2.48×10^{12}
	B. Maximum thermal at end of core life	2.76×10^{12}
III.	Reactor Materials	
	A. Fuel plates	U-Al alloy, Al cladding
	1. Weight of ^{235}U in 12 annular elements, kg	5.286
	2. Weight of ^{235}U in 8 inner elements, kg	2.819
	3. Weight of ^{235}U in 4 lune-shaped cover plates on control mechanism housing	0.233
	4. Weight of ^{235}U in cylindrical plug element	0.031
	5. Total fuel loading of ^{235}U, kg	8.369
	B. Coolant	H_2O
	C. Inner reflector	H_2O - 20,000 cc Al - 16.75 in-diam sphere with openings for control plates
	D. Shim safety and regulating plates	B_4C powder canned in stainless steel
	E. Outer reflector	H_2O, Al - other materials may be used

IV. Heat Transfer and Coolant Data

A. General

1.	Design heat load, kW	1,000
2.	System operating pressure psi	
	a. Maximum	94
	b. Minimum	36.5
3.	Coolant flow rates, gpm	
	a. Through fuel	800
	b. Minimum through control mechanism housing	5.5
4.	Design coolant temperature at 1,000 kW, °F	
	a. Fuel inlet	125
	b. Maximum bulk water (fuel outlet)	134
	c. Maximum surface (fuel plate - water interface)	156

B. Fuel Region

1. Geometry: spherical annulus with 3.2 in. diam opening for controls. Fuel is divided into a main region with three types of elements (inner, annular, plug) and a thin spherical shell on the outside of the control mechanism housing.

2. Main fuel region data, in.

a.	Inner diameter (fuel)	9.0
b.	Outer diameter (fuel)	14.5
c.	Fuel plate thickness	0.060
d.	Cladding thickness (each surface)	0.020
e.	Fuel plate core thickness	0.020
f.	Coolant channel thickness	0.120
g.	Plate dimension, length, width, curvature	All vary to obtain spherical core

h.	Number of elements	
	(1) Annular	12
	(2) Inner	8
	(3) Cylindrical plug	1
i.	Number of fuel plates (per element)	
	(1) Annular	41
	(2) Inner	33
	(3) Cylindrical plug	6
3.	Spherical fuel shell data	
a.	Number of pieces	4
b.	Shape	lune
c.	Outer diameter, in.	17.0
d.	Shell thickness, in.	0.125
e.	Cladding thickness (each side), in.	0.034
f.	Fuel plate core thickness, in.	0.046
4.	Total heat transfer area, ft^2	657.5
5.	Volume of core, cc	
	Main fuel annulus only	158,456
	Total fuel volume	168,218
6.	Heat load in fuel, kW	1,000
7.	Heat flux, for main fuel annulus, Btu $hr^{-1}ft^{-2}$	
a.	Average for clean cold core	5,075
b.	Average for end of core life	5,062
c.	Peak to average for clean cold core	1.20
d.	Peak to average for end of core life	1.37

8.	Heat flux from spherical fuel shell (heat transfer assumed for one side only), Btu hr^{-1} ft^{-2}	
	a. For clean cold core	18,270
	b. At end of core life	20,246
9.	Coolant flow rate, gpm	800
10.	Pressure drop across core, psi	30.5
11.	Temperature, ^{o}F	
	a. Design saturation	274
	b. Maximum fuel plate surface in upper region of inner fuel	137
	c. Maximum surface for spherical cover shell	144
	d. Maximum surface in annular elements	156

C. Control Region

1. Geometry: aluminum sphere with sections cut out for control plates. Outer surface is fuel loaded spherical shell. There are five shim-safety plates and one regulating plate. Control plate motion is radial.

2.	Control region dimensions	
	a. Overall region diameter, in.	17.0
	b. Control plate	
	(1) Plate thickness, in.	0.5
	(2) Can thickness, in.	0.025
	(3) Approximate area of plate outer surface, $in.^2$	80
	(4) Radial plate movement, in.	1.7
3.	Heat generation inside control region, kW	8.8
4.	Minimum water flow rate through region, gpm	5.5
5.	Temperature rise of water, ^{o}F	11.0

6. For heat generation and removal for spherical cover shell (see fuel region)

D. Outer reflector

1. Geometry: spherical shell made in five sections (lower hemisphere and four upper sections that form a hemisphere with opening at top)

2. Materials can be varied (see Appendix A - Vol. 1) Al - H_2O used most often

3. Dimensions

a. Inner diameter of first solid material must be, in.	36.75
b. Aluminum thickness, in.	0.75

4. Heat load — Negligible

V. Reactivities

A. Summary of reactivities

1. Fuel worth, $\Delta k/k$, for no fission products, 70°F, shield for maximum reactivity worth	0.019
2. Shim-safety plate worth, $\Delta k/k$, (all plate inserted)	0.038
3. Shut down margin, $\Delta k/k$	0.019
4. Temperature defect from 70 - 140°F, $\Delta k/k$	0.007
5. Fuel depletion, $\Delta k/k$, for 1000 MWhr	-0.00122
2000 MWhr	-0.00244
3000 MWhr	-0.00366
6. Samarium, $\Delta k/k$, for 1000 MWhr	-0.00325
2000 MWhr	-0.00552
3000 MWhr	-0.00710

7. Xenon, $\Delta k/k$, for 1 MW cyclic operation (2 hr on 2 hr off, 16 hr per day, 5 days per week)	-0.0034
B. Shim-safety plate characteristics	
1. Worth with all plates inserted, i.e. close to fuel, $\Delta k/k$	0.038
2. Reactivity insertion rate, $\Delta k/k$ per sec	
a. Maximum, exists at position of maximum shutdown	0.015×10^{-2}
b. At position where clean core is just critical	0.065×10^{-2}
c. Minimum, rate, occurs late in core life with plates completely withdrawn	0.05×10^{-2}
C. Regulating plate characteristics	
1. Worth with plate inserted, i.e. against fuel, $\Delta k/k$	0.40×10^{-2}
2. Reactivity insertion rates, $\Delta k/k$ per sec	
a. Maximum, exists at position of maximum shutdown	0.108×10^{-2}
b. Near normal operating position	0.047×10^{-2}
c. Minimum, plate withdrawn to limit	0.034×10^{-2}
D. Reactivity coefficients	
1. Isothermal temperature coefficient of reactivity, $\Delta k/k$ per $^{\circ}F$, at $50^{\circ}F$	-0.67×10^{-4}
at $145^{\circ}F$	-1.24×10^{-4}
2. Void reactivity coefficients, $\Delta k/k$ per cc of void	
a. Main fuel annulus (volume average)	-2.15×10^{-6}
b. Between main fuel annulus and fuel loaded spherical shell on control mechanism housing	-6.3×10^{-7}

c.	Inside control mechanism housing	$+8.2 \times 10^{-7}$
3.	Fuel coefficient, $\Delta k/k$ per kg of ^{235}U	
a.	Main fuel region, (average)	-0.027
b.	Spherical shell on control mechanism housing	0.086
E.	Miscellaneous	
1.	Prompt neutron generation time, μsec	53